Master Thesis

Distinguishing Spins in Decay Chains with Photons

Author: A. Landwehr
Supervisor: D. Wyler, A. Freitas

2008-03-11

Abstract

There are several alternatives for extending physics beyond the Standard Model. The two most prominent examples are supersymmetry (SUSY) and universal extra dimensions (UED). These models predict new particles, which differ in mass spectra and spin and may provide us with a suitable dark matter candidate.

If new particles are discovered at the LHC, it will be vital to measure their spins, in order to distinguish SUSY from UED. In this thesis we concentrate on gauge mediated SUSY breaking (GMSB) and 2 universal extra dimensions (2UED). These models lead to decay chains involving leptons and photons. As proposed by Barr [1] we investigate the invariant mass distributions for the different decay products for sample mass spectra of both GMSB and 2UED. In order to extend this analysis in a more model-independent way we investigated all possible spin assignments.

For a typical hierarchichal GMSB mass spectrum a χ^2 analysis gives a good chance of distinguishing the two models at the LHC. However for a degenerate 2UED mass spectrum it would be more difficult to observe spin correlations.

Acknowledgment

I would like to thank all people who helped and inspired me during my study — family, friends, colleagues and the members of the theoretical and experimental physics institutes.

Especially, my gratitude goes to Prof. Dr. Ayres Freitas for his great support, even over the Atlantic. I thought it would be more difficult with my supervisor being far away, but he really took his time to write extensive emails, so that my questions never stayed unanswered. I also would like to thank Prof. Dr. Daniel Wyler for giving me the possibility to write this thesis in his research group. Further, I thank Dr. Wolfgang Ehrenfeld, whom it was a pleasure to work with.

Contents

Chapter 1

Introduction

The Electroweak Standard Model (SM) includes all the known elementary particles and describes their interactions (i.e. the electric, weak and strong forces). The only exception is gravity, which, from a phenomenological point of view, is irrelevant, since the gravitational force is orders of magnitude weaker than the other forces and so is its effect on the observable quantities. This is reflected by high energy experiments, which show high agreement between theory and experiment.

Although the SM is experimentally successfull it has some theoretical shortcomings. One is the large number of free parameters, in the SM 19 — although some extensions to the SM introduce even more free parameters. Another mystery is their scale compared to the one of gravity — why is gravity so weak? Why are there three generations of particles?

There are candidates for a fundamental description of elementary particles, for instance Superstring theory. However these theories are far from predicting measurable results and it is questionable whether they really will be THE fundamental theory, irrespective to the fact that it might not even exist. Anyways, in quest of such a theory - whether we will ever find it is another story - it is reasonable to concentrate on few shortcomings and not burden oneself with the task of finding a final description of the universe. This is the way embarked by the different extensions to the SM. Tackling some of this deficiencies gives us a deeper insight into nature and gives us hints how such a fundamental theory might look like.

In string theory for instance space time is supersymmetric. Herefore it makes sense to consider supersymmetric extensions of the SM. If we gain insights about supersymmetry for example through collider experiments, that could give us clues about the underlying string theory. This applies also to other extensions such as extra dimensions.

As a matter of fact these extensions often predict new particles which might have an impact on future high energy experiments such as the LHC. The spin of these new particles gives us important information about the extensions and so maybe about the fundamental theory. It is therefore sensible to inspect measurable quantities which are sensible to the spin of these new particles. In this thesis we consider exemplary one supersymmetric and one extra dimensional theory - gauge mediated supersymmetry breaking (GMSB) and two universal extra dimensions (2UED). In these two models the spins of the new particles

differ by a value of 1/2. Another specialty of these models is that the last decay of the whole decay chain of these new particles contains a photon which is very useful to separate these events from the usual Standard Model background.

Suited quantities to observe spin effects in colliders are invariant mass distributions. Some groups studied decays of the quark partner with one outgoing quark and two outgoing leptons where they constructed different invariant mass distributions from these decay products. Since in the models we are inspecting, a photon is emitted, we study invariant mass distributions constructed from one photon and two leptons.

In a first step we calculated these different mass distributions analytically, which could be useful to fit the values of the new particles masses to measured distributions. Next we generated Monte Carlo events with the parton level generator CompHEP. In order to distinguish the different spin configurations, we generated histograms for the different invariant masses and compared them with the χ^2 test. In real-life experiments such as the LHC diverse effects tend to wash out these invariant mass distributions. Thus, at last we have to calculate these distributions with the Monte Carlo generator *Pythia* and include detector effects with *ATLFAST*. This has not been accomplished within the period of this master thesis.

Chapter 2

Theoretical Prelude

2.1 The Standard Model

The SM is described by a Lagrangian $\mathcal{L}$ which contains fields for all elementary particles. There are two fundamentally different sorts of particles, fermions and bosons. The former are described by spinors Ψ and latter come into play if we require invariance under a local gauge symmetry and are described by a vector A_μ. The gauge symmetry of the Standard model is $SU(3)_c \times SU(2)_L \times U(1)_Y$. The subscript c denotes that this symmetry acts on colored spinors, i.e. $SU(3)$ triplets, L denotes that the symmetry only acts on left handed spinors which are aligned in $SU(2)$ doublets, right handed ones are $SU(2)$ singlets and Y the weak hypercharge. To express this in a more formal way let us define the projection operators

$$P_{R/L} = \frac{1}{2}(1 \pm \gamma^5). \tag{2.1}$$

Then the right-/left-handed spinors are $\Psi_R = P_R\Psi$ and $\Psi_L = P_L\Psi$. For further convenience we will just stick to the $SU(2) \times U(1)$ case. Table 2.1 lists all SM fermionic particles. The left-handed particles are aligned in $SU(2)$ dublets, the right-handed ones in singlets.

				I^3	Y	Q
$L =$	$\begin{pmatrix} \nu_e \\ e^- \end{pmatrix}_L$	$\begin{pmatrix} \nu_\mu \\ \mu^- \end{pmatrix}_L$	$\begin{pmatrix} \nu_\tau \\ \tau^- \end{pmatrix}_L$	$1/2$ $-1/2$	-1 -1	0 -1
	e_R	μ_R	τ_R	0	-2	-1
$Q =$	$\begin{pmatrix} u \\ d \end{pmatrix}_L$	$\begin{pmatrix} c \\ s \end{pmatrix}_L$	$\begin{pmatrix} t \\ b \end{pmatrix}_L$	$1/2$ $-1/2$	$1/3$ $1/3$	$2/3$ $-1/3$
	u_R	c_R	t_R	0	$4/3$	$2/3$
	d_R	s_R	b_R	0	$-2/3$	$-1/3$

Table 2.1: Fermions described by the SM and their quantum numbers

Then the free Dirac equation reads

$$\mathcal{L} = \sum i \left[\bar{Q}\partial\!\!\!/^{(L)}Q + \bar{u}_R\partial\!\!\!/ u_R + \bar{d}_R\partial\!\!\!/ d_R + \bar{L}\partial\!\!\!/^{(L)}L + \bar{e}_R\partial\!\!\!/ e_R\right], \tag{2.2}$$

where summation runs over the three families. Interactions emerge if we require invariance under local gauge transformations. As mentioned before left handed spinors have to be invariant under $SU(2)\times U(1)$, right handed ones under $U(1)$. Mathematically a local gauge transformation is a map $\Psi \to e^{iT^a\alpha^a(x)}\Psi$ where T^a are the generators of the Lie group and $\alpha^a(x)$ are scalar functions of space-time. In our case we have the following transformations:

$$\begin{aligned} L &\longrightarrow e^{iT^a\alpha^a(x)}e^{i\hat{y}\beta(x)}L, \\ e_R &\longrightarrow e^{i\hat{y}\beta(x)}e_R, \end{aligned} \tag{2.3}$$

$T^a = \tau^a/2$ are the $SU(2)$ generators and $\hat{y}$ is the hypercharge operator. In order to construct local gauge invariance under these groups we have to perform the replacements

$$\begin{aligned} \partial_\mu^{(L)} &\longrightarrow D_\mu^{(L)} = \partial_\mu + igT^aW_\mu^a + ig'\hat{y}B_\mu, \\ \partial_\mu &\longrightarrow D_\mu = \partial_\mu + ig'\hat{y}B_\mu. \end{aligned} \tag{2.4}$$

W_μ^a and B_μ are the gauge fields, they transform as

$$\begin{aligned} W_\mu^a &\longrightarrow W_\mu'^a = W_\mu^a - \epsilon^{abc}\alpha^b W_\mu^c - \frac{1}{g'}\partial_\mu\beta, \\ B_\mu &\longrightarrow B'_\mu = B_\mu - \frac{1}{g'}\partial_\mu\beta. \end{aligned} \tag{2.5}$$

If we want to regard these fields as physical objects, we have to add a term corresponding to their kinetic energy to the Lagrangian. So we define the field strength tensors

$$\begin{aligned} B_{\mu\nu} &= \partial_\mu B_\nu - \partial_\nu B_\mu, \\ W_{\mu\nu}^a &= \partial_\mu W_\nu^a - \partial_\nu W_\mu^a + g\epsilon^{abc}W_\mu^b W_\nu^c. \end{aligned} \tag{2.6}$$

The complete Lagrangian then is

$$\begin{aligned} \mathcal{L} = &\sum_{families} i\left[\bar{Q}\not{D}^{(L)}Q + \bar{u}_R\not{D}u_R + \bar{d}_R\not{D}d_R + \bar{L}\not{D}^{(L)}L + \bar{e}_R\not{D}e_R\right] \\ &- \frac{1}{4}B_{\mu\nu}B^{\mu\nu} - \frac{1}{4}W_{\mu\nu}^a W^{a\mu\nu}. \end{aligned} \tag{2.7}$$

The physical fields are linear combinations of the gauge fields and are obtained by

$$\begin{aligned} W_\mu^\pm &= \frac{1}{\sqrt{2}}(W_\mu^1 \pm iW_\mu^2), \\ \begin{pmatrix} Z_\mu \\ A_\mu \end{pmatrix} &= \begin{pmatrix} \cos\theta_W & \sin\theta_W \\ -\sin\theta_W & \cos\theta_W \end{pmatrix}, \end{aligned} \tag{2.8}$$

where θ_W is the Weinberg angle. The relation between the electric charge, the hypercharge and the weak isospin turns out to be

$$Q = T^3 + \frac{y}{2}. \tag{2.9}$$

So far we have only considered massless particles. Introducing fermion mass terms $\sim m\bar{\Psi}\Psi = m(\bar{\Psi}_R\Psi_L + \bar{\Psi}_L\Psi_R)$ and boson mass terms $\sim \frac{1}{2}m^2B_\mu B^\mu$ would break gauge invariance. In order to describe massive particles we have to introduce a new scalar field, the Higgs field.

2.1.1 The Higgs Mechanism

The recipe is to introduce a Lagrangian $\mathcal{L} = \mathcal{T} - \mathcal{V}$ for a scalar $SU(2)$ doublet $\Phi = \binom{\phi^+}{\phi^0}$ which is invariant under $SU(2)_L \times U(1)_Y$. In order to produce the right mass terms the ground state of the scalar potential $\mathcal{V}$ has to break the $SU(2)_L \times U(1)_Y$ symmetry down to $U(1)_{em} \subset SU(2)_L \times U(1)_Y$ such that the photon remains massless. This is achieved in choosing the following Lagrangian:

$$\mathcal{L} = (D_\mu \Phi^\dagger)(D^\mu \Phi) - \mu^2 \Phi^\dagger \Phi + \lambda (\Phi^\dagger \Phi)^2. \tag{2.10}$$

We choose $\lambda > 0$ to avoid instability at large values of the field. For $\mu^2 > 0$ the ground state is obtained with the field being zero $\langle \Phi \rangle = 0$ and is invariant under $SU(2)_L \times U(1)_Y$. On the other hand if $\mu^2 < 0$ the ground state is not at $\langle \Phi \rangle = 0$ but its reached at $\langle \Phi \rangle = \sqrt{-\mu^2/2\lambda} \equiv v/\sqrt{2}$, hence it is not invariant under $SU(2)_L \times U(1)_Y$ anymore. In order to keep the photon massless we choose Φ to have the hypercharge $y = 1$. With relation (2.9) we note that ϕ^+ has the electric charge $Q = +1$ and ϕ^0 is electrically neutral. Using an $SU(2)$ rotation, we have the freedom to choose the ground state $\Phi = \binom{0}{v/\sqrt{2}}$, which makes the invariance under $U(1)_{em}$ explicit. Inserting this into the Lagrangian (2.10) and using the transformation property of the Higgs field, the $W^\pm$ and Z gauge bosons acquire masses

$$\begin{aligned} M_W &= \frac{vg}{2}, \\ M_Z &= \frac{vg}{2\cos\theta_W}. \end{aligned} \tag{2.11}$$

In order to expand the Lagrangian about the ground state we write the Higgs-doublet field as

$$\Phi(x) = \begin{pmatrix} G^+(x) \\ \frac{1}{2}\left(v + h(x) + iG^0(x)\right) \end{pmatrix}. \tag{2.12}$$

The fields G^+ and G^0 are unphysical degrees of freedom — the would-be Goldstone bosons — and can be eliminated by applying a specific gauge transformation. However, $h(x)$ is a physical field with mass

$$M_h = \sqrt{-2\mu^2} \tag{2.13}$$

and gives rise to the physical Higgs boson.

For the fermion masses we have to introduce Yukawa couplings between the spinors and the scalar Higgs field which turn out to be mass terms when the Higgs field acquires the vacuum expectation value (VEV). Physically speaking, fermions get mass through interactions with a scalar field which fills the complete space.

Another point is the mixing between the different flavors. For instance, if we write down the most general Yukawa term for the quarks we end up with

$$\sum_i c_{ik} (\bar{u}_{iL}, \bar{d}_{iL}) \binom{\phi^+}{\phi^0} d_{kR} \tag{2.14}$$

where summation goes over the different families. c_{ik} are some further arbitrary constants added to the Lagrangian.

2.2 Theoretical Issues

In high energy experiments the SM shows very high agreement with experimental data. However, from cosmological observations (such as galactic rotation curves, structure formation and gravitational lensing) we assume that the space is filled with 22% by *dark matter* and only 4% by baryons. From a particle physicists point of view, it would be desirable to describe dark matter in the framework of elementary particles.

On the other hand the SM is also not completely satisfactory from a theoretical point of view. To name few issues:

- Inspecting the free parameters of the SM one counts 19. For a fundamental theory of nature one may wish a smaller number.
- After symmetry breakdown the fermion mass terms have the form $m = c\langle\Phi\rangle = \frac{v}{\sqrt{2}}$, c being the Yukawa coupling and $v = 246\,\text{GeV}$. Assuming the *natural* value of the Yukawa coupling to be of order 1 we would expect the fermion masses to be of order 100 GeV which only applies for the top quark mass $m_t = 175\,\text{GeV}$, all the other masses are orders of magnitudes smaller. This constitutes the fermion mass hierarchy problem.

Lastly we would like to discuss a shortcoming envisaged by most extensions to the SM: the gauge hierarchy problem, mostly just called hierarchy problem.

2.2.1 Naturalness and the Hierarchy Problem

For the next thought it will suffice to consider a spinor (ψ) and a scalar (S) field interacting through a Yukawa term. Thus our Lagrangian is

$$\mathcal{L}_1 = \bar{\psi}\left(i\partial\!\!\!/ - m_F\right)\psi + \frac{1}{2}(\partial_\mu S)(\partial^\mu S) - \frac{1}{2}m_S^2 S^2 - \frac{\lambda_F}{2}S\bar{\psi}\psi \tag{2.15}$$

Considering the boson mass correction to the first order we have to calculate the Feynman diagram pictured in Figure (2.1).

$$\begin{aligned}\delta m_S^2 &= -\left(-i\frac{\lambda_F}{2}\right)^2 \int^\Lambda \frac{d^4l}{(2\pi)^4}\frac{\text{Tr}\left[i(l\!\!\!/ + m)i(p\!\!\!/ - l\!\!\!/ + m)\right]}{(l^2 - m^2)((p-l)^2 - m^2)} \\ &= -\frac{\lambda_F^2}{8\pi^2}\left(\Lambda^2 - m_F^2 \log\frac{\Lambda^2}{m_F^2}\right)\end{aligned} \tag{2.16}$$

Accordingly in the SM the Higgs boson mass receives the following one-loop

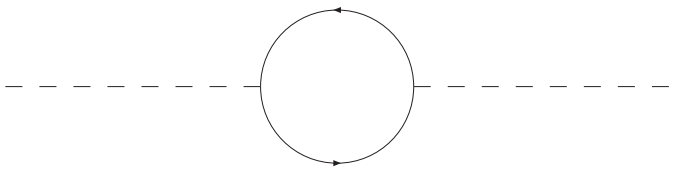

Figure 2.1: One-loop contribution to the boson mass in a theory with one spinor and one real scalar field.

correction

$$\delta M_h^2 = \frac{3\Lambda^2}{8\pi^2 v^2}\left((4m_t^2 - 2M_W^2 - M_Z^2 - M_h^2)\right) + \mathcal{O}\left(\log\frac{\Lambda}{\mu}\right) \tag{2.17}$$

Λ is the momentum cutoff used to regulate the loop integral, it should be interpreted as an energy scale at which new physics enters to alter the high energy behavior of the theory. If we assume Λ to be of order $M_P \sim 10^{19}\,\mathrm{GeV}$ and we plug $M_h \sim 100\,\mathrm{GeV}$ we see that δM_h^2 is some 30 orders of magnitude larger than the actual Higgs mass. This means that we have to adjust the bare Higgs mass M_h^2 in the SM Lagrangian to one part in 10^{30} what seems rather unnatural and is called the (gauge) hierarchy problem. Simply speaking, the Higgs mass which is of order the weak scale ($\sim 100\,\mathrm{GeV}$) receives corrections of order the Planck scale. So we are tempted to ask: why is the weak scale so much smaller than the Planck scale?

2.2.2 Possible Solutions to the Gauge Hierarchy Problem

Inspecting eq. (2.16) we have two possibilities to cure the Hierarchy problem. The first one is to add further contributions which cancel with the SM terms and the Higgs mass thus will be stabilized. This approach will lead us to Supersymmetric (SUSY) theories[1]. On the other hand one can pursue the question why the weak and Planck scales are so widely separated. Herefore we find nice answers in Extra Dimensional (XD) theories.

Tackling the Hierarchy Problem with Supersymmetry

Let us return to the simple Lagrangian in eq. (2.15) where we have only one spinor and one real scalar field and add another Lagrangian containing one complex scalar field $\Phi = \phi_1 + i\phi_2$ interacting with the real one:

$$\mathcal{L}_2 = (\partial_\mu\phi_1)(\partial^\mu\phi_1) + (\partial_\mu\phi_2)(\partial^\mu\phi_2) - m_\phi^2(\phi_1^2 + \phi_2^2) + \frac{\lambda_S}{2}S^2(\phi_1^2 + \phi_2^2) \tag{2.18}$$

If we now calculate the S mass correction for the total Lagrangian $\mathcal{L}_{\mathrm{tot}} = \mathcal{L}_1 + \mathcal{L}_2$ we get the same term as in (2.16) but in addition we have to calculate the Feynman diagram fig. 2.2 which results in

$$\delta m'^2_S = +\frac{\lambda_S^2}{8\pi^2}\left(\Lambda^2 - m_\phi^2\log\frac{\Lambda^2}{m_\phi^2}\right) \tag{2.19}$$

Adding the two corrections together we get

$$\begin{aligned}\delta m_S^2|_{\mathrm{tot}} = \delta m_S^2 + \delta m'^2_S = \frac{1}{8\pi^2}\Bigg(&\Lambda^2(\lambda_S^2 - \lambda_F^2) \\ &- m_\phi^2\log\frac{\Lambda^2}{m_\phi^2} + m_F^2\log\frac{\Lambda^2}{m_F^2}\Bigg)\end{aligned} \tag{2.20}$$

[1] Primarily Supersymmetry was not introduced to cure the Hierarchy problem. In fact it was considered much more due to symmetry reasons and it was later noticed that it solves the Hierarchy problem.

Requiring the couplings to be equal $\lambda_S = \lambda_F$ we see that the quadratic divergences vanish. On the other hand, assuming the real scalar mass to be of order of the weak scale ($m_S \sim \mathcal{O}(100\,\text{GeV})$), the mass of the complex scalar has to be in the TeV range ($m_\phi \leq \mathcal{O}(\text{TeV})$) in order to keep the logarithmic divergences small.

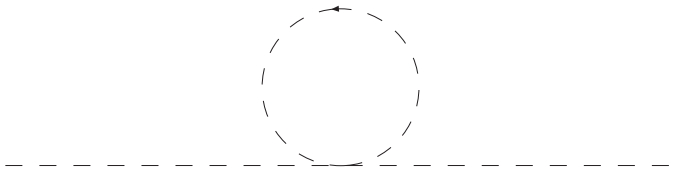

Figure 2.2: Further one-loop contribution to the boson mass if a complex scalar field is added.

This is exactly what SUSY models achieve: they introduce a new symmetry between bosons and fermions and so double the particle spectrum (i.e. to each fermionic field a bosonic field is added and vice versa), keeping the fermionic and bosonic couplings equal. Since we have not observed any SUSY particle yet SUSY must be broken and the superpartners have to be heavier than the SM particles. Here the latter condition gives us some bounds on the SUSY breaking mechanisms.

Tackling the Hierarchy Problem with Extra Dimensions

Let us assume the universe has $4+n$ dimensions where n is the number of the compact extra dimensions. The higher dimensional Einstein-Hilbert action is then given by

$$S_{4+n} = -M_*^{2+n} \int d^{4+n}x \sqrt{g^{(4+n)}} R^{(4+n)}, \tag{2.21}$$

where M_* denotes the fundamental Planck mass, $g^{(4+n)}$ and $R^{(4+n)}$ the $4+n$ dimensional metric respectively Ricci tensor. We now want to know how this is related to the usual 4 dimensional action

$$S_4 = -M_P^2 \int d^4x \sqrt{g^{(4)}} R^{(4)}. \tag{2.22}$$

Especially we are interested in the relation between the fundamental Planck mass M_* and the 4 dimensional one $M_P \sim 10^{19}$ GeV. To do so we take the line element as

$$ds^2 = (\eta_{\mu\nu} + h_{\mu\nu}) dx^\mu dx^\nu - r^2 d\Omega_{(n)}^2, \tag{2.23}$$

where x^μ is the 4-dimensional coordinate, $h_{\mu\nu}$ a small fluctuation around $\eta_{\mu\nu} = \text{diag}(1,-1,-1,-1)$ and $r^2 d\Omega_{(n)}^2$ describes the line element of the XDs. With it the quantities appearing in S_{4+n} can be calculated

$$\sqrt{g^{(4+n)}} = r^n \sqrt{g^{(4)}}, \quad R^{(4+n)} = R^{(4)}. \tag{2.24}$$

This said we can calculate the $4+n$ dimensional action

$$\begin{aligned} S_{4+n} &= -M_*^{2+n} \int d^{4+n}x \sqrt{g^{(4+n)}} R^{(4+n)} \\ &= -M_*^{2+n} \int r^n d\Omega_{(n)} \int d^4x \sqrt{g^{(4)}} R^{(4)} \\ &= M_*^{2+n} V_{(n)} M_P^{-2} S_4, \end{aligned} \tag{2.25}$$

r is the compactification radius and so $V_{(n)} = (2\pi r)^n$ is the volume of the extra dimensions. Requiring the 4-dimensional and $4+n$-dimensional actions to be equal we find the desired relation between the different Planck masses

$$M_P^2 = M_*^{2+n} V_{(n)}. \tag{2.26}$$

Thus the 4 dimensional Planck mass is a derived quantity determinded by the fundamental mass M_* and the volume $V_{(n)}$ of the XDs. For instance having in mind solving the hierarchy problem we could choose $M_* \sim \mathcal{O}(1\,\mathrm{TeV})$. For $n = 1$ we get that the compactification radius of the extra dimensions is $r \sim \mathcal{O}(10^8\,\mathrm{km})$ which is certainly excluded. Taking $n = 2$ we have $r \sim \mathcal{O}(1\,\mathrm{mm})$ what is in the reach of todays Cavendish type experiments [2]. For $n > 3$ the radius needs to be $r < 10^{-6}\,\mathrm{mm}$ which is not going to be reached by gravity experiments any time soon.

In the extra dimensional models fine tuning of the Higgs mass is resolved by lowering the mass scale for new physics: A fundamental mass scale of $\sim 1\,\mathrm{TeV}$ can produce a Planck mass of the actual size. Recently, the interesting features of extra-dimensional models have spurred research in a larger class of models where the extra dimension(s) can be much smaller, of order TeV^{-1}. While these models do not offer a straightforeward solution to the hierarchy problem, they still have many interesting phenomenological consequences, as discussed in section 2.3.4.

2.3 Supersymmetry

As a matter of fact SUSY was not introduced to solve specially the hierarchy problem. As its name suggests it can be constructed by symmetry arguments. The stumbling block was the no-go theorem by Coleman and Mandula [3] which could be rephrased in a non-technical way as [4]:

> The only conserved charges which transform as tensors under the Lorentz group are:
>
> - P_μ, the generators of translation,
> - $M_{\mu\nu}$, the generators of Lorentz transformations.

They obey the following commutation relations:

$$\begin{aligned} &[P_\mu, P_\nu] = 0, \\ &[P_\mu, M_{\rho\sigma}] = i(g_{\mu\rho}P_\sigma - g_{\mu\sigma}P_\rho), \\ &[M_{\mu\nu}, M_{\rho\sigma}] = i(g_{\nu\rho}M_{\mu\sigma} - g_{\nu\sigma}M_{\mu\rho} - g_{\mu\rho}M_{\nu\sigma} + g_{\mu\sigma}M_{\nu\rho}). \end{aligned} \tag{2.27}$$

However there is a possibility to evade the Coleman Mandula theorem, since their argument turns out to not exclude charges which transform under Lorentz transformations as spinors, that is to say as a fermionic field Ψ. We denote such a charge as Q_r where the index r denotes the spinor component. Acting on a state of definite spin $|J\rangle$ we obtain

$$Q_r|J\rangle \sim |J \pm 1/2\rangle. \tag{2.28}$$

Now we already see that this charge switches between states of different spins, that is to say between bosons and fermions. Since these charges are fermionic objects we expect them to obey some sort of anticommutation relations. The commutator $\{Q_r, Q_s\}$ is a symmetric combination of two spin $1/2$ objects and thus of spin 1 — it transforms as a vector under Lorentz transformations. With Q_a the commutator is also a conserved quantity and since it is of bosonic nature, it underlies to the Coleman Mandula theorem. The only vector-like object is P_μ and thus we expect a relation of the form $\{Q_r, Q_s\} \sim P_\mu$.

Let us now abandon this handwaving arguments and just list the SUSY algebra. By convention we choose the charge Q_α to be a two component Weyl spinor. The SUSY algebra then extends the Poincaré algebra by

$$\begin{aligned}
&\{Q_\alpha, Q_\beta\} = \{\bar{Q}_{\dot{\alpha}}, \bar{Q}_{\dot{\beta}}\} = 0,\\
&\{Q_\alpha, \bar{Q}_{\dot{\alpha}}\} = 2\sigma^\mu_{\alpha\dot{\alpha}} P_\mu,\\
&[Q_\alpha, P^\mu] = \left[\bar{Q}_{\dot{\alpha}}, P^\mu\right] = 0,\\
&[Q_\alpha, M^{\mu\nu}] = i(\sigma^{\mu\nu})_\alpha{}^\beta Q_\beta,\\
&\left[\bar{Q}_{\dot{\alpha}}, M^{\mu\nu}\right] = i(\bar{\sigma}^{\mu\nu})^{\dot{\beta}}{}_{\dot{\alpha}} \bar{Q}_{\dot{\beta}}.
\end{aligned} \tag{2.29}$$

$\sigma^\mu_{\alpha\dot{\beta}}$ are the Pauli matrices and $\bar{\sigma}^\mu$ are defined as $\bar{\sigma}^{\mu\,\alpha\dot{\beta}} = \epsilon^{\dot{\alpha}\dot{\beta}}\epsilon^{\alpha\beta}\sigma^\mu_{\beta\dot{\beta}}$ where $\epsilon^{\alpha\beta}$, $\epsilon^{\dot{\alpha}\dot{\beta}}$ are the anisymmetric tensors ($\epsilon^{12} = \epsilon^{\dot{1}\dot{2}} = 1$). Further we use

$$\begin{aligned}
\sigma^{\mu\nu}{}_\alpha{}^\beta &= \frac{1}{4}\left(\sigma^\mu_{\alpha\dot{\alpha}}\bar{\sigma}^{\nu\,\dot{\alpha}\beta} - \sigma^\nu_{\alpha\dot{\alpha}}\bar{\sigma}^{\mu\,\dot{\alpha}\beta}\right),\\
\sigma^{\mu\nu\dot{\alpha}}{}_{\dot{\beta}} &= \frac{1}{4}\left(\bar{\sigma}^{\mu\,\alpha\dot{\alpha}}\sigma^\nu_{\alpha\dot{\beta}} - \bar{\sigma}^{\nu\,\alpha\dot{\alpha}}\sigma^\mu_{\alpha\dot{\beta}}\right).
\end{aligned} \tag{2.30}$$

The one-particle states of a supersymmetric theory fall into irreducible representations of of the SUSY algebra, called supermultiplets. Since a supermultiplet is invariant under Q_α it has to contain bosons and fermions. We list the simplest case (called $N = 1$ supersymmetry) which also will be used to construct the minimal supersymmetric extension to the Standard model (Minimal Supersymmetric Model MSSM):

- **chiral supermultiplet:** [spin 0, spin 1/2]
- **vector supermultiplet:** [spin 1, spin 1/2]

Furthermore one can show that the number of fermionic degrees of freedom n_F matches the number of bosonic degrees of freedom n_B. Under the gauge symmetries the particles in one supermultiplet all have the same quantum numbers for these symmetries. So we have to introduce new particles (i.e. double the particle spectrum): For each SM particle we have to introduce a new one with the same gauge quantum numbers but with spin differing by $\pm 1/2$.

Another problem is that the SUSY generator Q_α commutes with the squared mass operator $P_\mu P^\mu$ what leads immediately to the fact that particles in the same supermultiplet have the same mass. Since we do not observe in nature a bosonic particle with the same mass as a fermionic one we conclude that the vacuum is not invariant under SUSY, i.e. it is spontaneously broken.

2.3.1 Chiral Supermultiplet

We are going to construct a supersymmetric Lagrangian with a Weyl spinor from a top down approach. That means we are just going to state the supersymmetric Lagrangian and transformations in order to see what it typically consists of.

The Lagrangian we are considering consists of complex scalar fields ϕ_i and a left-handed two component Weyl spinors ψ_i:

$$\mathcal{L} = -\partial^\mu \phi^{i*} \partial_\mu \phi_i - \psi^{\dagger i} i\bar{\sigma}^\mu \partial_\mu \psi_i. \tag{2.31}$$

SUSY invariance means that the action $\mathcal{S} = \int d^4x \mathcal{L}$ is invariant under SUSY transformations. Thus the Lagrangian has to be invariant up to a total derivative. This is ensured for the supersymmetry transformation

$$\delta\phi_i = \epsilon\psi_i, \tag{2.32}$$

$$\delta(\psi_i)_r = i(\sigma^\mu \epsilon^\dagger)_r \partial_\mu \phi_i, \tag{2.33}$$

where ϵ is the infinitesimal Weyl spinor of the transformation. One can show that in this case the SUSY algebra only closes if we require the on-shell condition. In order to close the SUSY algebra even off-shell we have to introduce new complex scalar fields F_i, which do not have a kinetic term.[2] The Lagrangian receives in addition a term $F^{i*}F_i$ such that we end with

$$\mathcal{L} = -\partial^\mu \phi^{i*} \partial_\mu \phi_i - \psi^{\dagger i} i\bar{\sigma}^\mu \partial_\mu \psi_i + F^{i*}F_i. \tag{2.34}$$

The transformation rule for ψ_i changes and F_i also transforms under supersymmetry, thus

$$\begin{aligned} \delta(\psi_i)_r &= i(\sigma^\mu \epsilon^\dagger)_r \partial_\mu \phi_i + \epsilon_r F_i, \\ \delta F_i &= i\epsilon^\dagger \bar{\sigma}^\mu \partial_\mu \psi_i. \end{aligned} \tag{2.35}$$

The next step is to introduce interactions with respect both renormalization and invariance under SUSY transformation. The most general interaction Lagrangian respecting this is

$$\begin{aligned} \mathcal{L}_{\text{int}} &= \left(-\frac{1}{2} W^{ij} \psi_i \psi_j + W^i F_i \right) + cc.\,, \\ W^{ij} &= M^{ij} + y^{ijk} \phi_k, \\ W^i &= M^{ij} \phi_j + \frac{1}{2} y^{ijk} \phi_j \phi_k, \\ M^{ij} &= M^{ji}. \end{aligned} \tag{2.36}$$

[2] This can also be exemplified by a handwaving argument: The LHS of transformation (2.33) is a Weyl spinor and thus has four degrees of freedom (DOF) if we do not imply the on-shell condition. The RHS contains a complex scalar field with two DOF. In order to have the same amount of DOF on both sides we have to add a complex scalar field on the RHS such that we have four DOF on both sides.

M^{ij} is a symmetric mass matrix for the fermion fields and y^{ijk} is a Yukawa coupling of a scalar ϕ_k and two fermions ψ_i, ψ_j that must be totally symmetric under interchange of i, j, k. Introducing the *superpotential* $W = \frac{1}{2}M^{ij}\phi_i\phi_j + \frac{1}{6}y^{ijk}\phi_i\phi_j\phi_k$ we can write

$$W^{ij} = \frac{\delta^2 W}{\delta\phi_i\delta\phi_j}, \qquad W^i = \frac{\delta W}{\delta\phi_i}. \tag{2.37}$$

Furthermore we can apply the Euler-Lagrange equation for the axillary field F and obtain the equations of motion

$$F_i = -W_i^*, \qquad F^{*i} = -W^i. \tag{2.38}$$

Thus the field F_i can be expressed in terms of the superpotential of the scalar fields ϕ_i and we end up with

$$\begin{aligned}\mathcal{L}_c = &-\partial^\mu\phi^{*i}\partial_\mu\phi_i - V(\phi,\phi^*) - i\psi^{\dagger i}\bar{\sigma}^\mu\partial_\mu\psi_i,\\ &-\frac{1}{2}\left(M^{ij}\psi_i\psi_j + y^{ijk}\phi_i\phi_j\phi_k + cc.\right).\end{aligned} \tag{2.39}$$

$V(\phi,\phi^*)$ is the scalar potential of the theory obtained from the term $F^{*i}F_i$

$$\begin{aligned}V(\phi,\phi^*) = &M^*_{ik}M^{kj}\phi^{*i}\phi_j + \frac{1}{2}M^{in}y^*_{jkn}\phi_i\phi^{*j}\phi^{*k}\\ &+\frac{1}{2}M^*_{in}y^{jkn}\phi^{*i}\phi_j\phi_k + \frac{1}{4}y^{ijn}y^*_{kln}\phi_i\phi_j\phi^{*k}\phi^{*l}.\end{aligned} \tag{2.40}$$

Since V is a sum of squares ($V = \sum_i |W_i|^2$) it is always non-negative and the potential is automatically bounded from below. It is noteworthy that we obtain *naturally* a scalar potential that looks like the Higgs potential and Yukawa terms for the fermions. Hence we do not have to insert them by hand as we had to in the SM.

2.3.2 Gauge Supermultiplet

The propagating fields in a gauge supermultiplet are a massless gauge boson A^a_μ and a two component Weyl fermion λ^a_r where the index a runs over the adjoint representation of the gauge group and r is the spinor index. The infinitesimal gauge transformations then read

$$\begin{aligned}\delta_g A^a_\mu &= \partial_\mu\Lambda^a + g f^{abc}A^b_\mu\Lambda^c,\\ \delta_g\lambda^a_r &= f^{abc}\lambda^b_r\Lambda^c,\end{aligned} \tag{2.41}$$

where Λ^a is an infinitesimal gauge transformation parameter, g the gauge coupling and f^{abc} the structure constant of the gauge group. Aiming for the SUSY transformation we again have to introduce an auxiliary field: The Weyl fermion λ^a_r has to transform into the vector field A^a_μ. In the general (off-shell) case the former has four DOF and the latter three, thus we have to introduce a real scalar field D^a, which also transforms as an adjoint of the gauge group. Therefore the Lagrangian of the gauge supermultiplet is

$$\mathcal{L}_g = -\frac{1}{4}F^a_{\mu\nu}F^{a\mu\nu} - i\lambda^{a\dagger}\bar{\sigma}^\mu D_\mu\lambda^a + \frac{1}{2}(D^a)^2, \tag{2.42}$$

where $F^a_{\mu\nu}$ is the field strength tensor and D_μ the covariant derivative:

$$\begin{aligned} F^a_{\mu\nu} &= \partial_\mu A^a_\nu - \partial_\nu A^a_\mu + g f^{abc} A^b_\mu A^c_\nu, \\ D_\mu \lambda^a &= \partial_\mu \lambda^a + g f^{abc} A^b_\mu \lambda^c. \end{aligned} \tag{2.43}$$

The SUSY transformations of the fields then are

$$\begin{aligned} \delta A^a_\mu &= \frac{1}{\sqrt{2}} \left(\epsilon^\dagger \bar{\sigma}_\mu \lambda^a + \lambda^\dagger \bar{\sigma}_\mu \epsilon \right), \\ \delta \lambda^a_r &= \frac{i}{2\sqrt{2}} (\sigma^\mu \bar{\sigma}^\nu \epsilon)_r F^a_{\mu\nu} + \frac{1}{\sqrt{2}} \epsilon_r D^a, \\ \delta D^a &= \frac{i}{\sqrt{2}} \left(\epsilon^\dagger \bar{\sigma}^\mu D_\mu \lambda^a - D_\mu \lambda^{a\dagger} \bar{\sigma}^\mu \epsilon \right). \end{aligned} \tag{2.44}$$

The action obtained by integrating $\mathcal{L}$ is indeed invariant under these transformations. Now we are ready to couple the chiral to the gauge supermultiplet.

2.3.3 Coupling a Chiral to an Abelian Supermultiplet

Our goal is to construct a Lagrangian with both chiral and gauge supermultiplets. Let the chiral spinor ψ_i transform under a gauge group in a representation with matrices T^a satisfying $\left[T^a, T^b\right] = i f^{abc} T^c$. Since SUSY and gauge transformations commute, the scalar ϕ_i and auxiliary field F_i must be in the same representation, so

$$\delta_g X_i = i g \Lambda^a (T^a X)_i, \qquad X_i = \psi_i,\, \phi_i,\, F_i. \tag{2.45}$$

In order to have a gauge invariant Lagrangian we have to replace the ordinary derivatives with covariant ones: $\partial_\mu \longrightarrow D_\mu = \partial_\mu - i g A^a_\mu T^a$. This achieves the coupling of the vector boson of the gauge supermultiplet A^a_μ with the scalars ϕ_i and fermions ψ_i of the chiral supermultiplet. Therefore it makes sense that the gaugino λ^a and the axillary field D^a also couple to the chiral fermions and scalars. In fact the only renormalizable interaction terms are

$$(\phi^* T^a \psi)\lambda^a, \quad \lambda^{a\dagger} (\psi^\dagger T^a \phi), \quad (\phi^* T^a \phi) D^a. \tag{2.46}$$

The couplings for these terms have to be chosen such that the Lagrangian stays invariant up to a total derivative. The SUSY transformations for the gauge supermultiplet stay the same as (2.44) and the transformations for the chiral supermultiplet have to be altered to

$$\begin{aligned} \delta \phi_i &= \epsilon \psi_i, \\ \delta (\psi_i)_r &= i (\sigma^\mu \epsilon^\dagger)_r D_\mu \phi_i + \epsilon_r F_i, \\ \delta F_i &= i \epsilon^\dagger \bar{\sigma}^\mu D_\mu \psi_i + \sqrt{2} g (T^a \phi)_i \epsilon^\dagger \lambda^{a\dagger}. \end{aligned} \tag{2.47}$$

As a matter of fact these are the familiar transformations (2.32), (2.35) where we have replaced the ordinary derivatives by covariant ones and added an extra term to δF_i. The SUSY-invariant Lagrangian containing gauge and chiral supermultiplets and the interactions (2.46) is

$$\mathcal{L} = \mathcal{L}_c + \mathcal{L}_g - \sqrt{2} g (\phi^* T^a \psi)\lambda^a - \sqrt{2} g \lambda^{a\dagger} (\psi^\dagger T^a \phi) + g (\phi^* T^a \phi) D^a. \tag{2.48}$$

For the pure gauge supermultiplet Lagrangian (2.42), the equation of motion for the D^a-field results in $D^a = 0$. However now the last term of (2.48) gives us the following equation of motion

$$D^a = -g(\phi^* T^a \phi). \tag{2.49}$$

As before with the fields F_i we can express the fields D^a in terms of the scalar fields ϕ and add to the scalar potential (2.40). So we end with

$$V(\phi, \phi^*) = F^{i*} F_i + \frac{1}{2} \sum_a (D^a)^2 = W_i^* W^i + \frac{1}{2} \sum_a g_a^2 (\phi^* T^a \phi)^2. \tag{2.50}$$

The first term is called "F-term" and the second one "D-term". The former contains Yukawa couplings and mass terms, the latter consists of gauge couplings.

2.3.4 The Minimal Supersymmetric Standard Model

So far we have presented the SUSY framework, now we have to insert the SM particles and their superpartners. Since all particles in one supermultiplet must have the same gauge quantum numbers we cannot construct supermultiplets from SM particles alone. Thus to each SM particle we have to introduce a new superpartner. As already mentioned the particles are aligned in chiral supermultiplets (spin 0, spin 1/2) or gauge supermultiplets (spin 1, spin 1/2). All SM fermions are members of the former. Since the left- and right-handed components transform differently under $SU(2)$ we have to treat the the two parts as different particles with their own partners. The names of the scalar superpartners are constructed by prepending an "s" (e.g. the superpartner of a *quark* is called *squark*). The symbols of the sfermions are the same as for the corresponding fermions, but with a tilde (e.g. the superpartner of the left-handed electron e_L is denoted by $\tilde{e}_L$)[3]. A further chiral supermultiplet consists of the (spin-0) Higgs and (spin-1/2) higgsino. As we will see later there have to be two Higgs supermultiplets denoted as $(\tilde{H}_u, H_u)$ and $(\tilde{H}_d, H_d)$ with weak hypercharges $Y = 1/2$, $Y = -1/2$. The SM gauge bosons are aligned together with their partners in gauge supermultiplets. Similarly, the names of the spin-1/2 superpartners are obtained by appending "-ino" to the name of the SM particle (e.g. gluon - gluino). The whole particle spectrum is presented in tables 2.2 and 2.3.

Further we have to construct the superpotential W, where we have the restriction that it has to be invariant under gauge transformations. The MSSM consists of the choice

$$W = \tilde{\bar{u}} \mathbf{y_u} \tilde{Q} \tilde{H}_u - \tilde{\bar{d}} \mathbf{y_d} \tilde{Q} \tilde{H}_d - \tilde{\bar{e}} \mathbf{y_e} \tilde{L} \tilde{H}_d + \mu \tilde{H}_u \tilde{H}_d. \tag{2.51}$$

We have suppressed all of the gauge and family indices. For example the first term can be written out as $\tilde{\bar{u}}^{ia} (\mathbf{y_u})_i^j \tilde{Q}_{j\alpha a} (\tilde{H}_u)_\beta \epsilon^{\alpha\beta}$ where i, j are the family indices, α, β the $SU(2)$ indices and a the color index. The dimensionless Yukawa couplings $\mathbf{y_u}$ are 3×3 matrices in family space. The different Yukawa and interaction terms are then obtained with (2.51). Since W has to be an analytic

[3] One has to keep in mind that the index L in $\tilde{e}_L$ has nothing to do with the helicity of the selectron (it is a spin-0 particle and has no helicity). In fact $\tilde{e}_L$ and $\tilde{e}_R$ are completely different particles.

Name		spin 0	spin 1/2	$SU(3)$, $SU(2)$, $U(1)$
squarks, quarks	Q	$(\tilde{u}_L, \tilde{d}_L)$	(u_L, d_L)	$(\mathbf{3}, \mathbf{2}, \frac{1}{6})$
	$\bar{u}$	$\tilde{u}_R^*$	u_R^*	$(\bar{\mathbf{3}}, \mathbf{1}, -\frac{2}{3})$
	$\bar{d}$	$\tilde{d}_R^*$	$d_R^\dagger$	$(\bar{\mathbf{3}}, \mathbf{1}, \frac{1}{3})$
sleptons, leptons	L	$(\tilde{\nu}_L, \tilde{e}_L)$	(ν_L, e_L)	$(\mathbf{1}, \mathbf{2}, -\frac{1}{2})$
	$\bar{e}$	$\tilde{e}_R^*$	$e_R^\dagger$	$(\mathbf{1}, \mathbf{1}, 1)$
Higgs, higgsinos	H_u	(H_u^+, H_u^0)	$(\tilde{H}_u^+, \tilde{H}_u^0)$	$(\mathbf{1}, \mathbf{2}, \frac{1}{2})$
	H_d	(H_d^0, H_u^+)	$(\tilde{H}_d^0, \tilde{H}_d^+)$	$(\mathbf{1}, \mathbf{2}, -\frac{1}{2})$

Table 2.2: Chiral supermultiplets

Name	spin 1/2	spin 1	$SU(3)$, $SU(2)$, $U(1)$
gluino, gluon	$\tilde{g}$	g	$(\mathbf{8}, \mathbf{1}, 0)$
winos, W bosons	$\tilde{W}^\pm$, $\tilde{W}^0$	$W^\pm$, W^0	$(\mathbf{1}, \mathbf{3}, 0)$
bino, B boson	$\tilde{B}^0$	B^0	$(\mathbf{1}, \mathbf{1}, 0)$

Table 2.3: Gauge supermultiplets

function of the scalar fields we cannot add terms like $\tilde{u}\tilde{Q}\tilde{H}_d^*$. In order to have Yukawa terms for up- and down-quarks (and thus masses) we need two different Higgs fields with $Y = \pm 1/2$.

For the superpotential we have not taken into account terms violating lepton (L) or baryon number (B). Therefore one adds a new symmetry to the MSSM which eliminates the possibility of any B- and L-violating terms, which is called "R-parity". R-parity is a multiplicatively conserved quantum number defined as

$$P_R = (-1)^{3(B-L)+2s}, \tag{2.52}$$

where s is the spin of the particle. Now, all SM particles have R-parity $P_R = +1$ and all SUSY particles have $P_R = -1$. Thus every interaction vertex has to contain an even number of SUSY particles. This has important phenomenological consequences:

- The lightest supersymmetric particle (LSP) must be absolute stable. Thus every sparticle other than the LSP decays to an odd number of LSPs. If the LSP is electrically neutral, it interacts only weakly with SM particles and is an attractive dark matter (DM) candidate.
- In collider experiments sparticles can only be produced pairwise.

2.3.5 Supersymmetry Breaking

Since no sparticle has yet been detected, they have to be more massive and thus SUSY has to be broken. From a theoretical point of view the most elegant way is to break SUSY spontaneously. That means that a vacuum state $|0\rangle$ is not invariant under transformations Q_α: $Q_\alpha|0\rangle \neq 0$. From eq. (2.29) it follows for the Hamiltonian H

$$H = P_0 = \frac{1}{4}(Q_1 Q_1^\dagger + Q_1^\dagger Q_1 + Q_2 Q_2^\dagger + Q_2^\dagger Q_2). \tag{2.53}$$

Thus, if the vacuum state is not invariant under SUSY transformations, the vacuum has positive energy:

$$\langle 0|H|0\rangle = \frac{1}{4}(\|Q_1^\dagger|0\rangle\|^2 + \|Q_1|0\rangle\|^2 + \|Q_2^\dagger|0\rangle\|^2 + \|Q_2|0\rangle\|^2) > 0. \tag{2.54}$$

Assuming the kinetic terms don't contribute in the vacuum, we can write $\langle 0|H|0\rangle = \langle 0|V|0\rangle$, where V is the scalar potential (2.50). Thus in order to break SUSY spontaneously F_i and D^a must not vanish simultaneously in the vacuum. So spontaneous SUSY breaking can be achieved by constructing models in which $F_i = 0$ and $D^a = 0$ cannot hold for any field values simultaneously. This leads to the two *Fayet-Ilipopoulos* (D-term) [5] and *O'Raifeartaigh* (F-term) [6] breaking mechanisms.

As a matter of fact, simple D-term SUSY breaking models do not agree with phenomenological data and F-term SUSY breaking requires us to extend the MSSM. Therefore we need a heavier particle sector where SUSY is spontaneously broken. This "hidden" sector and the "visible sector" of the MSSM do share some interactions such that SUSY breaking can be communicated down to the MSSM sector. There are two major candidates: *Planck-scale-mediated* and *gauge-mediated* SUSY breaking (GMSB).

In the former the SUSY breaking sector connects with the MSSM sector through non-renormalizable terms suppressed by powers of the Planck mass. If the F-term of the hidden sector then acquires a VEV they constitute the MSSM mass terms. On the other hand in GMSB models the ordinary gauge interactions are responsible for the transport of SUSY breaking down to the MSSM sector. This transport is provided by some new chiral supermultiplets, called messengers, that couple to the breaking sector and indirectly to the MSSM sector through ordinary $SU(3) \times SU(2) \times U(1)$ gauge interactions. Gauginos get their masses through one-loop Feynman graphs involving virtual messenger particles, scalar particles acquire their masses in leading order through two-loop Feynman graphs. The LSP in GMSB is the gravitino ($\tilde{G}$). Thus the next-lightest SUSY particle decays into $\tilde{G}$, however, its lifetime is very model dependent ($\mathcal{O}(\mu\text{m}) < c\tau < \mathcal{O}(\text{km})$).

Since we do not know how SUSY breaking exactly should be done, it is very useful to just introduce extra terms that break SUSY explicitly. As we have seen unbroken SUSY resolves the hierarchy problem by introducing scalars to each spinor field and vice versa. Furthermore the dimensionless couplings have to stay the same as it is required below (2.20). Thus the effective SUSY breaking terms contain only couplings parameters with positive mass dimension and scale of $\mathcal{O}(\text{TeV})$, the Lagrangian is called to be *softly* broken.

2.3.6 Some Selected Phenomenological Aspects

SUSY Mass Spectrum

In the MSSM there are 33 masses corresponding to undiscovered particles (including the gravitino). Assuming a specific SUSY breaking model one can compute the masses in terms of few parameters[4]. A further important point is that the higgsinos and charginos in the MSSM Lagrangian are no mass eigenstates:

[4] For instance the simplest gauge-mediated SUSY breaking model needs 6 parameters to predict masses

The neutral higgsinos ($\tilde{H}_u^0$, $\tilde{H}_d^0$) and neutral gauginos ($\tilde{B}$, $\tilde{W}^0$) mix to mass eigenstates called neutralinos ($\tilde{\chi}_i^0$, $i = 1, 2, 3, 4$) and the charged higgsinos ($\tilde{H}_u^+$, $\tilde{H}_d^-$) and gauginos ($\tilde{W}^\pm$) form mass eigenstates with charge ± 1 and are called charginos ($\tilde{\chi}_i^\pm$, $i = 1, 2$). Generally sleptons and squarks do also appear in mixed mass eigenstates. This implies however flavor mixing and/or CP-violation that is severely restricted by experiment. In GMSB, sfermion flavor mixing and CP phases are highly suppressed and the first two families (up, down, strange, charm respectively electrons and muons) do not mix, only the third family mix the fields ($\tilde{t}_L$, $\tilde{t}_R$, $\tilde{b}_L$, $\tilde{b}_R$) to ($\tilde{t}_1$, $\tilde{t}_2$, $\tilde{t}_3$, $\tilde{t}_4$) and ($\tilde{\tau}_L$, $\tilde{\tau}_R$, $\tilde{\nu}_\tau$) to ($\tilde{\tau}_1$, $\tilde{\tau}_2$, $\tilde{\nu}_\tau$) respectively.

Our later analysis will be based on the G1a parameter point of [7], where some phenomenological aspects of GMSB are discussed.

Sparticle	mass [GeV]	Sparticle	mass [GeV]
$\tilde{g}$	747		
$\tilde{\chi}_1^\pm$	223	$\tilde{\chi}_2^\pm$	469
$\tilde{\chi}_1^0$	119	$\tilde{\chi}_2^0$	224
$\tilde{\chi}_3^0$	451	$\tilde{\chi}_4^0$	570
$\tilde{u}_L$	986	$\tilde{u}_R$	942
$\tilde{d}_L$	989	$\tilde{d}_R$	939
$\tilde{t}_1$	846	$\tilde{t}_2$	962
$\tilde{b}_1$	935	$\tilde{b}_2$	945
$\tilde{e}_L$	326	$\tilde{e}_R$	164
$\tilde{\nu}_e$	317	$\tilde{\tau}_2$	326
$\tilde{\tau}_1$	163	$\tilde{\nu}_\tau$	316
h^0	110	H^0	557
A^0	555	$H^\pm$	562

Table 2.4: Masses of sparticles, in GeV, for the G1a point of [7]. Note that the first and second generation squarks and sleptons are degenerate and thus are not listed separately .

2.4 Universal Extra Dimensions

In universal extra dimensions (UED) [8] space-time consists of a 4-dimensional Minkowski space and d compactified dimensions. In the simplest case we have one additional dimension that is compactified to a circle. The total space-time would then be understood to be the usual Minkowski space where at each point a circle is placed. In contrast to other ED-models in UED all SM fields do propagate in this $4 + d$-dimensional space. A 4-dimensional theory in the low-energy limit is obtained by integrating over the d dimensions. Let us study this for the simple case of one extra dimension compactified on a circle of radius R. Later we will see that compactifying on a circle will not lead to chiral fermions. In order to get a chiral theory we will have to compactify on a circle where the opposed points are identified.

2.4.1 Scalar Fields

The action S for a real scalar field ϕ in five flat dimensions is

$$S[\phi] = \frac{1}{2}\int d^4x dy \left(\partial^A \phi \partial_A \phi - m^2\phi^2\right), \tag{2.55}$$

where the index A goes from 0 to $3+d=4$ and y denotes the compactified dimension. The compactness of the fifth dimension is reflected in the periodicity of the field: $\phi(y) = \phi(y+2\pi)$. Thus we can expand the fifth dimension in Fourier modes

$$\phi(x,y) = \frac{1}{\sqrt{2\pi R}}\phi_0(x) + \sum_{n=1}^{\infty}\frac{1}{\sqrt{\pi R}}\left[\phi_n(x)\cos\left(\frac{ny}{R}\right) + \hat{\phi}_n(x)\sin\left(\frac{ny}{R}\right)\right]. \tag{2.56}$$

The first term ϕ_0 is called the zero mode, the other Fourier modes ϕ_n and $\hat{\phi}_n$ are called the n^{th} Kaluza-Klein (KK) modes. Plugging this expansion into the action S gives

$$S[\phi] = \sum_{n=0}^{\infty}\frac{1}{2}\int d^4x\left(\partial^\mu\phi_n\partial_\mu\phi_n - m_n^2\phi_n^2\right) + \sum_{n=1}^{\infty}\frac{1}{2}\int d^4x\left(\partial^\mu\hat{\phi}_n\partial_\mu\hat{\phi}_n - m_n^2\hat{\phi}_n^2\right), \tag{2.57}$$

where the KK-mass is given by $m_n^2 = m^2 + n^2/R^2$. Thus in the effective theory we end up with a infinite tower of fields with masses m_n (spin and all quantum numbers stay the same) whereas the odd fields have no zero mode.

2.4.2 Spinor Fields

For the spinor fields we first have to write down the five dimensional representation of the Poincare algebra Γ^M where $\{\Gamma^M, \Gamma^N\} = 2\eta^{MN}$. Now the algebra involves more matrices than in four dimensions:

$$\Gamma^\mu = \gamma^\mu \text{ and } \Gamma^4 = i\gamma_5. \tag{2.58}$$

Analogously spinors Ψ are elements of the five dimensional representation space. The Dirac equation for massless fermions is $i\partial_M\Gamma^M\Psi(x,y) = 0$. Further γ_5 is the only matrix that anticommutes with all γ^μ and satisfies $(\gamma_5)^2 = \mathbf{1}$. Since γ_5 is now included in the five dimensional Clifford algebra one cannot define chiral spinors anymore. We will fix that by choosing a different compactification manifold - namely $U(1)/Z_2$ - that is a circle where the opposed points are identified. The action for a massless fermion is

$$S = \int d^4x dy i\bar{\Psi}\Gamma^A\partial_A\Psi = \int d^4x dy\left[i\bar{\Psi}\gamma^\mu\partial_\mu\Psi + \bar{\Psi}\gamma_5\partial_y\Psi\right]. \tag{2.59}$$

The spinor field can be decomposed in Fourier modes

$$\begin{aligned}\Psi(x,y) =& \frac{1}{\sqrt{2\pi R}}\Psi^{(0)}(x) \\ &+ \sum_{n=1}^{\infty}\frac{1}{\sqrt{\pi R}}\left[\Psi^{(n)}(x)\cos\left(\frac{ny}{R}\right) + \hat{\Psi}^{(n)}(x)\sin\left(\frac{ny}{R}\right)\right].\end{aligned} \tag{2.60}$$

Plugging this expansion into eq. (2.59) gives us

$$S = \int d^4x \Bigg\{ i\bar{\Psi}^{(0)}\gamma^\mu \partial_\mu \Psi^{(0)} + i\sum_{n=1}^{\infty} \Bigg[\bar{\Psi}^{(n)}\gamma^\mu \partial_\mu \Psi^{(n)} + \bar{\hat{\Psi}}^{(n)}\gamma^\mu \partial_\mu \hat{\Psi}^{(n)} + \frac{n}{R}\left(\bar{\Psi}^{(n)}\gamma_5 \hat{\Psi}^{(n)}\right) \Bigg] \Bigg\}. \tag{2.61}$$

Since we cannot define projector operators anymore the theory consists of 4-component spinors. Now if we choose to compactify the fifth dimension on $U(1)/Z_2$ we have to identify y and $-y$ and impose that the Lagrangian is invariant under the transformation $P(\Psi)(x^\mu, y) = \Psi(x^\mu, -y)$: $\mathcal{L}(x^\mu, y) = \mathcal{L}(x^\mu, -y)$. In order to ensure the invariance of the Lagrangian the spinor fields have to transform as $P(\Psi)(x^\mu, y) = \gamma^5 \Psi(x^\mu, y)$. Writing $\Psi = \binom{\psi_R}{\psi_L}$ gives us the following relation for the two component spinors $\psi_{L/R}$:

$$P(\psi_L) = \psi_L, \quad P(\psi_R) = -\psi_R. \tag{2.62}$$

If we now write out the Fourier decomposition of the Weyl spinors and impose the above constraints we get

$$\begin{aligned} \psi_L(x^\mu, y) =& \frac{1}{\sqrt{2\pi R}}\psi_L^{(0)}(x) + \sum_{n=1}^{\infty} \frac{1}{\sqrt{\pi R}}\psi_L^{(n)}(x)\cos\left(\frac{ny}{R}\right), \\ \psi_R(x^\mu, y) =& \sum_{n=1}^{\infty} \frac{1}{\sqrt{\pi R}}\psi_R^{(n)}(x)\sin\left(\frac{ny}{R}\right) \end{aligned} \tag{2.63}$$

Thus the right-handed spinor component has no zeroth mode and therefore at lowest mode level the theory appears as if fermions were chiral. Analogously if we want to compactify the scalar field on $U(1)/Z_2$ we have to assign the parity transformation $P(\Phi)(x^\mu, y) = \pm\Phi(x^\mu, y)$. Even (odd) fields are only expanded into cosine (sine) modes, thus the KK spectrum has only half of the modes and odd fields have no zero modes and thus do not appear in the low energy theory.

2.4.3 Gauge Fields

For simplicity we will only consider the case of a free gauge Abelian theory. As usual the Lagrangian in five dimensions is

$$S = -\int d^4x dy \frac{1}{4} F_{MN}F^{MN} = \int d^4x dy \left\{ -\frac{1}{4}F_{\mu\nu}F^{\mu\nu} + \frac{1}{2}F_{\mu 5}F^{\mu 5} \right\} \tag{2.64}$$

where $F_{MN} = \partial_M A_N - \partial_N A_M$ and A_M is the five component vector field. Again we proceed by writing out the Fourier decomposition of the gauge field

$$\begin{aligned} A_M(x^\mu, y) = \frac{1}{\sqrt{2\pi R}}A_M^{(0)}(x^\mu) + \sum_{n=1}^{\infty} \frac{1}{\sqrt{\pi R}} \Bigg[& A_M^{(n)}(x^\mu)\cos\left(\frac{ny}{R}\right) \\ & + A_M^{(n)}(x^\mu)\sin\left(\frac{ny}{R}\right) \Bigg]. \end{aligned} \tag{2.65}$$

Furthermore we can use that the Lagrangian is invariant under gauge transformations $A_M \to A_M + \partial_M \Lambda(x^\mu, y)$. After inserting the above expansion into

(2.64) and compactifying on a circle one can choose a gauge such that the scalars $A_5^{(n)}$ vanish for $n \geq 1$ and only the zero component $A_5^{(0)}$ remains.

$$S = \int d^4x \Bigg\{ \sum_{n=0}^{\infty} \left[-\frac{1}{4} F_{\mu\nu}^{(n)} F^{(n)\mu\nu} + \frac{1}{2} \left(\frac{n}{R}\right)^2 A_\mu^{(n)} A^{(n)\mu} + \frac{1}{2} \left(\partial_\mu A_5^{(0)}\right)^2 \right] + (\text{odd modes}) \Bigg\} \tag{2.66}$$

Now all the KK modes acquire mass by absorbing the scalars $A_5^{(n)}$, only the zero mode stays massless. The last term represents a massless scalar field. Nevertheless, compactifying on a $U(1)/Z_2$ orbifold the extra degree of freedom $A_5^{(0)}$ can be projected out, since $A_5^{(0)}$ can be chosen to be an odd function under y parity P.

2.4.4 Two Extra Dimensions and their Phenomenology

Until now we have just considered a simple model of one extra dimension. However later on we will examine two universal extra dimensions (2UED) [9, 10]. Here we will state some phenomenological consequences. Now the gauge fields have six components. Thus corresponding to each KK vector boson we have two additional fields. As in the five dimensional case one field gets eaten up to give the KK gauge bosons mass. The other degree of freedom represents a physical spin-0 particle transforming in the adjoint representation of the gauge group, thus it is called *spinless adjoint* and denoted as $A_H^{(m,n)}$ for the (m,n)th KK mode of the gauge field $A_\mu^{(m,n)}$. Since two extra dimensions have been compactified the EP now carry two indices (m,n). In our later analysis we will concentrate on the $(0,1)$ KK-mode and simply denote it as the (1) mode.

Another important point is that momentum conservation in the compactified dimensions leads to what we call *KK-parity* conservation. KK-parity can simply be written as $P = (-1)^{(m+n)}$ where (m,n) denote the (m,n)th KK mode. This has similar consequences as R-parity conservation in SUSY:

- The lightest level-one KK particle (LKP) is stable and is a suitable DM candidate;
- Odd level KK modes (especially the first one) can only be produced in pairs.

Finally we present the mass spectrum of the first KK level. At tree-level the masses of KK particles m_{KK} are

$$m_{\text{KK}}^2 = \frac{1}{R^2} + m_{\text{SM}}^2 \tag{2.67}$$

where m_{SM} is the mass of the Standard Model particle and R the compactification radius. This suggests a high degeneracy for the KK excitations of light SM particles. However, the radiative corrections [11] to the KK-masses are often much larger that the SM masses themselves. Without going through the calculations we list the first KK level masses from [12, 13] in table 2.5. Further phenomenological aspects of 2UED can be found in [12].

SM particle	KK excitation	MR
3rd generation quarks	$Q_+^{(1)3}$	$1.265 + \frac{1}{2}(m_t R)^2$
top quark	$T_-^{(1)}$	$1.252 + \frac{1}{2}(m_t R)^2$
1/2nd generation quarks	$Q_+^{(1)}$	1.247
up/strange quark	$U_-^{(1)}$	1.216
down/charm quark	$D_-^{(1)}$	1.211
leptons	$L_+^{(1)}$	1.041
leptons	$E_-^{(1)}$	1.015
Gluon	$G_\mu^{(1)}$	1.392
W boson	$W_\mu^{(1)}$	$1.063 + \frac{1}{2}(M_W R)^2$
B boson	$B_\mu^{(1)}$	0.974
	$G_H^{(1)}$	1.0
	$W_H^{(1)}$	$0.921 + \frac{1}{2}(M_W R)^2$
	$B_H^{(1)}$	0.855

Table 2.5: The + and − subscripts denote the six dimensional chirality. + containt left-handed and − the right handed zero modes. In the later analysis we use the compactification radius $R^{-1} = 500\ \mathrm{GeV}^{-1}$.

Chapter 3

Discrimination

There are a lot of similarities between the two different models 2UED and GMSB (including the graviton). The most important ones are:

- Both extensions predict at least one "partner" - let us call them extra particles (EP) - to the existing SM particles.
- Due to R-/KK-parity these EP can only interact in pairs.
- The lightest EP is stable and neutral (lightest stable neutral particle LSNP). Thus it is a valid DM candidate. In the detector events containing EP will have missing energy as the LSNP escapes the detector.

However, there are also some important differences:

- In 2UED scenarios the masses are very degenerate whereas in GMSB scenarios the masses are less degenerate.
- The spins of the EP differ by 1/2 to the SM particles for SUSY whereas for 2UED models the spins stay the same.

More phenomenological aspects of GMSB and 6-dimensional 2UED can be found in [7] and [12] respectively.

Thus there are in principle two possibilities to distinguish 2UED and GMSB. The first is to measure the masses of the EP. The fact that events containing EP have missing energy helps to separate them from the SM background. On the other hand it makes mass (and spin) measurements more complicated since it is impossible to reconstruct the momentum and therefore the restframes of the decaying particles. However, invariant mass distributions from the visible particles in a decay chain do depend on the masses of the decaying particles and through end-point analyses it is possible to extract the masses of the intermediate particles [14].

Although the EP masses can give a hint about the nature of the extension of the SM, they give no clear answer. For instance the nature of SUSY breaking and thus the SUSY masses are widely unknown. To get a deeper insight one has to measure the spins of the intermediary EPs. In the past attention has been concentrated on decays containing a quark and a dilepton pair of the same family and opposite charge. In a SUSY scenario that would be evoked by the decay chain $\tilde{q}_L \rightarrow \tilde{\chi}_2^0\ q_L \rightarrow \tilde{l}_R^{\pm}\ l_n^{\mp} q_L \rightarrow \tilde{\chi}_1^0\ l_f^{\pm}\ l_n^{\mp}\ q_L$. The first emitted lepton is

called *near* and the second one *far* lepton, thus the indices n and f. In a UED scenario the same decay products are caused by a decay $Q_+^{(1)} \to Z^{(1)}\ q_L \to L^{(1)}\ l_n^{\mp} q_L \to A^{(1)}\ l_f^{\pm}\ l_n^{\mp}\ q_L$. Spin determination for these decay chains has been studied by [1, 15, 16, 17, 18][1].

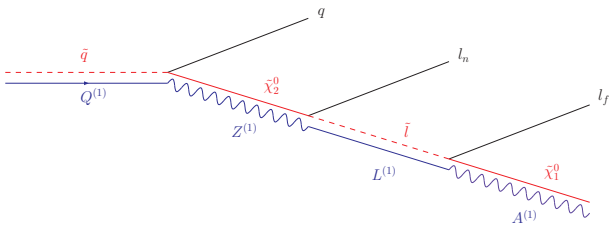

Figure 3.1: SUSY (red) and 2UED (blue) decay chains with observable final state $q\ l^+\ l^-\not{E}_T$

However [21] pointed out that GMSB models with the gravitino as LSP the next-lightest SUSY particle (NLSP) decays into a gravitino by emitting a photon. Thus one has the decay chain $\tilde{\chi}_2^0 \to \tilde{l}_R^{\pm}\ l_n^{\mp} \to \tilde{\chi}_1^0\ l_f^{\pm}\ l_n^{\mp} \to \tilde{G}\ \gamma\ l_f^{\pm}\ l_n^{\mp}$. In 2UED one can construct an analogous decay chain where the KK hypercharge boson decays into a spinless adjoint and a photon: $Z^{(1)} \to L^{(1)}\ l_n^{\mp} \to A^{(1)}\ l_f^{\pm}\ l_n^{\mp} \to A_H^{(1)}\ \gamma\ l_f^{\pm}\ l_n^{\mp}$ [12]. We will refer to them as *long* decay chains.

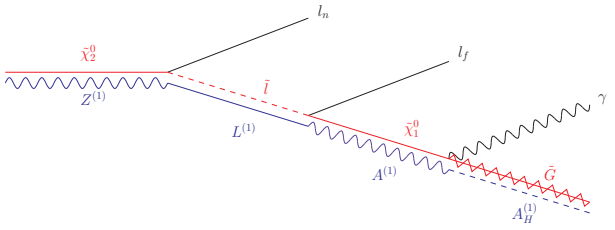

Figure 3.2: GMSB (red) and 2UED (blue) decay chains with observable final state $l^+\ l^-\ \gamma\ \not{E}_T$

Other decay chains revealing information about the spin of the intermediate particle are $\tilde{q}_R \to q_R\ \chi_1^0 \to q_R\ \gamma\ \tilde{G}$ and $Q_-^{(1)} \to q_R\ \gamma\ A^{(1)}$ respectively which we will be referring to as *short* decay chains. Although they have a considerably bigger SM background at the LHC they also have a larger branching ratio.

In this thesis we will focus on the *long* and *short* decay chains to discriminate between GMSB and 2UED models or generally speaking to study the effect of spin correlations.

3.1 General Thoughts about Spin Correlations in Cascade Decays

In this section we review decay probabilities and their angular distributions for decays of scalars, fermions and gauge bosons based on [17]. These will serve as

[1] Other methods of spin determination can be found in [19, 20].

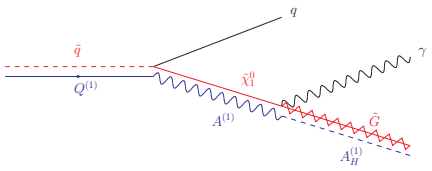

Figure 3.3: GMSB (red) and 2UED (blue) decay chains with observable final state $q_L\ \gamma\ \not{E}_T$

building blocks in our understanding of spin correlations of the above cascade decays.

Scalar Decay

Since a scalar particle has no spin it does not pick any special direction in space and its decay is isotropic in its rest frame.

Fermion Decay

In the simplest case a fermion ψ_1 decays to a fermion ψ_2 and a scalar ϕ through the interaction $\bar{\psi}_2\Gamma\psi_1\phi$. If the coupling is chiral Γ is a linear combination of P_L and P_R, otherwise if it is non-chiral, it is proportional to some constant. Since the decaying fermion has a spin it picks a direction in space and the decay may be anisotropic. However this is only the case if the decaying fermion is polarized and the coupling chiral. To show that we will have to calculate the associated decay rates where we will refer to the notation of [22].

Let us assume the incoming particle to have spin up in its rest frame and the coupling to be left-handed. If its spin is aligned along the z-axis the spinor is

$$u^\dagger_{\psi_1} \propto (0,1,0,1)\,. \tag{3.1}$$

If the outgoing fermion ψ_2 is boosted it is mostly right-handed and its spinor then is

$$u^\dagger_{\psi_2} \propto (0,0,1,0)\,, \tag{3.2}$$

if ψ_2 moves along the z-axis. To describe the decaying fermion in this coordinate frame we have to rotate it by the angle θ:

$$u_{\psi_1} \propto \begin{pmatrix} 0\\1\\0\\1 \end{pmatrix} \to \begin{pmatrix} \cos\frac{\theta}{2} & -\sin\frac{\theta}{2} & 0 & 0\\ \sin\frac{\theta}{2} & \cos\frac{\theta}{2} & 0 & 0\\ 0 & 0 & \cos\frac{\theta}{2} & -\sin\frac{\theta}{2}\\ 0 & 0 & \sin\frac{\theta}{2} & \cos\frac{\theta}{2} \end{pmatrix} \begin{pmatrix} 0\\1\\0\\1 \end{pmatrix} = \begin{pmatrix} \sin\frac{\theta}{2}\\ \cos\frac{\theta}{2}\\ \sin\frac{\theta}{2}\\ \cos\frac{\theta}{2} \end{pmatrix}. \tag{3.3}$$

The matrix element therefore has the form

$$\mathcal{M} \propto (0,0,1,0)\,\gamma^0 \begin{pmatrix} \sin\frac{\theta}{2}\\ \cos\frac{\theta}{2}\\ \sin\frac{\theta}{2}\\ \cos\frac{\theta}{2} \end{pmatrix} = \sin\frac{\theta}{2}, \tag{3.4}$$

and the squared matrix element is proportional to $\sin^2\frac{\theta}{2}$. A similar calculation shows that the squared matrix element for a inverse polarized fermion is $\propto \cos^2\frac{\theta}{2}$.

Thus if the decaying particle ψ_1 is not polarized the angular dependences cancel and the decay is indeed isotropic. Exactly the same thing happens if the coupling is non-chiral.

In an analogous manner one can show for the decay of a fermion in a fermion and gauge boson that one only has angular dependences if the decaying particle is polarized and the coupling chiral. Further we note that there is no angular dependence between the fermions and the gauge boson/scalar.

Gauge Boson Decay

In general the decay of a gauge boson shows angular dependence. For instance the decay rate of a transversal gauge boson is proportional to $1 + \cos^2\theta$.

Comparing the Decay Chains

In the GMSB case the first decay is $\tilde{\chi}_2^0 \to l_n\, \tilde{l}$. As we have mentioned before, there is no angular dependence between the scalar and the near lepton. Since the scalar decays isotropically there is no angular dependence between the two leptons. The last coupling between the neutralino, graviton and photon [23, 24] in momentum space is written down in figure 3.4. Since this coupling is non-

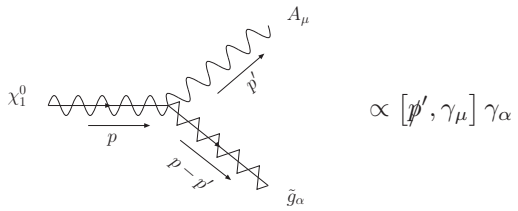

Figure 3.4: Neutralino-gravitino-photon vertex from [25], Appendix A.

chiral, spin-effects between the photon and the far lepton (and so also between the photon and the near lepton) are absent. Thus in the complete decay chain only the phase space contribution plays a role. That is also seen when we calculate the matrix element for this decay chain, it is not dependent of the angles between the near/far lepton and the photon.

On the other hand, the 2UED decay chain has potential angular dependences between all outgoing particles. Thus in this case the matrix element will play an important role in calculating the invariant mass distributions.

Chapter 4

Invariant Mass Distributions

Our aim is to obtain analytical expressions for the invariant mass distributions of the cascade decays discussed in the previous chapter and to check whether spin effects can be measured at the LHC. Analytical expressions have already been obtained for the decay chains $E \to D\ q \to C\ l_n\ q \to B\ l_f\ l_n\ q$, where E, D, C and B are the new particles belonging to the particular SM extension, in [26]. In [15] invariant mass distributions neglecting the spin contributions are calculated at full length. We take their calculations as a base and extend them with the spin correlations of the *long* decay chain involving a photon $D \to C\ l_n \to B\ l_n\ l_f \to A\ l_n\ l_f\ \gamma$. Further we calculate invariant mass distributions for the *short* decay chain $C \to B\ q \to A\ q\ \gamma$.

There are two possibilities to calculate invariant mass distributions with one photon and one lepton — the far-lepton–photon and the near-lepton–photon mass distribution. However since one cannot distinguish the near and far lepton one can only measure the sum of these two distributions. Another possibility is to build observable distributions by taking the maximum/minimum invariant lepton-photon mass giving us the high/low lepton-photon invariant mass distribution.

For the sake of completeness we consider all different spin configurations by interchanging vector bosons through scalars and vice-versa, leading to the different decay chains displayed in figure 4.1. The spin configurations FSFG/VFVS correspond to the *long* and SFG/FVS to the *short* GMSB/2UED decay chains.

4.1 Preliminary Remarks

A particle of mass M, energy E and momentum $\boldsymbol{P}$ decays into n products with masses m_f, energies E_f and momenta $\boldsymbol{p}_f$. The decay rate then has the well known form

$$d\Gamma = \frac{1}{2E} \prod_{f=1}^{n} \left(\frac{d^3\boldsymbol{p}_f}{(2\pi)^3} \frac{1}{2E_f} \right) |\mathcal{M}|^2 (2\pi)^4 \delta^{(4)}(P - \sum_{f=1}^{n} p_f). \tag{4.1}$$

In order to calculate the invariant mass distribution $d\Gamma/dm$ for some decay products p we have to express one component of one momentum through the invariant mass and integrate over the remaining momenta. That way we obtain

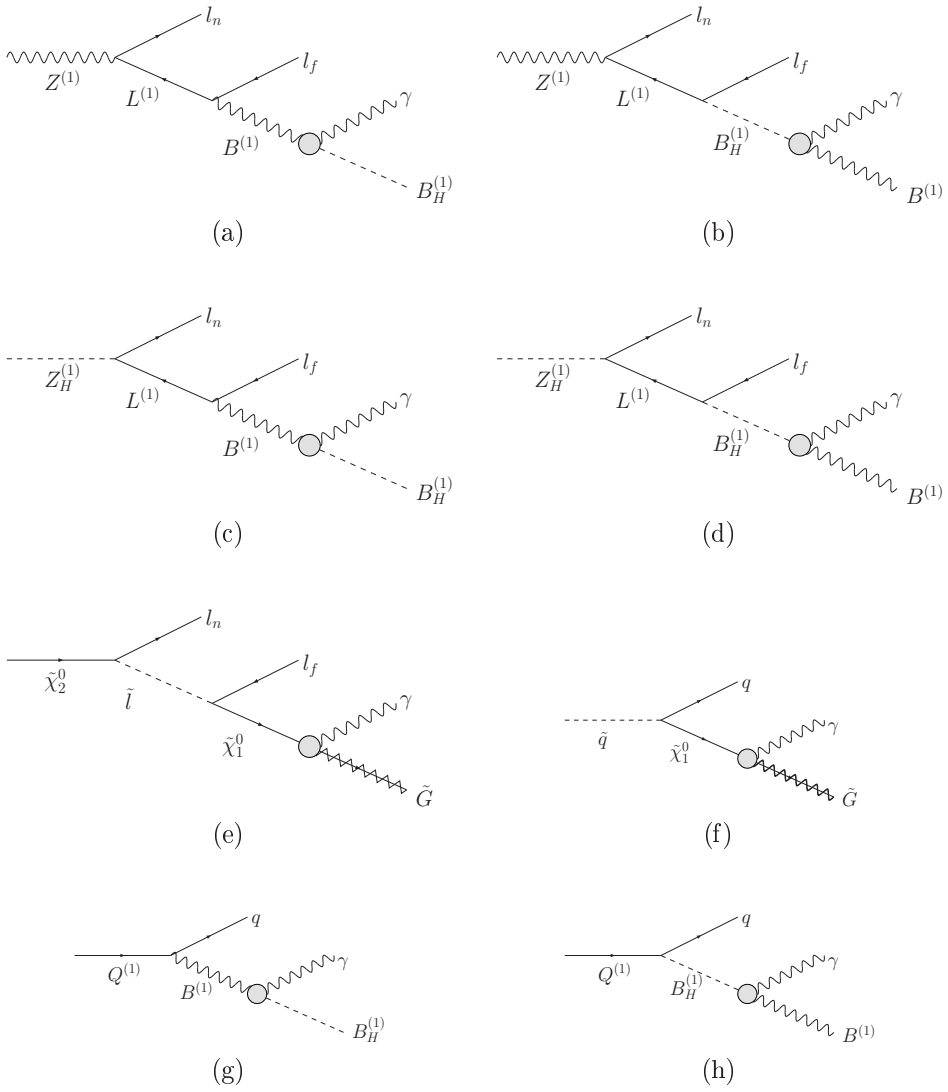

Figure 4.1: Different 2UED decay chains leading to the different spin configurations in the long decay chain: (a) vector-fermion-vector-scalar (VFVS), (b) vector-fermion-scalar-vector (VFSV), (c) scalar-fermion-vector-scalar (SFVS), (d) scalar-fermion-scalar-vector (SFSV), (e) fermion-scalar-fermion-gravitino (FSFG). In the short decay chain: (f) scalar-fermion-gravitino (SFG), (g) fermion-vector-scalar (FVS), (h) fermion-scalar-vector (FSV).

an expression $d\Gamma = f(m)dm$ and thus the invariant mass distribution $\frac{d\Gamma}{dm} = f(m)$. Moreover, since our knowledge about the force of the couplings is model-dependent and we are more interested in the qualitative behavior of the invariant mass distributions, we just calculate $\frac{1}{\Gamma_0}\frac{d\Gamma}{dm}$, where Γ_0 is the total decay width. Thus we will not be interested in overall constants (such as coupling constants). Anyway that calculation can be lengthy and thus we will first discuss a simple toy model.

4.1.1 A Simple Toy Model

Let us assume the decay rate is given by the following simple expression

$$d\Gamma = \hat{\theta}(x)\hat{\theta}(y)dx\,dy \tag{4.2}$$

where we have defined $\hat{\theta}(x) = \theta(x)\theta(1-x)$. The step functions just define the integration borders $[0,1]$ for the variables x and y. Now let us define a new variable $m = x + y$ with the integration limits $[0,2]$. The decay rate then reads

$$d\Gamma = |\frac{\partial(x,y)}{\partial(m,y)}|\hat{\theta}(m-y)\hat{\theta}(y)dm\,dy, \tag{4.3}$$

where the first expression is the Jacobi determinant, in this case just 1. Integrating over the remaining dy we get the invariant mass distribution

$$\frac{d\Gamma}{dm} = \int_{-\infty}^{\infty} \hat{\theta}(m-y)\hat{\theta}(y)dy. \tag{4.4}$$

The step functions give the following bounds on y

$$\begin{array}{llll} \hat{\theta}(m-y): & m-y>0 \Rightarrow & \boldsymbol{y < m} & m-y<1 \Rightarrow \quad \boldsymbol{y > m-1} \\ \hat{\theta}(y): & & \boldsymbol{y > 0} & \qquad\qquad\quad \boldsymbol{y < 1} \end{array} \tag{4.5}$$

Since $m \in [0,2]$ the bounds on the left-hand side hold if $m < 1$ the ones on the right hand side if $m \geq 1$. Thus we have to evaluate $\frac{d\Gamma}{dm}$ for these two cases separately:

$$\begin{aligned} m < y: \quad & \frac{d\Gamma}{dm} = \int_0^m dy = m, \\ m \geq y: \quad & \frac{d\Gamma}{dm} = \int_{m-1}^1 dy = 2 - m. \end{aligned} \tag{4.6}$$

And we end up with

$$\frac{d\Gamma}{dm} = \begin{cases} m & m < 1 \\ 2-m & m \geq 1. \end{cases} \tag{4.7}$$

As we see in figure 4.1.1 the distribution gets a kink at $m = 1$ whereas in the old variables the decay rate is smooth (constant). That property will often occur when calculating invariant mass distributions.

4.1.2 Approximations

Since we assume the intermediary particles to have very small width we can make a further simplification. The propagator of an intermediary particle with

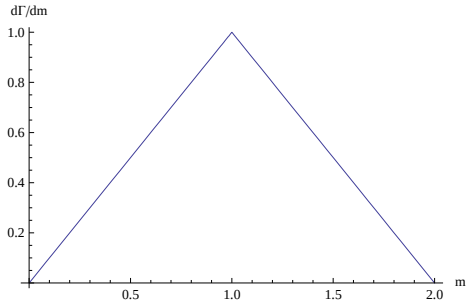

Figure 4.2: Plot of the invariant mass distribution $\frac{d\Gamma}{dm}$ for the simple play model.

momentum q, mass m and width Γ is proportional to $\frac{1}{q^2-m^2+im\Gamma}$. The expression appearing in the squared matrix element is then

$$\left|\frac{1}{q^2-m^2+im\Gamma}\right|^2 = \frac{1}{q^4-2q^2m^2+m^4+m^2\Gamma^2} = \frac{\pi}{m\Gamma}\frac{m\Gamma}{\pi\left[(q^2-m^2)^2+m^2\Gamma^2\right]} \xrightarrow[\Gamma\to 0]{} \frac{\pi}{m\Gamma}\delta(q^2-m^2). \quad (4.8)$$

Thus the intermediate particle is on-shell and the denominator of the propagator is just an overall constant and can be neglected in our case. This is called the *zero width approximation*.

Since the new particles of the extensions to the SM have not been observed yet, they have to be much heavier than most SM particles, except the top quark, W, Z and Higgs boson, which do not play a role in our analysis. Thus we work in an approximation where the SM masses are zero.

4.2 Kinematics

The invariant masses depend on the masses of the intermediate particles and on the angles between the outgoing ones. In order to calculate the invariant mass distributions we have to express the phase space integration (4.1) with the right angles. For the long decay chain we will use the following choices:

1. For the lepton-lepton invariant mass distribution: $\theta_{cb}^{(C)}$, the angle between the momenta of c and b in the rest frame of C, analogously $\theta_{ca}^{(B)}$ and $\phi_{cbca}^{(B)}$, which is the angle between the two planes spanned by (c, b) and (c, a) (figure 4.3). For this decay it will suffice to consider the subprocess $D \to c\,C \to c\,b\,B$ and so only the angular dependence on $\theta_{cb}^{(C)}$, the other angles are integrated out.

2. For the far-lepton–photon distribution: $\theta_{ab}^{(B)}$, $\theta_{ac}^{(C)}$ and $\phi_{abac}^{(C)}$ (figure 4.4). Similarly the only relevant angle is $\theta_{ab}^{(B)}$ and the others are integrated out.

3. For the near-lepton–photon distribution: $\theta_{cb}^{(C)}$, $\theta_{ca}^{(B)}$ and $\phi_{cbca}^{(B)}$. The angles θ are defined as before and $\phi_{cbca}^{(B)}$ is the angle between the two planes spanned by (c, b) and (c, a) (figure 4.3).

4. For the high/low lepton-photon distribution: $\theta_{ab}^{(B)}$, $\theta_{ac}^{(C)}$ and $\phi_{abac}^{(C)}$ (figure 4.4).

The short decay chain only consists of $C \to b\ B \to b\ a\ A$ and has only one angular dependence $\theta_{ab}^{(B)}$.

4.2.1 $\theta_{cb}^{(C)}$, $\theta_{ca}^{(B)}$ and $\phi_{cbca}^{(B)}$

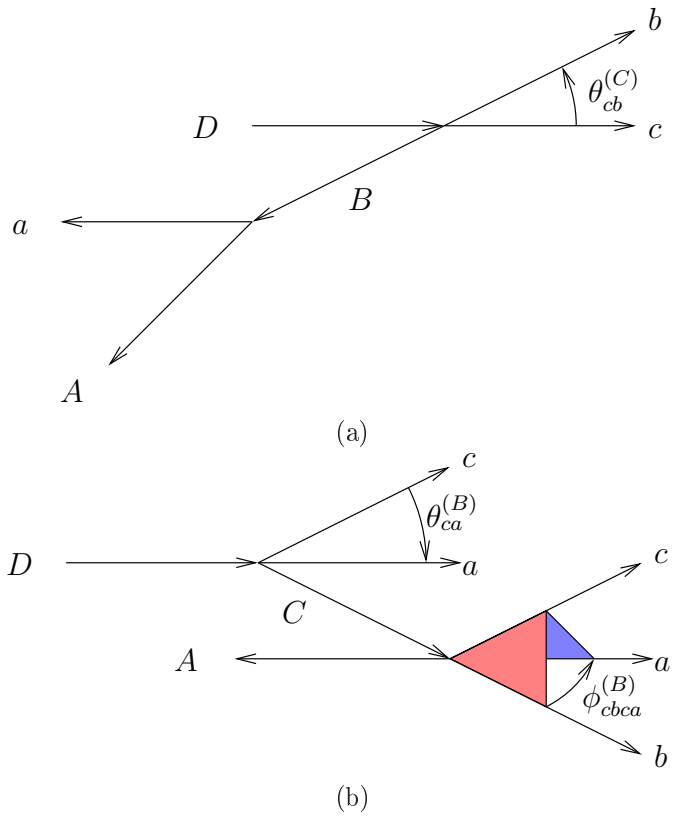

Figure 4.3: a) angles in the rest frame of C; b) angles in the rest frame of B

In order to calculate the matrix elements one has to express the scalar products by means of these angles and the masses of the intermediary particles. First it will be useful to get an expression of $\theta_{ba}^{(B)}$ by means of $\theta_{ca}^{(B)}$, $\theta_{cb}^{(B)}$ and $\phi_{cbca}^{(B)}$. To do so we define

$$\begin{aligned} \boldsymbol{x} &= \boldsymbol{p}_c^{(B)} \wedge \boldsymbol{p}_b^{(B)}, \quad x^i = \varepsilon^{ijk} p_c^{(B)j} p_b^{(B)k}, \quad |\boldsymbol{x}| = E_c^{(B)} E_b^{(B)} \sin\theta_{cb}^{(B)}, \\ \boldsymbol{y} &= \boldsymbol{p}_a^{(B)} \wedge \boldsymbol{p}_c^{(B)}, \quad y^i = \varepsilon^{ilm} p_a^{(B)l} p_c^{(B)m}, \quad |\boldsymbol{y}| = E_a^{(B)} E_c^{(B)} \sin\theta_{ca}^{(B)}. \end{aligned} \tag{4.9}$$

The scalar product between $\boldsymbol{x}$ and $\boldsymbol{y}$ then is

$$\begin{aligned} x^i y^i &= \varepsilon^{ijk}\varepsilon^{ilm} p_c^{(B)j} p_b^{(B)k} p_a^{(B)l} p_c^{(B)m} \\ &= \left(\boldsymbol{p}_c^{(B)} \cdot \boldsymbol{p}_a^{(B)}\right)\left(\boldsymbol{p}_c^{(B)} \cdot \boldsymbol{p}_b^{(B)}\right) - |\boldsymbol{p}_c^{(B)}|^2 \left(\boldsymbol{p}_a^{(B)} \cdot \boldsymbol{p}_b^{(B)}\right) \\ &= E_a^{(B)} E_b^{(B)} \left(E_c^{(B)}\right)^2 \left(\cos\theta_{ca}^{(B)} \cos\theta_{cb}^{(B)} - \cos\theta_{ba}^{(B)}\right) \\ &\stackrel{!}{=} E_a^{(B)} E_b^{(B)} \left(E_c^{(B)}\right)^2 \sin\theta_{ca}^{(B)} \sin\theta_{cb}^{(B)} \cos\left(\pi - \phi_{cbca}^{(B)}\right). \end{aligned} \tag{4.10}$$

This can be solved for $\cos\theta_{ba}^{(B)}$:

$$\cos\theta_{ba}^{(B)} = \cos\theta_{ca}^{(B)} \cos\theta_{cb}^{(B)} + \sin\theta_{ca}^{(B)} \sin\theta_{cb}^{(B)} \cos\phi_{cbca}^{(B)}. \tag{4.11}$$

Next we want to express $\theta_{cb}^{(B)}$ by means of $\theta_{cb}^{(C)}$. For this purpose we use

$$\begin{aligned} &\boldsymbol{p}_c^{(B)} \cdot \boldsymbol{p}_b^{(B)} = E_c^{(B)} E_b^{(B)} - p_c p_b, \\ &\Rightarrow \cos\theta_{cb}^{(B)} = 1 - \frac{E_b^{(C)} E_c^{(C)}}{E_b^{(B)} E_c^{(B)}} (1 - \cos\theta_{cb}^{(C)}). \end{aligned} \tag{4.12}$$

Lastly we need to calculate the energies of all outgoing particles in the two rest frames (B) and (C). To calculate $E_c^{(C)}$ we begin with

$$m_D^2 = \left(E_D^{(C)}\right)^2 - \left(\boldsymbol{p}_D^{(C)}\right)^2 = \left(E_c^{(C)} + m_C\right)^2 - \left(\boldsymbol{p}_c^{(C)}\right)^2, \tag{4.13}$$

where the second equals sign follows from momentum conservation. This expression can now be solved for $E_c^{(C)}$:

$$E_c^{(C)} = \frac{m_D^2 - m_C^2}{2m_C}. \tag{4.14}$$

In the same way we obtain

$$E_b^{(C)} = \frac{m_C^2 - m_B^2}{2m_C}, \quad E_b^{(B)} = \frac{m_C^2 - m_B^2}{2m_B}, \quad E_a^{(B)} = \frac{m_B^2 - m_A^2}{2m_B}. \tag{4.15}$$

For the energy $E_c^{(B)}$ we calculate

$$\begin{aligned} m_D^2 &= \left(E_D^{(B)}\right)^2 - \left(\boldsymbol{p}_D^{(B)}\right)^2 = \left(E_c^{(B)} + E_b^{(B)} + m_B\right)^2 - \left(\boldsymbol{p}_c^{(B)} + \boldsymbol{p}_b^{(B)}\right)^2 \\ &= m_B^2 + 2E_c^{(B)} m_B + 2E_b^{(B)} m_B + 2E_b^{(C)} E_c^{(C)} \left(1 - \cos\theta_{cb}^{(C)}\right), \end{aligned} \tag{4.16}$$

where we used (4.12) to get the expression on the second line. Solved for $E_c^{(B)}$ this leads to

$$E_c^{(B)} = \frac{\left(m_D^2 - m_C^2\right)\left(m_C^2 + m_B^2 + \left(m_C^2 - m_B^2\right)\cos\theta_{cb}^{(C)}\right)}{4m_B m_C^2}. \tag{4.17}$$

Analogously

$$E_a^{(C)} = \frac{\left(m_B^2 - m_A^2\right)\left(m_C^2 + 2m_B^2 - 2m_A^2 - \left(m_C^2 - m_A^2\right)\cos\theta_{ba}^{(B)}\right)}{4m_B^2 m_C}. \tag{4.18}$$

This can be further calculated using (4.11).

Now we have calculated the energies of all outgoing particles and all angles between them. This allows us to calculate the scalar products appearing in the squared matrix element.

4.2.2 $\theta_{ab}^{(B)}$, $\theta_{ac}^{(C)}$ and $\phi_{abac}^{(C)}$

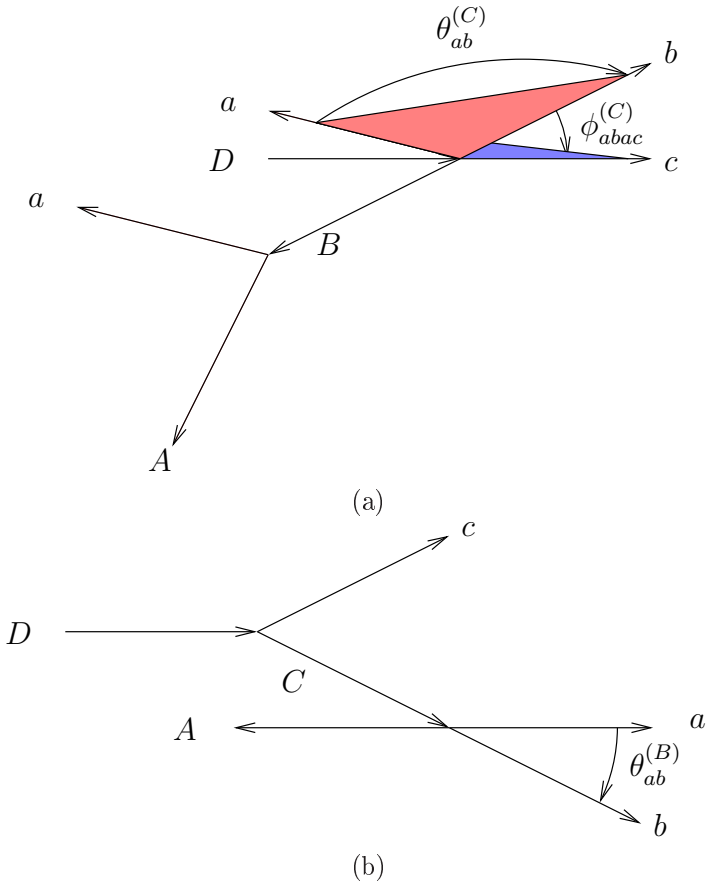

Figure 4.4: a) angles in the rest frame of C; b) angles in the rest frame of B

Since the energies $E_a^{(B)}$, $E_b^{(B)}$, $E_b^{(C)}$ and $E_c^{(C)}$ only depend on the masses, their expressions stay the same. The only two masses depending on the angles become

$$E_a^{(C)} = \frac{\left(m_B^2 - m_A^2\right)\left(m_C^2 + m_B^2 - \left(m_C^2 - m_B^2\right)\cos\theta_{ab}^{(B)}\right)}{4m_C m_B^2} \tag{4.19}$$

$$E_c^{(B)} = \frac{\left(m_D^2 - m_C^2\right)\left(m_C^2 + m_B^2 + \left(m_C^2 - m_B^2\right)\cos\theta_{bc}^{(C)}\right)}{4m_B m_C^2}, \tag{4.20}$$

with the angles

$$\cos\theta_{bc}^{(C)} = \cos\theta_{ac}^{(C)}\cos\theta_{ab}^{(C)} + \sin\theta_{ac}^{(C)}\sin\theta_{ab}^{(C)}\cos\phi_{abac}^{(C)}, \tag{4.21}$$

$$\cos\theta_{ab}^{(C)} = 1 - \frac{E_a^{(B)}E_b^{(B)}}{E_a^{(C)}E_b^{(C)}}\left(1 - \cos\theta_{ab}^{(B)}\right). \tag{4.22}$$

4.3 Matrix Elements

In order to calculate the partial decay width (4.1) we first need to calculate the squared matrix elements. As we already have discussed in the chapter before, the GMSB decay has no spin correlation and thus the squared matrix element is proportional to some overall constant. For the other decay chains we do expect non-trivial matrix elements and using the Feynman rules from Appendix A.1 on graph in figure 4.5 we get for the *long* decay chain VFVS

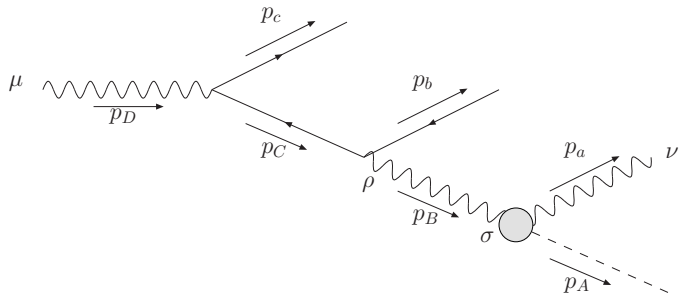

Figure 4.5: Feynman diagram for the VFVS decay.

$$\begin{aligned}\mathcal{M}_{VFVS} \propto\ & \bar{u}(p_c)\gamma^\mu P_L(-\not{p}_C + m_C)\gamma^\rho P_L v(p_b) \\ & \times (-g_{\rho\sigma} + \frac{p_{B\rho}p_{B\sigma}}{m_B^2})\varepsilon^{\nu\sigma\alpha\beta}p_{B\alpha}p_{A\beta}\epsilon_\mu(p_D)\epsilon_\nu^*(p_a).\end{aligned} \tag{4.23}$$

In the same way we obtain matrix elements for the other 2UED decays:

$$\begin{aligned}\mathcal{M}_{VFSV} \propto\ & \bar{u}(p_c)\gamma^\mu P_L(-\not{p}_C + m_C)P_L v(p_b) \\ & \times \varepsilon^{\nu\rho\alpha\beta}p_{A\alpha}p_{B\beta}\epsilon_\mu(p_D)\epsilon_\nu^*(p_a)\epsilon_\rho^*(p_A),\end{aligned} \tag{4.24}$$

$$\begin{aligned}\mathcal{M}_{SFVS} \propto\ & \bar{u}(p_c)P_L(-\not{p}_C + m_C)\gamma^\rho P_L v(p_b) \\ & \times (-g_{\rho\sigma} + \frac{p_{B\rho}p_{B\sigma}}{m_B^2})\varepsilon^{\nu\sigma\alpha\beta}p_{B\alpha}p_{A\beta}\epsilon_\nu^*(p_a),\end{aligned} \tag{4.25}$$

$$\begin{aligned}\mathcal{M}_{SFSV} \propto\ & \bar{u}(p_c)P_L(-\not{p}_C + m_C)P_L v(p_b) \\ & \times \varepsilon^{\nu\rho\alpha\beta}p_{A\alpha}p_{B\beta}\epsilon_\nu^*(p_a)\epsilon_\rho^*(p_A).\end{aligned} \tag{4.26}$$

For the *short* decay chains we only have to calculate the FVS matrix element. The FSV decay shows no angular dependence between the quark and the photon since the intermediate particle is a scalar.

$$\mathcal{M}_{FVS} \propto\ \bar{v}(p_C)\gamma^\rho P_L v(p_b)(-g_{\rho\sigma} + \frac{p_{B\rho}p_{B\sigma}}{m_B^2})\varepsilon^{\nu\sigma\alpha\beta}p_{B\alpha}p_{A\beta}\epsilon_\nu^*(p_a). \tag{4.27}$$

The squared matrix elements have been evaluated with the Tracer.m Mathematica package [27]. These rather lengthy expressions are consigned to Appendix A.2.

4.4 Invariant Mass Distributions

It will be useful to define the quantities

$$(m_{ab}^{\max})^2 = (m_{ba}^{\max})^2 = \frac{(m_C^2 - m_B^2)(m_B^2 - m_A^2)}{m_B^2}, \tag{4.28}$$

$$(m_{ac}^{\max})^2 = (m_{ca}^{\max})^2 = \frac{(m_D^2 - m_C^2)(m_B^2 - m_A^2)}{m_B^2}, \tag{4.29}$$

$$(m_{c2}^{\max})^2 = \frac{(m_D^2 - m_C^2)(m_B^2 - m_A^2)}{2m_C^2 - m_D^2}, \tag{4.30}$$

$$a = 1 - \frac{m_B^2}{m_C^2}. \tag{4.31}$$

4.4.1 The Lepton-Lepton Invariant Mass Distribution

With the above notation and defining $u = 1/2(1-\cos\theta_{cb}^{(C)})$, $v = 1/2(1-\cos\theta_{ac}^{(C)})$ we can write the far-lepton–photon invariant mass as

$$m_{bc}^2 = 4E_b^{(C)}E_c^{(C)}u. \tag{4.32}$$

Thus m_{cb} lies in the range $[0, m_{bc}^{(max)}]$ where we have defined $m_{bc}^{(max)} \equiv 4E_b^{(C)}E_c^{(C)}$. With eq. (4.1) we can calculate $1/\Gamma_0 d\Gamma/du$

$$\begin{aligned} \frac{1}{\Gamma_0}d\Gamma &= \frac{1}{\int |\mathcal{M}|^2 du\ dv\ d\phi_{cbca}^{(B)}} |\mathcal{M}|^2 du\ dv\ d\phi_{cbca}^{(B)} \\ \Rightarrow \frac{1}{\Gamma_0}\frac{d\Gamma}{du} &= \frac{1}{\int |\mathcal{M}|^2 du\ dv\ d\phi_{cbca}^{(B)}} \int |\mathcal{M}|^2\ dv\ d\phi_{cbca}^{(B)}, \end{aligned} \tag{4.33}$$

where $|\mathcal{M}|^2$ is the squared matrix element associated to the different decay chains in figure 4.1 written down in Appendix A.2. Thus we can calculate the invariant mass distribution

$$\frac{1}{\Gamma_0}\frac{d\Gamma}{dm_{bc}^2} = \frac{1}{\Gamma_0}\frac{du}{dm_{bc}^2}\frac{d\Gamma}{du} = \frac{1}{\Gamma_0}\frac{1}{4E_b^{(c)}E_c^{(C)}}\frac{d\Gamma}{du}, \tag{4.34}$$

which is displayed in figures 4.6 and 4.7

4.4.2 The Far-Lepton–Photon Invariant Mass Distribution

Analogously the far-lepton–photon invariant mass distribution is

$$\frac{1}{\Gamma_0}\frac{d\Gamma}{dm_{ab}^2} = \frac{1}{\Gamma_0}\frac{1}{4E_a^{(B)}E_b^{(B)}}\frac{d\Gamma}{du}, \tag{4.35}$$

where $u = 1/2(1-\cos\theta_{ab}^{(B)})$, $v = 1/2(1-\cos\theta_{ac}^{(C)})$ and

$$\frac{1}{\Gamma_0}\frac{d\Gamma}{du} = \frac{1}{\int |\mathcal{M}|^2 du\, dv\, d\phi_{abac}^{(C)}} \int |\mathcal{M}|^2\, dv\, d\phi_{abac}^{(C)}. \tag{4.36}$$

The invariant mass m_{ab} lies in the range $[0, m_{ab}^{(max)}]$, $m_{ab}^{(max)} \equiv 4E_a^{(B)}E_b^{(B)}$. These distributions are plotted in figures 4.8 and 4.9.

4.4.3 The Near-Lepton–Photon Invariant Mass Distribution

Using the angles 2) the $l_n\ \gamma$ invariant mass can be written as

$$m_{ca}^2 = 2E_a^{(B)}E_c^{(B)}\cos\theta_{ca}^{(B)}. \tag{4.37}$$

Rewriting this with (4.15), (4.17), (4.29) and

$$u = \frac{1}{2}(1-\cos\theta_{cb}^{(C)}), \quad v = \frac{1}{2}(1-\cos\theta_{ca}^{(B)}), \tag{4.38}$$

we end up with

$$m_{ca}^2 = m_{ca}^{\max 2}(1-au)v \Rightarrow 0 \le m_{ac} \le m_{ac}^{\max}. \tag{4.39}$$

The distribution $\partial^2 P/(\partial u\,\partial v)$ can be obtained expressing the squared matrix element from Appendix A.2 with the angles 2), integrating over $\phi_{cbca}^{(B)}$ and normalizing to 1:

$$\frac{1}{\Gamma_0}\frac{\partial^2\Gamma}{\partial u\,\partial v} = \underbrace{\frac{\int |\mathcal{M}|^2\, d\phi_{cbca}^{(B)}}{\int |\mathcal{M}|^2 du\, dv\, d\phi_{cbca}^{(B)}}}_{\equiv P(u,v)} \hat{\theta}(u)\hat{\theta}(v). \tag{4.40}$$

We have added the step functions $\hat{\theta}(u) = \theta(u)\theta(1-u)$ to assure the integration borders for u and v. The differential distribution with respect to u and m_{ca}^2 then is

$$\begin{aligned}\frac{1}{\Gamma_0}\frac{\partial^2\Gamma}{\partial u\,\partial m_{ca}^2} &= \left|\frac{\partial(u,v)}{\partial(u,m_{ca}^2)}\right| P(u,v)\hat{\theta}(u)\hat{\theta}(v) \\ &= \frac{P(u,v)}{(m_{ac}^{\max})^2(1-au)}\hat{\theta}\left(\frac{m_{ac}^2}{(m_{ac}^{\max})^2(1-au)}\right)\hat{\theta}(u).\end{aligned} \tag{4.41}$$

Finally we have to integrate over u to find the distribution of m_{ac}^2:

$$\begin{aligned}\frac{1}{\Gamma_0}\frac{\partial\Gamma}{\partial m_{ca}^2} &= \int_{-\infty}^{\infty} \frac{P(u,v)}{(m_{ac}^{\max})^2(1-au)}\hat{\theta}\left(\frac{m_{ac}^2}{(m_{ac}^{\max})^2(1-au)}\right)\hat{\theta}(u)du \\ &= \int_0^1 \frac{P(u,v)}{(m_{ac}^{\max})^2(1-au)}\hat{\theta}\left(\frac{m_{ac}^2}{(m_{ac}^{\max})^2(1-au)}\right)du.\end{aligned} \tag{4.42}$$

The last step function gives us the following restriction on u

$$\frac{m_{ac}^2}{(m_{ac}^{\max})^2(1-au)} < 1 \Rightarrow u < \frac{1}{a}\left(1-\frac{m_{ac}^2}{(m_{ac}^{\max})^2}\right), \tag{4.43}$$

giving us the following distribution:

$$\frac{1}{\Gamma_0}\frac{\partial\Gamma}{\partial m_{ca}^2} = \int_0^{u^{\max}} \frac{P(u,v)}{(m_{ac}^{\max})^2(1-au)}du, \tag{4.44}$$

where the upper bound of u is

$$u^{\max} = \min\left(1, \frac{1}{a}\left(1 - \frac{m_{ac}^2}{(m_{ac}^{\max})^2}\right)\right). \tag{4.45}$$

Thus we find for the invariant mass distribution

$$\frac{1}{\Gamma_0}\frac{\partial\Gamma}{\partial m_{ca}^2} = \begin{cases} \int_0^1 \frac{P(u,v)}{(m_{ac}^{\max})^2(1-au)}du & 0 < m_{ac} < \frac{m_B}{m_C}m_{ac}^{\max} \\ \int_0^{u^{\max}} \frac{P(u,v)}{(m_{ac}^{\max})^2(1-au)}du & \frac{m_B}{m_C}m_{ac}^{\max} < m_{ac} < m_{ac}^{\max}. \end{cases} \tag{4.46}$$

The plots can be found in figures 4.10 and 4.11.

4.4.4 The Observable Lepton-Photon Invariant Mass Distribution

The observable lepton-photon invariant mass distribution (figures 4.12 and 4.13) is the sum of the two preceding distributions. Another possibility to create observable quantities is to calculate the maximum/ minimum of the lepton-photon invariant masses.

4.4.5 The High Lepton-Photon Invariant Mass Distribution

Working with the angles 3) we first define

$$u = \frac{1}{2}(1 - \cos\theta_{ba}^{(B)}),\ v = \frac{1}{2}(1 - \cos\theta_{ca}^{(C)}) \tag{4.47}$$

Now we can write the invariant masses as

$$m_{ab}^2 = (m_{ab}^{max})^2 u,\ m_{ac}^2 = (m_{ac}^{max})^2(1-a+au)v \tag{4.48}$$

m_{abac}^{high} is now defined as

$$m_{abac}^{high} = \max[m_{ab}, m_{ac}] \tag{4.49}$$

Let us define the variable x which is positive for $m_{ab} > m_{ac}$ and negative vice versa

$$x = m_{ab}^2 - m_{ac}^2 = (m_{ab}^{max})^2 u - (m_{ac}^{max})^2(1-a+au)v \tag{4.50}$$

m_{abac}^{high} can now be written as

$$(m_{abac}^{high})^2 = \theta(x)(m_{ab}^{max})^2 u + \theta(-x)(m_{ac}^{max})^2(1-a+au)v \tag{4.51}$$

In the following we will denote m_{abac}^{high} simply as m. The two latter formulas can be solved for u and v, thus

$$\begin{aligned} u &= \frac{m^2 + x\theta(-x)}{(m_{ab}^{max})^2}, \\ v &= \frac{(m_{ab}^{max})^2(m^2 - x\theta(x))}{(m_{ac}^{max})^2((m_{ab}^{max})^2 + a(m^2 - (m_{ab}^{max})^2 + x\theta(-x)))}. \end{aligned} \tag{4.52}$$

As before the distribution $1/\Gamma_0 \partial^2\Gamma/(\partial u \partial v)$ can be calculated by expressing the matrix element from Appendix A.2 through the angles 3), integrating over $\phi^{(C)}_{abac}$ and normalizing to 1:

$$\frac{1}{\Gamma_0}\frac{\partial^2\Gamma}{\partial u\,\partial v} = \underbrace{\frac{\int |\mathcal{M}|^2\, d\phi^{(C)}_{abcb}}{\int |\mathcal{M}|^2 du\, dv\, d\phi^{(C)}_{abcb}}}_{\equiv P(u,v)} \hat{\theta}(u)\hat{\theta}(v). \tag{4.53}$$

With the the Jacobian

$$J = \left|\frac{\partial(u,v)}{\partial(x,m^2)}\right| = \frac{1}{(m^{max}_{ab})^2 (m^{max}_{ac})^2 (1-a+au)} \tag{4.54}$$

we get the differential distribution with respect to m^2 and x:

$$\frac{1}{\Gamma_0}\frac{\partial^2\Gamma}{\partial x \partial m^2} = \frac{P(u,v)\,\hat{\theta}(u)\hat{\theta}(v)}{(m^{max}_{ab})^2 (m^{max}_{ac})^2 (1-a+au)} \tag{4.55}$$

where we have defined $\hat{\theta}(u) = \theta(u)\theta(1-u)$. These step functions just assure the integration borders for u and v. To obtain the desired distribution, we have to integrate over x

$$\begin{aligned}\frac{1}{\Gamma_0}\frac{\partial\Gamma}{\partial m^2} = &\int_0^\infty \frac{P(u,v)\,\hat{\theta}(u_+)\hat{\theta}(v_+)}{(m^{max}_{ab})^2 (m^{max}_{ac})^2 (1-a+au_+)} dx_+ \\ &+ \int_{-\infty}^0 \frac{P(u,v)\,\hat{\theta}(u_-)\hat{\theta}(v_-)}{(m^{max}_{ab})^2 (m^{max}_{ab})^2 (1-a+au_-)} dx_-.\end{aligned} \tag{4.56}$$

u_+/u_- and v_+/v_- are the values of u and v for positive / negative x, they are

$$\begin{aligned} u_- &= \tfrac{m^2+x_-}{(m^{max}_{ab})^2}, & u_+ &= \tfrac{m^2}{(m^{max}_{ab})^2} \\ v_- &= \frac{m^2}{(m^{max}_{ac})^2(1-a+a\frac{m^2+x_-}{(m^{max}_{ab})^2})}, & v_+ &= \frac{m^2-x_+}{(m^{max}_{ac})^2(1-a+a\frac{m^2}{(m^{max}_{ab})^2})} \end{aligned} \tag{4.57}$$

The step functions restrict $0 < u_\pm < 1$ and $0 < v_\pm < 1$, which in turn give restrictions on x and m:

$$\hat{\theta}(u_+) \neq 0 \Rightarrow \boldsymbol{0 < m^2 < (m^{max}_{ab})^2}, \tag{4.58}$$

$$\hat{\theta}(v_+) \neq 0 \Rightarrow \boldsymbol{m^2(1 - a\frac{(m^{max}_{ac})^2}{(m^{max}_{ab})^2}) - (m^{max}_{ac})^2(1-a) < x < m^2}, \tag{4.59}$$

$$\hat{\theta}(u_-) \neq 0 \Rightarrow \boldsymbol{-m^2 < x < (m^{max}_{ab})^2 - m^2}, \tag{4.60}$$

$$\hat{\theta}(v_-) \neq 0 \Rightarrow \boldsymbol{-\frac{1-a}{a}(m^{max}_{ab})^2 - m^2(1 - \frac{(m^{max}_{ab})^2}{a(m^{max}_{ac})^2}) < x}. \tag{4.61}$$

Let us now have a close look which of these inequalities provide the strongest bounds.

- **lower bound of** x_+ There are two possible lower bounds of x_+: either 0 or the left hand side of eq. (4.59). In order that 0 is the lower bound:

$$0 > m^2(1 - a\frac{(m^{max}_{ac})^2}{(m^{max}_{ab})^2}) - (m^{max}_{ac})^2(1-a). \tag{4.62}$$

Solving this inequality we have to consider two cases: $m_D^2 < 2m_C^2$ and $m_D^2 > 2m_C^2$. The first one leads to $m^2 > (m_{c2}^{max})^2$ and the second one to $m^2 < (m_{c2}^{max})^2$. The last of these inequalities is never fullfilled since $m_D^2 > 2m_C^2 \Rightarrow (m_{c2}^{max})^2 < 0$. So, in the first case there are two possible lower bounds for x_+:

$$m^2 < (m_{c2}^{max})^2 \;\Rightarrow\; x_+ > 0, \tag{4.63}$$

$$m^2 > (m_{c2}^{max})^2 \;\Rightarrow\; x_+ > m^2(1 - a\frac{(m_{ac}^{max})^2}{(m_{ab}^{max})^2}) - (m_{ac}^{max})^2(1-a). \tag{4.64}$$

In the second case 0 is always the lower bound of x_+

- **upper bound of** x_+ As long as eq. (4.58) holds the upper bound of x_+ is m^2, otherwise there is no integration over x_+.

- **lower bound of** x_- In order to the step function of eq. (4.61) being non-zero, the left hand side of eq. (4.61) has to be smaller than zero, which is the case for $m^2 < (m_{c2}^{max})^2$. Otherwise there is no integration over x_-. There are now two possible lower bounds given in eq. (4.60) and (4.61). Let us discriminate the stronger one:

$$-m^2 > -\frac{1-a}{a}(m_{ab}^{max})^2 - m^2(1 - \frac{(m_{ab}^{max})^2}{a(m_{ac}^{max})^2}),$$
$$m^2 > \frac{m_B^2}{m_C^2}(m_{ac}^{max})^2 \Rightarrow x_- > -m^2. \tag{4.65}$$

In the other case eq. (4.61) is the lower bound:

$$m^2 < \frac{m_B^2}{m_C^2}(m_{ac}^{max})^2 \Rightarrow x_- > -\frac{1-a}{a}(m_{ab}^{max})^2 - m^2(1 - \frac{(m_{ab}^{max})^2}{a(m_{ac}^{max})^2}). \tag{4.66}$$

- **upper bound of** x_- The upper bound is either 0 or the right hand side of eq. (4.60):

$$m^2 > (m_{ab}^{max})^2 \Rightarrow x_- < (m_{ab}^{max})^2 - m^2, \tag{4.67}$$
$$m^2 < (m_{ab}^{max})^2 \Rightarrow x_- < 0. \tag{4.68}$$

Assuming $m_D > m_C > m_B > m_A$ we have to treat the two cases $m_D^2 < 2m_C^2$ and $m_D^2 > 2m_C^2$ separately. For the first one we see that $m_{c2}^{max} > \frac{m_B}{m_C}(m_{ac}^{max})$ and $m_{ac}^{max} > \frac{m_B}{m_C}(m_{ac}^{max})$. Thus there are two hierarchies between these three invariant masses

$$A1) \quad m_{c2}^{max} > m_{ac}^{max} > \frac{m_B}{m_C}(m_{ac}^{max}),$$
$$A2) \quad m_{ac}^{max} > m_{c2}^{max} > \frac{m_B}{m_C}(m_{ac}^{max}).$$

Into these mass hierarchies we have to place m_{ab}^{max}. In hierarchy A1 we assumed $m_{c2}^{max} < m_{ac}^{max}$. Thus $m_B^2 > 2m_C^2 - m_D^2$ and this leads to

$$(m_{ab}^{max})^2 = \frac{(m_C^2 - m_B^2)(m_B^2 - m_A^2)}{m_B^2} < \frac{(m_D^2 - m_C^2)(m_B^2 - m_A^2)}{m_B^2} = (m_{ac}^{max})^2,$$
$$\Rightarrow m_{ab}^{max} < m_{ac}^{max}. \tag{4.69}$$

Therefore there are two possibilities to place m_{ab}^{max} in hierarchy A1. This leads to

$$A11) \quad m_{ab}^{max} < m_{ac}^{max}\frac{m_B}{m_C} < m_{ac}^{max} < m_{c2}^{max},$$
$$A12) \quad m_{ac}^{max}\frac{m_B}{m_C} < m_{ab}^{max} < m_{ac}^{max} < m_{c2}^{max}.$$

To obtain hierarchy A2 we assumed $m_{c2}^{max} < m_{ac}^{max}$ which leads to $m_B^2 < 2m_C^2 - m_D^2$ and we see that $m_{ab}^{max} > m_{ac}^{max}$. Now there is only one possibility to place m_{ab}^{max} in hierarchy A2:

$$A2) \quad m_{ac}^{max}\frac{mB}{mC} < m_{c2}^{max} < m_{ac}^{max} < m_{ab}^{max}.$$

For the second case ($m_D^2 > 2m_C^2$) we note

$$\begin{aligned}(m_{ab}^{max})^2 &= \frac{(m_C^2 - m_B^2)(m_B^2 - m_A^2)}{m_B^2} = \frac{(2m_C^2 - m_C^2 - m_B^2)(m_B^2 - m_A^2)}{m_B^2} \\ &< \frac{(m_D^2 - m_C^2 - m_B^2)(m_B^2 - m_A^2)}{m_B^2} < \frac{(m_D^2 - m_C^2)(m_B^2 - m_A^2)}{m_B^2} \\ &= (m_{ac}^{max})^2. \end{aligned} \tag{4.70}$$

Thus we end with two hierarchies:

$$B1) \quad m_{ab}^{max} < m_{ac}^{max}\frac{m_B}{m_C} < m_{ac}^{max},$$
$$B2) \quad m_{ac}^{max}\frac{m_B}{m_C} < m_{ab}^{max} < m_{ac}^{max}.$$

Now we can list the bounds on $x_\pm$ for the different hierarchies:

Hierarchy A11: $m_{ab}^{max} < m_{ac}^{max}\frac{m_B}{m_C} < m_{ac}^{max} < m_{c2}^{max}$

$\mathbf{0 < m < m_{ab}^{max}}$: $\quad 0 < x_+ < m^2$, $\quad -m^2 < x_- < 0$

$\mathbf{m_{ab}^{max} < m < m_{ac}^{max}\frac{m_B}{m_C}}$: $\quad 0 < x_+ < 0$, $\quad -m^2 < x_- < (m_{ab}^{max})^2 - m^2$

$\mathbf{m_{ac}^{max}\frac{m_B}{m_C} < m < m_{c2}^{max}}$: $\quad 0 < x_+ < 0$, $\quad -\frac{1-a}{a}(m_{ab}^{max})^2 - m^2(1 - \frac{(m_{ab}^{max})^2}{a(m_{ac}^{max})^2}) < x_- < (m_{ab}^{max})^2 - m^2$

Hierarchy A12: $m_{ac}^{max}\frac{m_B}{m_C} < m_{ab}^{max} < m_{ac}^{max} < m_{c2}^{max}$

$\mathbf{0 < m < m_{ac}^{max}\frac{m_B}{m_C}}$: $\quad 0 < x_+ < m^2$, $\quad -m^2 < x_- < 0$

$\mathbf{m_{ac}^{max}\frac{m_B}{m_C} < m < m_{ab}^{max}}$: $\quad 0 < x_+ < m^2$, $\quad -\frac{1-a}{a}(m_{ab}^{max})^2 - m^2(1 - \frac{(m_{ab}^{max})^2}{a(m_{ac}^{max})^2}) < x_- < 0$

$\mathbf{m_{ab}^{max} < m < m_{c2}^{max}}$: $\quad 0 < x_+ < 0$, $\quad -\frac{1-a}{a}(m_{ab}^{max})^2 - m^2(1 - \frac{(m_{ab}^{max})^2}{a(m_{ac}^{max})^2}) < x_- < (m_{ab}^{max})^2 - m^2$

Hierarchy A2: $m_{ac}^{max}\frac{m_B}{m_C} > m_{a2}^{max} > m_{ac}^{max} > m_{ab}^{max}$

$\mathbf{0 < m < m_{ac}^{max}\frac{m_B}{m_C}}$: $\quad 0 < x_+ < m^2$, $\; -m^2 < x_- < 0$

$\mathbf{m_{ac}^{max}\frac{m_B}{m_C} < m < m_{c2}^{max}}$: $\quad 0 < x_+ < m^2$, $\; -\frac{1-a}{a}(m_{ab}^{max})^2 - m^2(1 - \frac{(m_{ab}^{max})^2}{a(m_{ac}^{max})^2}) < x_- < 0$

$\mathbf{m_{c2}^{max} < m < m_{ab}^{max}}$: $\quad m^2 - (m_{ac}^{max})^2((1-a) + \frac{am^2}{(m_{ab}^{max})^2}) < x_+ < m^2$, $\; 0 < x_- < 0$

Hierarchy B1: $m_{ab}^{max} < m_{ac}^{max}\frac{m_B}{m_C} < m_{ac}^{max}$

$\mathbf{0 < m < m_{ab}^{max}}$: $\quad 0 < x_+ < m^2$, $\; -m^2 < x_- < 0$

$\mathbf{m_{ab}^{max} < m < m_{ac}^{max}\frac{m_B}{m_C}}$: $\quad 0 < x_+ < 0$, $\; -m^2 < x_- < (m_{ab}^{max})^2 - m^2$

$\mathbf{m_{ac}^{max}\frac{m_B}{m_C} < m < m_{ac}^{max}}$: $\quad 0 < x_+ < 0$, $\; -\frac{1-a}{a}(m_{ab}^{max})^2 - m^2(1 - \frac{(m_{ab}^{max})^2}{a(m_{ac}^{max})^2}) < x_- < (m_{ab}^{max})^2 - m^2$

Hierarchy B2: $m_{ac}^{max}\frac{m_B}{m_C} < m_{ab}^{max} < m_{ac}^{max}$

$\mathbf{0 < m < m_{ac}^{max}\frac{m_B}{m_C}}$: $\quad 0 < x_+ < m^2$, $\; -m^2 < x_- < 0$

$\mathbf{m_{ac}^{max}\frac{m_B}{m_C} < m < m_{ab}^{max}}$: $\quad 0 < x_+ < m^2$, $\; -\frac{1-a}{a}(m_{ab}^{max})^2 - m^2(1 - \frac{(m_{ab}^{max})^2}{a(m_{ac}^{max})^2}) < x_- < 0$

$\mathbf{m_{ab}^{max} < m < m_{ac}^{max}}$: $\quad 0 < x_+ < 0$, $\; -\frac{1-a}{a}(m_{ab}^{max})^2 - m^2(1 - \frac{(m_{ab}^{max})^2}{a(m_{ac}^{max})^2}) < x_- < (m_{ab}^{max})^2 - m^2$

The invariant mass distributions are displayed in figures 4.14 and 4.15.

4.4.6 The Low Lepton-Photon Invariant Mass Distribution

m_{abc}^{low} is defined as $\min[m_{ab}, m_{ac}]$. Keeping x as defined in the chapter before we write

$$(m_{abc}^{low})^2 = \theta(-x)(m_{ab}^{max})^2 u + \theta(x)(m_{ac}^{max})^2(1 - a + au)v. \tag{4.71}$$

This can now be inverted to give (again, we just write m for m_{abc}^{low}):

$$\begin{aligned} u &= \frac{m^2 + x\theta(x)}{(m_{ab}^{max})^2}, \\ v &= \frac{(m_{ab}^{max})^2(m^2 - x\theta(-x))}{(m_{ac}^{max})^2((m_{ab}^{max})^2 + a(m^2 - (m_{ab}^{max})^2 + x\theta(x)))}. \end{aligned} \tag{4.72}$$

We can write the differential distribution $1/\Gamma_0 \partial\Gamma/\partial m^2$ the same way as in the preceding chapter but now with

$$\begin{aligned} u_- &= \tfrac{m^2}{(m_{ab}^{max})^2}, & u_+ &= \tfrac{m^2+x}{(m_{ab}^{max})^2}, \\ v_- &= \tfrac{m^2-x}{(m_{ac}^{max})^2(1-a+a\frac{m^2}{(m_{ab}^{max})^2})}, & v_+ &= \tfrac{m^2}{(m_{ac}^{max})^2(1-a+a\frac{m^2+x}{(m_{ab}^{max})^2})}. \end{aligned} \tag{4.73}$$

The step functions of the integrand now give us the following restrictions

$$\hat{\theta}(u_+) \neq 0 \Rightarrow -m^2 < x < (m_{ab}^{max})^2 - m^2, \tag{4.74}$$

$$\hat{\theta}(v_+) \neq 0 \Rightarrow -\frac{1-a}{a}(m_{ab}^{max})^2 - m^2(1 - \frac{(m_{ab}^{max})^2}{a(m_{ac}^{max})^2}) < x, \tag{4.75}$$

$$\hat{\theta}(u_-) \neq 0 \Rightarrow 0 < m^2 < (m_{ab}^{max})^2, \tag{4.76}$$

$$\hat{\theta}(v_-) \neq 0 \Rightarrow m^2(1 - a\frac{(m_{ac}^{max})^2}{(m_{ab}^{max})^2}) - (m_{ac}^{max})^2(1-a) < x < m^2. \tag{4.77}$$

These inequalities coincide at the distinct values m_{ab}^{max}, m_{ac}^{max} and m_{c2}^{max}. There are the following hierarchies:

$$\begin{aligned} &A1) \quad m_{ab}^{max} < m_{ac}^{max} < m_{c2}^{max}, \\ &A2) \quad m_{c2}^{max} < m_{ac}^{max} < m_{ab}^{max}, \\ &B) \quad m_{ab}^{max} < m_{ac}^{max}. \end{aligned}$$

Again, for the hierarchies A1 and A2 $2m_C^2 - m_D^2 > 0$ and $2m_C^2 - m_D^2 < 0$ for B. Carefully checking the bounds on $x_\pm$ we find:

Hierarchy A1 & B: $m_{ab}^{max} < m_{ac}^{max}$

$\mathbf{0 < m < m_{ab}^{max}}$: $\quad m^2(1 - a\frac{(m_{ac}^{max})^2}{(m_{ab}^{max})^2}) - (m_{ac}^{max})^2(1-a) < x_- < 0$
$\qquad\qquad\qquad\qquad\quad 0 < x_+ < (m_{ab}^{max})^2 - m^2$

$\mathbf{m_{ab}^{max} < m}$: $\quad 0 < x_- < 0$
$\qquad\qquad\qquad\qquad\quad 0 < x_+ < 0$

Hierarchy A2: $m_{c2}^{max} < m_{ac}^{max} < m_{ab}^{max}$

$\mathbf{0 < m < m_{c2}^{max}}$: $\quad m^2(1 - a\frac{(m_{ac}^{max})^2}{(m_{ab}^{max})^2}) - (m_{ac}^{max})^2(1-a) < x_- < 0$
$\qquad\qquad\qquad\qquad\quad 0 < x_+ < (m_{ab}^{max})^2 - m^2$

$\mathbf{m_{c2}^{max} < m < m_{ac}^{max}}$: $\quad 0 < x_- < 0$
$\qquad\qquad\qquad\qquad\quad -\frac{1-a}{a}(m_{ab}^{max})^2 - m^2(1 - \frac{(m_{ab}^{max})^2}{a(m_{ac}^{max})^2}) < x_+ < (m_{ab}^{max})^2 - m^2$

$\mathbf{m_{ac}^{max} < m < m_{ab}^{max}}$: $\quad 0 < x_- < 0$
$\qquad\qquad\qquad\qquad\quad 0 < x_+ < 0$

The plots can be found in figures 4.16 and 4.17.

4.4.7 The Dilepton-Photon Invariant Mass Distribution

This distribution (figures 4.18 and 4.19) was calculated only numerically since analytical results become very large. The full expression for the phase space distribution can be found in [15].

4.4.8 The Short Decay Chain

For the short decay chain we only have to consider the quark-photon invariant mass distribution. As before the invariant mass distribution (figures 4.20 and 4.21) is

$$\frac{1}{\Gamma_0}\frac{d\Gamma}{dm_{ab}^2} = \frac{1}{\Gamma_0}\frac{1}{4E_a^{(B)}E_b^{(B)}}\frac{d\Gamma}{du}, \tag{4.78}$$

where $u = 1/2(1 - \cos\theta_{ba}^{(B)})$ and

$$\frac{1}{\Gamma_0}\frac{d\Gamma}{du} = \frac{1}{\int |\mathcal{M}|^2 du}|\mathcal{M}|^2. \tag{4.79}$$

The invariant mass m_{ab} lies in the range $[0, m_{ab}^{(max)}]$, $m_{ab}^{(max)} \equiv 4E_a^{(B)}E_b^{(B)}$.

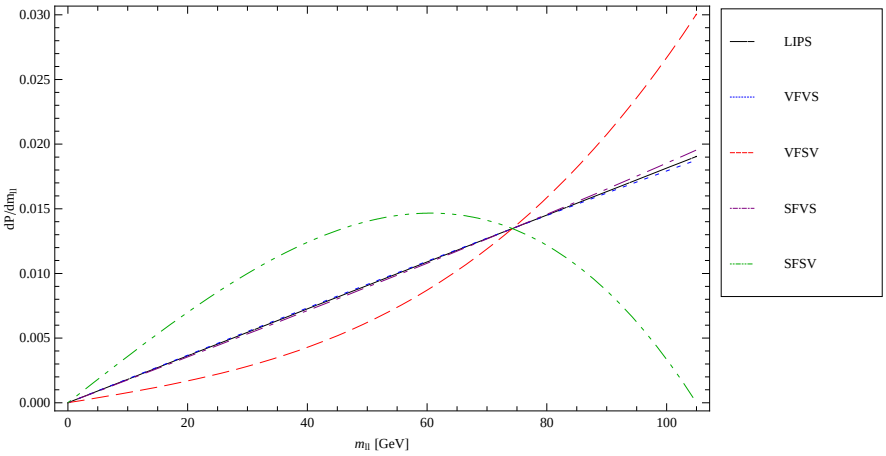

Figure 4.6: Lepton-lepton invariant mass distribution with GMSB masses.

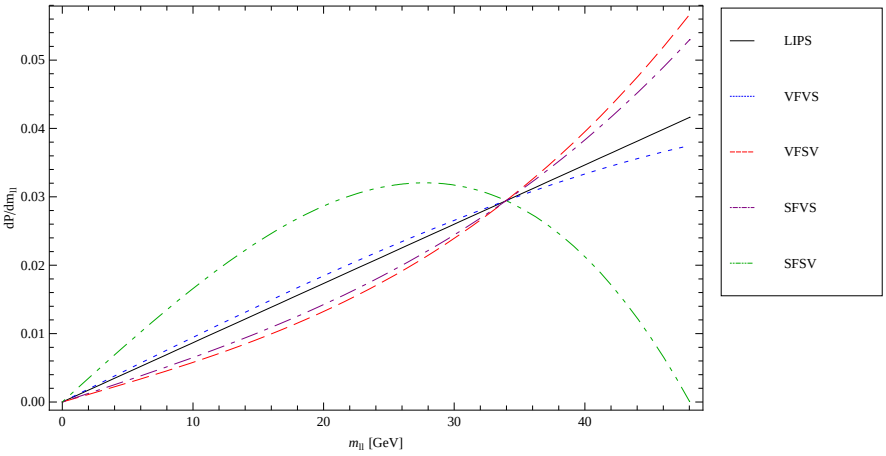

Figure 4.7: Lepton-lepton invariant mass distribution with 2UED masses.

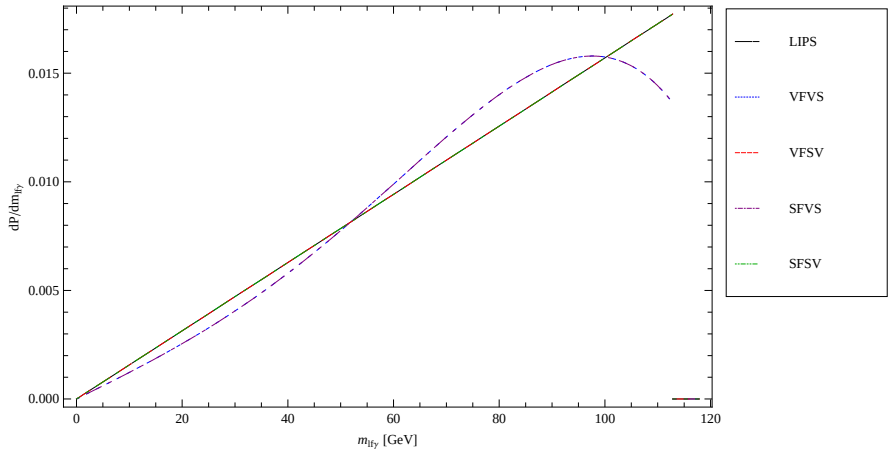

Figure 4.8: Far-lepton–photon invariant mass distribution with GMSB masses.

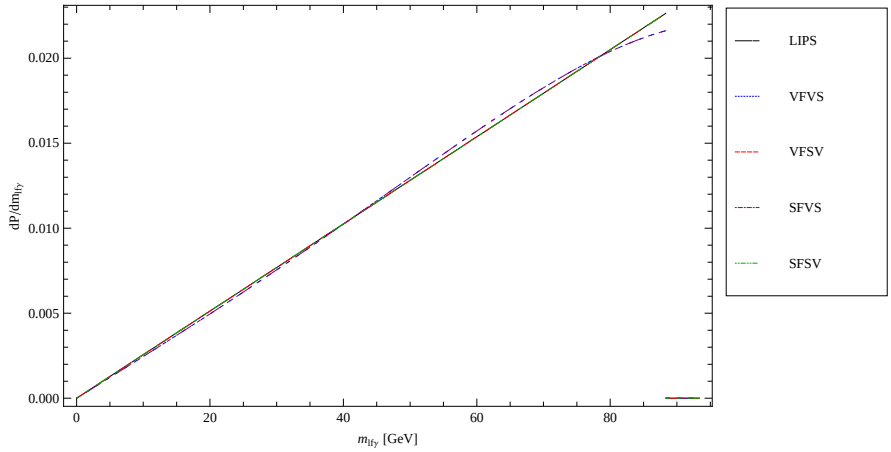

Figure 4.9: Far-lepton–photon invariant mass distribution with 2UED masses.

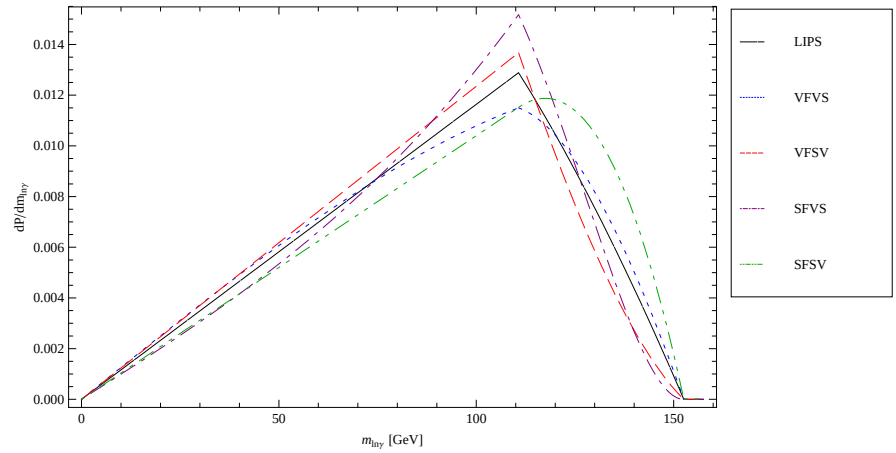

Figure 4.10: Near-lepton–photon invariant mass distribution with GMSB masses.

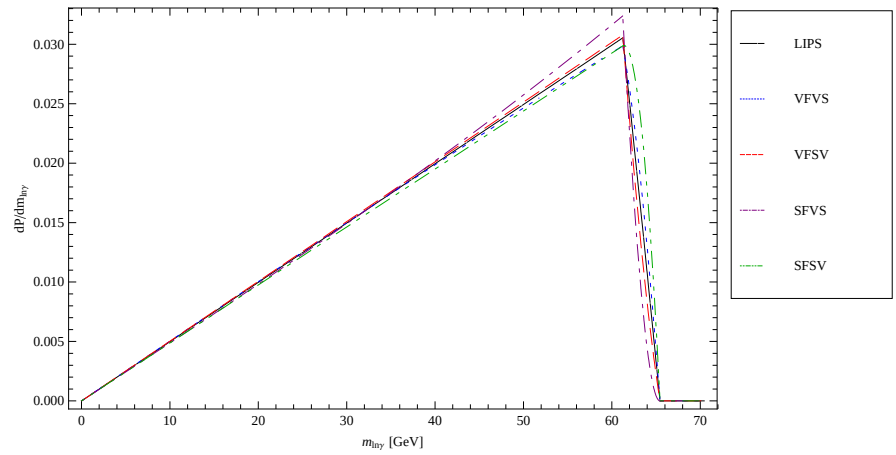

Figure 4.11: Near-lepton–photon invariant mass distribution with 2UED masses.

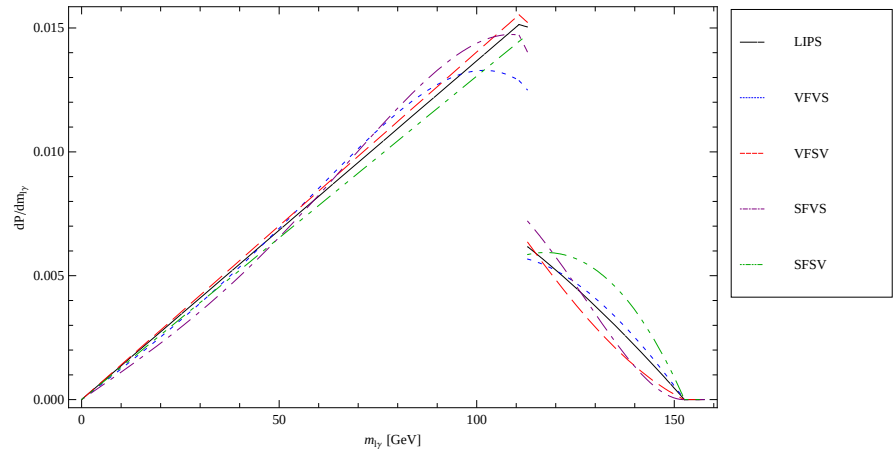

Figure 4.12: Observable lepton-photon invariant mass distribution with GMSB masses.

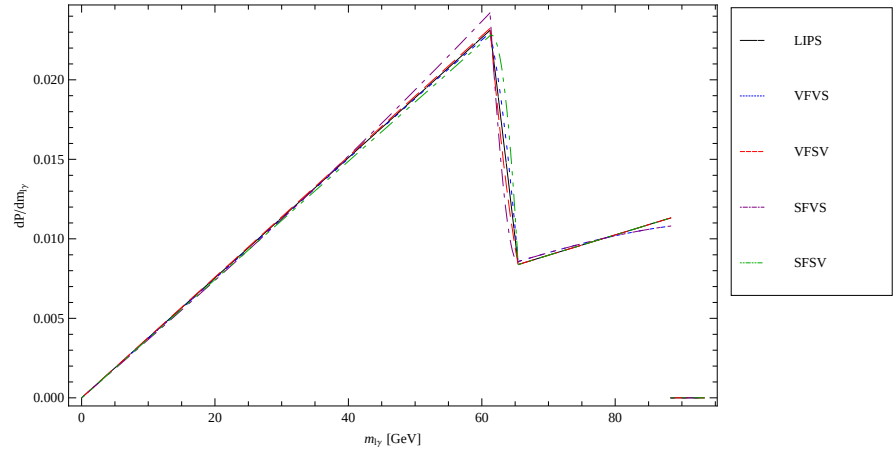

Figure 4.13: Observable lepton-photon invariant mass distribution with 2UED masses.

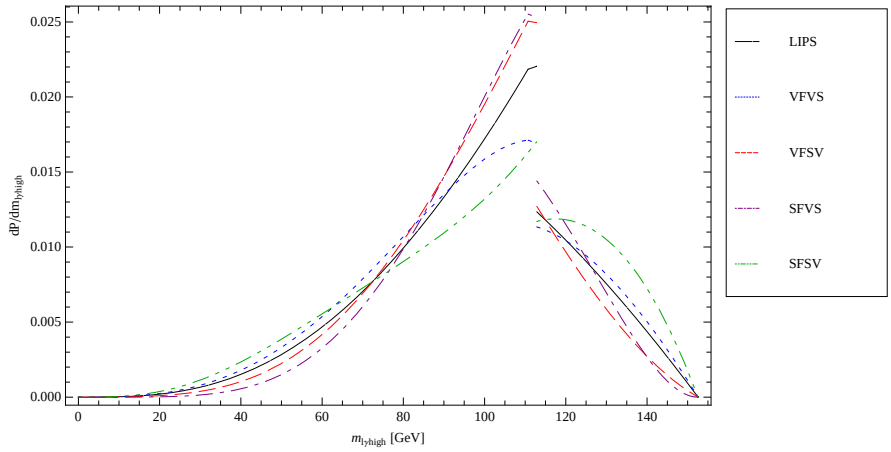

Figure 4.14: High lepton-photon invariant mass distribution with GMSB masses.

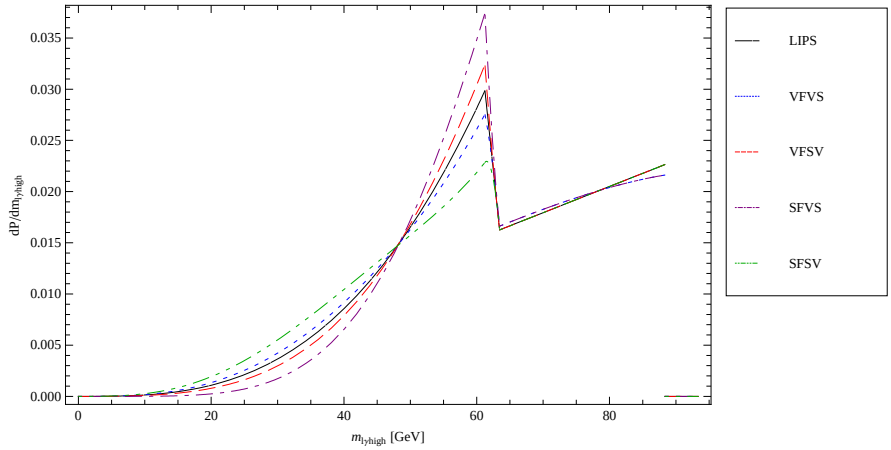

Figure 4.15: High lepton-photon invariant mass distribution with 2UED masses.

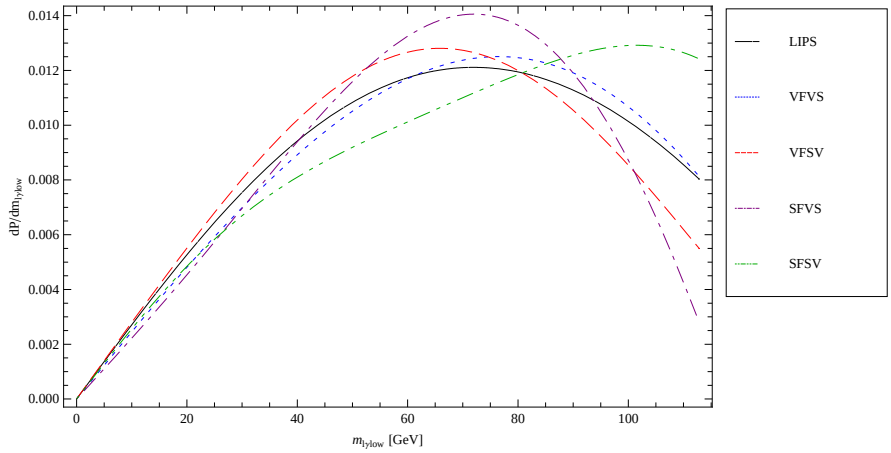

Figure 4.16: Low lepton-photon invariant mass distribution with GMSB masses.

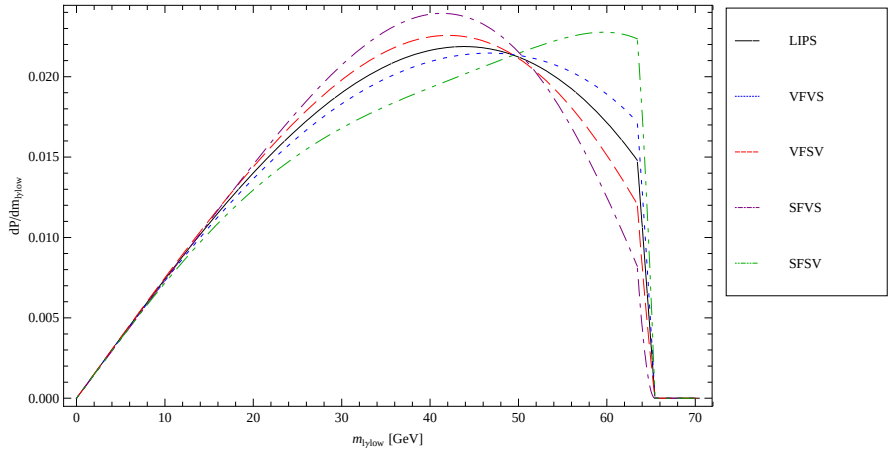

Figure 4.17: Low lepton-photon invariant mass distribution with 2UED masses.

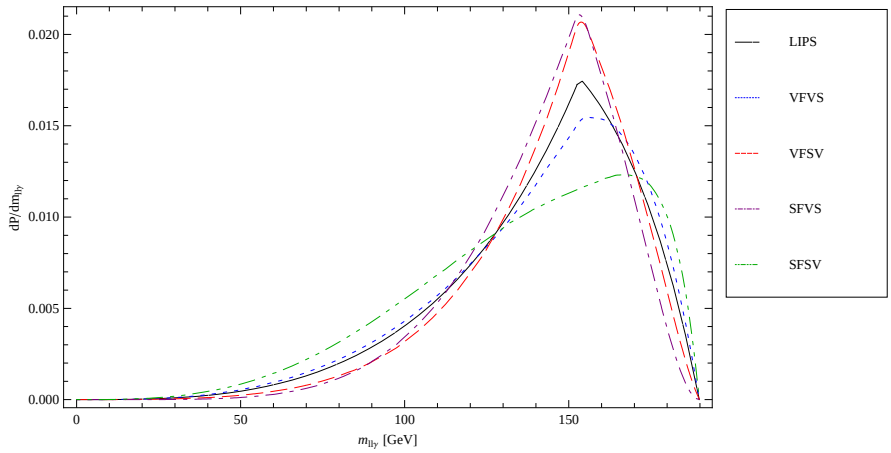

Figure 4.18: Lepton-lepton-photon invariant mass distribution with GMSB masses.

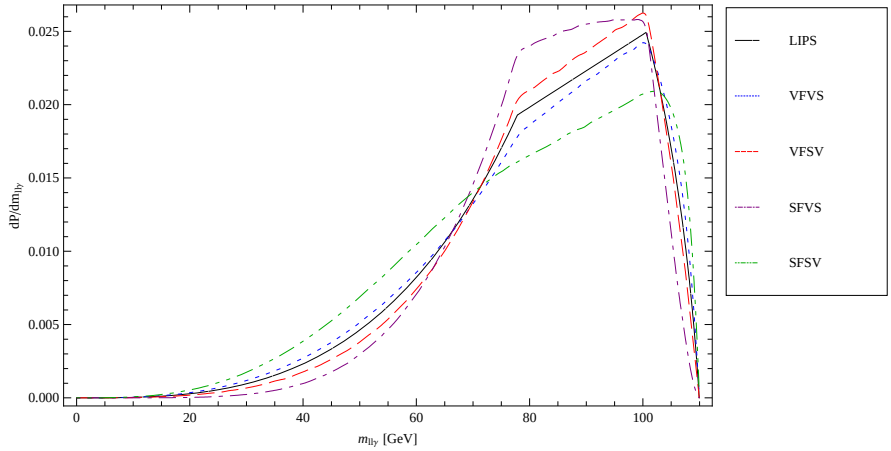

Figure 4.19: Lepton-lepton-photon invariant mass distribution with 2UED masses.

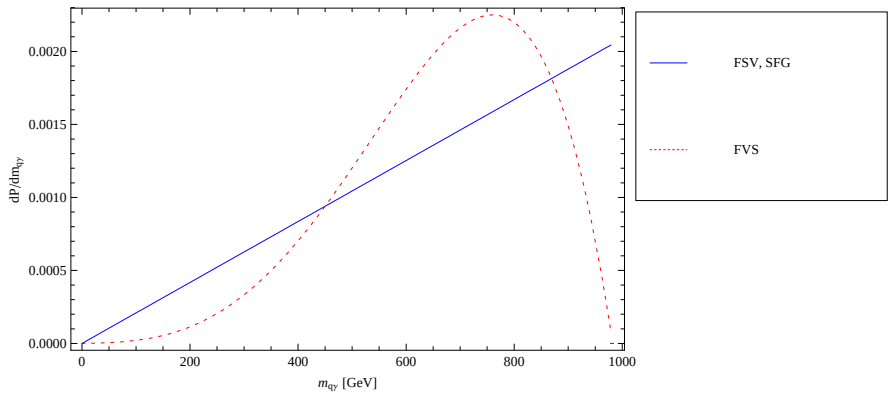

Figure 4.20: Quark-photon invariant mass distribution with GMSB masses.

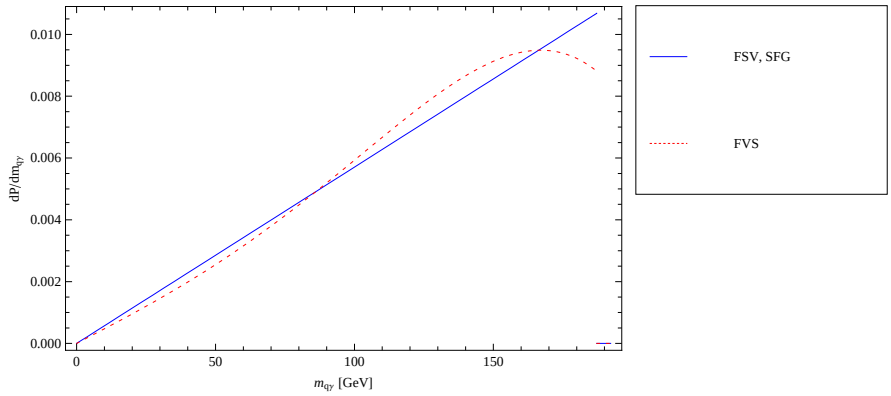

Figure 4.21: Quark-photon invariant mass distribution with 2UED masses.

Chapter 5

Monte Carlo Simulations

Lastly we approach the question whether from real experimental data it would be possible to determine the spin of these EP, given the invariant mass distributions of Chapter 4. As a first step, we generated Monte Carlo events at the parton level with CompHEP [28]. We have chosen the number events arbitrarily and in order to simulate realistic experiments, the histograms have to be normalized taking in account the production cross sections, the branching ratios, the luminosity of the collider and the experimental cuts, which separate the GMSB/2UED events from the SM background.

5.1 Normalization

In order to get normalized histograms for the decay chains with GMSB masses, we scale them with the factor

$$k_{GMSB} = \frac{N_H}{N}, \tag{5.1}$$

where $N_H = 2457$ is the number of events of [7] for a luminosity 10 fb^{-1} and after applying their cuts. N is the number of events of the histograms we generated. For the 2UED mass spectrum, we have to scale the histograms with the factor

$$k_{2UED} = k_{GMSB} \frac{\sigma_{2UED}}{\sigma_{GMSB}}, \tag{5.2}$$

where σ_{GMSB} and σ_{2UED} are the cross sections of the GMSB and 2UED decay chains. This gives us histograms taking account to the points listed above.

The GMSB cross section is calculated by multiplying the squark production cross section with branching ratio for the specific decay chain. Since the gluino mass is smaller than the squark mass, the squark mainly decays through cascades with a gluino ($\tilde{g} \to q\ \tilde{q}_R \to q\ q\ \tilde{\chi}_2^0$). The branching ratio for a gluino decaying to a 2 neutralino is

$$\mathrm{BR}\left(\tilde{g} \to q\ q\ \tilde{\chi}_2^0\right) \sim 16\,\%. \tag{5.3}$$

The neutralino then chooses our decay chain with a branching ratio

$$\mathrm{BR}\left(\tilde{\chi}_2^0 \to e^+\ e^-\ \gamma\ \tilde{G}\right) \sim 26\,\%. \tag{5.4}$$

Lastly, the total squark production cross section, including squarks from gluino decays, is written down in [7]: $\sigma_{\tilde{q}} = 7.6$ pb. So, the cross section for the decay chain in the GMSB model is

$$\sigma_{GMSB} = \mathrm{BR}\left(\tilde{g} \to q\, q\, \tilde{\chi}_2^0\right) \times \mathrm{BR}\left(\tilde{\chi}_2^0 \to e^+\, e^-\, \gamma\, \tilde{G}\right) \times \sigma_{\tilde{q}} \sim 0.3 \text{ pb}. \tag{5.5}$$

The cross section for the 2UED decay chain is calculated in a similar way. The branching ratios for a KK-quark decaying to a KK-Z-boson and the KK-Z-boson to a electron pair and a photon are

$$\mathrm{BR}\left(Q_+^{(1)} \to Z^{(1)}\, q\right) \sim 6.4\,\%, \tag{5.6}$$

$$\mathrm{BR}\left(Z^{(1)} \to e^+\, e^-\, \gamma\, B_H^{(1)}\right) \sim 0.5\%. \tag{5.7}$$

With a compactifying radius $R^{-1} = 500\,\mathrm{GeV}$ the KK-quark production cross sections are

$$\begin{aligned} &\sigma_{Q_+^{(1)}\, Q_+^{(1)}} \sim 7 \text{ pb}, && \sigma_{Q_+^{(1)}\, Q_-^{(1)}} \sim 18 \text{ pb}, \\ &\sigma_{G_\mu^{(1)}\, G_\mu^{(1)}} \sim 10 \text{ pb}, && \sigma_{G_\mu^{(1)}\, Q_+^{(1)}} \sim 24 \text{ pb}, \\ &\sigma_{G_\mu^{(1)}\, Q_-^{(1)}} \sim 26 \text{ pb}. \end{aligned} \tag{5.8}$$

There are additional production channels involving the scalar $G_H^{(1)}$ and weakly coupled particles which have been neglected here. In the last three production channels the KK-gluon can decay to a weak-doublet KK-quark with a branching ratio of

$$\mathrm{BR}\left(G_\mu^{(1)} \to Q_+^{(1)}\, q\right) \sim 50\,\%. \tag{5.9}$$

These branching ratios and the different KK-quark production cross sections are listed in [12]. So we end up with the 2UED cross section for the decay chain

$$\begin{aligned} \sigma_{2UED} &= \mathrm{BR}\left(Q_+^{(1)} \to Z^{(1)}\, q\right) \times \mathrm{BR}\left(Z^{(1)} \to e^+\, e^-\, \gamma\, B_H^{(1)}\right) \\ &\times \Bigg(2\,\sigma_{Q_+^{(1)}\, Q_+^{(1)}} + \sigma_{Q_+^{(1)}\, Q_-^{(1)}} + 2\,\mathrm{BR}\left(G_\mu^{(1)} \to Q_+^{(1)}\, q\right)\, \sigma_{G_\mu^{(1)}\, G_\mu^{(1)}} \\ &+ \left(1 + \mathrm{BR}\left(G_\mu^{(1)} \to Q_+^{(1)}\, q\right)\right)\, \sigma_{G_\mu^{(1)}\, Q_+^{(1)}} + \mathrm{BR}\left(G_\mu^{(1)} \to Q_+^{(1)}\, q\right)\, \sigma_{G_\mu^{(1)}\, Q_-^{(1)}}\Bigg) \\ &\sim 0.03 \text{ pb}. \end{aligned} \tag{5.10}$$

Thus we obtain 10 times fewer events in the 2UED case compared to the GMSB model.

5.2 The χ^2 Test

In order to discriminate these normalized histograms [29] we calculated for each pair of spin configurations and each distribution a χ^2 value and so the χ^2 probability.

We consider two histograms with r bins. The number of events in the ith bin in the first histogram is denoted as n_i and in the second as m_i. The total

numbers of events are $N = \sum_{i=1}^{r} n_i$ and $M = \sum_{i=1}^{r} m_i$ respectively. In order to discriminate two histograms we test the hypothesis of homogeneity, which says that the two histograms represent random numbers with identical probability distributions. I.e. there exist r constants $p_1, \cdots, p_r$, such that $\sum_{i=1}^{r} p_i = 1$. p_i is the probability for a measured value of belonging to the ith bin. The number of events in the ith bin is distributed according to the Poisson distribution $e^{-Np_i}(Np_i)^{n_i}/n_i!$ for the first histogram and $e^{-Mp_i}(Mp_i)^{m_i}/m_i!$ for the second. If the hypothesis of homogeneity is valid, then the maximum likelyhood estimator of p_i is

$$\hat{p}_i = \frac{n_i + m_i}{N + M}, \quad i = 1, \cdots, r. \tag{5.11}$$

We define

$$X^2 = \sum_{i=1}^{r} \frac{(n_i - N\hat{p}_i)^2}{N\hat{p}_i} + \sum_{i=1}^{r} \frac{(m_i - M\hat{p}_i)^2}{M\hat{p}_i} = \frac{1}{MN} \sum_{i=1}^{r} \frac{(Mn_i - Nm_i)^2}{n_i + m_i}, \tag{5.12}$$

which has approximately a $\chi^2_{(r-1)}$ distribution, $r-1$ being the number of degrees of freedom.

The probability distribution for χ^2 is given by

$$P(\chi^2; r-1) = \frac{2^{-(r-1)/2}}{\Gamma((r-1)/2)} \chi^{r-3} e^{-\chi^2/2}. \tag{5.13}$$

The probability that an observed χ^2 exceeds the value X^2 by chance, even for a correct model, is

$$\text{Prob}(X^2; r-1) = \int_{X^2}^{\infty} P(\chi^2; r-1) d\chi^2. \tag{5.14}$$

This is called the χ^2 probability. It is the probability that two histograms with the same underlying distribution give a larger χ^2 than we already have. The hypotheses of homogeneity is rejected if the χ^2 probability is lower than some significance level. Traditionally significance levels 0.1, 0.05 and 0.01 are used.

5.3 Results

The χ^2 probability changes its value for different numbers of bins r. In our analysis $r = 2$ gave the best discrimination capability. In Appendix C we list the different results. A value of 1 implies that there is no discrimination possibility between the two distributions and 0 signifies that the two histograms are well distinguishable. We choose a confidence level of 95 %, i.e. two histograms with a χ^2 probability less than 0.05 are regarded as two different distributions, which is true in 95 % of the cases.

With this confidence level we can distinguish all spin configurations in the GMSB mass scenario assuming an integrated luminosity[1] of 10 fb^{-1} (table 5.1) — if we take in account all different invariant mass distributions. In the 2UED mass scenario it gets more difficult, where we cannot distinguish the spin configurations FSFG-VFVS, FSFG-VFSV, FSFG-SFVS and VFSV-SFVS with a confidence level of 95 % (table 5.2). Nevertheless, assuming a luminosity of 30 fb^{-1}, all histograms are distinguishable but FSFG-VFVS (table 5.3).

	FSFG	VFVS	VFSV	SFVS	SFSV
FSFG	—	0.019	0.000	0.000	0.000
VFVS		—	0.000	0.000	0.000
VFSV			—	0.000	0.000
SFVS				—	0.000
SFSV					—

Table 5.1: Minimal χ^2 probabilities for the GMSB mass spectrum at 10 fb^{-1}, taking in account all different invariant mass distributions

	FSFG	VFVS	VFSV	SFVS	SFSV
FSFG	—	0.574	0.074	0.142	0.000
VFVS		—	0.019	0.051	0.000
VFSV			—	0.257	0.000
SFVS				—	0.000
SFSV					—

Table 5.2: Minimal χ^2 probabilities for the 2UED mass spectrum at 10 fb^{-1}, taking in account all different invariant mass distributions

However it is important to point out that these numbers in the tables correspond to perfect experimental conditions. In real-life experiments a lot of different effects may affect these curves. To name a few:

- In order to isolate the decay chain from the SM background cuts have to be applied (e.g. on the missing energy) which can alter the distribution curves.
- Since the squarks/ KK-quarks are always produced in pairs, the "other" squark/ KK-quark also decays in the LSP, contributes to the missing energy and thus can affect cuts.
- The decaying particles can emit additional photons, which can be misstaken for the photon in the decay chain.
- The detector resolution and efficiency also effect the shapes of the invariant mass distribution.
- In order to carry out this spin analysis, the masses of the involved particles have to be quantified with some kinematical measurements, which account for a further uncertainity.

In order to take these effects into account we would have to interface the CompHEP events into Pythia [30] linked to a detector simulation such as ATLFAST [31]. However this has not been accomplished within this thesis.

[1] An integrated luminosity of 10 fb^{-1} corresponds to one year of running at 10^{33} cm^{-2}s^{-1}.

	FSFG	VFVS	VFSV	SFVS	SFSV
FSFG	—	0.330	0.002	0.011	0.000
VFVS		—	0.000	0.001	0.000
VFSV			—	0.050	0.000
SFVS				—	0.000
SFSV					—

Table 5.3: Minimal χ^2 probabilities for the 2UED mass spectrum at 30 fb^{-1}, taking in account all different invariant mass distributions

Chapter 6

Summary and Conclusions

The Standard Model of particle physics (SM) is very successful in describing fundamental interactions of elementary particles that have been explored in high energy experiments over the past century. However, there are shortcomings on the theoretical and on the phenomenological side. For example the Higgs boson gets corrections that are some 30 orders of magnitude bigger than its Lagrangian mass. This is considered as unnatural and composes one of several theoretical defects of the SM. From a phenomenological point of view, it would be nice to incorporate a description of dark matter, which is responsible for cosmological effects on different length scales (rotation curves of galaxies, cosmic microwave background, to name a few).

Extensions to the Standard Model are able to cure some of these deficiencies — but not all of them. Furthermore, they often provide us with a whole set of partners to the SM particles. So, gathering information about newly measured particles (such as spin and mass), may give us hints about the unterlying theory, which extends the SM. One way to learn something about these new particles is through high energy experiments, such as the LHC which is going to produce data within the next years.

Lately some groups have studied the decays of the quark partner with one quark jet and one lepton pair. In this thesis we compared a supersymmetric model — gauge mediated supersymmetry breaking (GMSB) — with an extra-dimensional model — two universal extra dimensions (2UED). Both have the characteristic to emit a photon when a SM-partner decays. So we concentrated ourselves on decay chains with one lepton pair and one photon. In order to study model discrimination in a general way we considered five generic decay chains FSFG, VFVS, VFSV, SFVS and SFSV (figure 4.1).

First, we calculated analytical expressions for the different invariant mass distributions (figures 4.6 to 4.21). The shapes of these distributions give us information about the spin of the decaying and the intermediate particles. In order to formulate this quantitatively we generated Monte Carlo events with the parton level generator CompHEP and created histograms for the different invariant masses at a collider luminosity of 10 fb^{-1}. These histograms can be compared for the different models using the χ^2 test (Appendix C). As table 5.1 shows, we can distinguish the different spin configurations assuming GMSB masses with a confidence level of 95 %, if we consider all different mass distributions. On the other hand, if we assume the masses to be of 2UED type,

it will be harder to separate the different models. Especially the spin configurations FSFG-VFVS, FSFG-VFSV, FSFG-SFVS and VFSV-SFVS cannot be distinguished with that confidence level. Calculating the χ^2 probabilities for an integrated luminosity of 30 fb^{-1} only the spin configurations FSFG-VFVS stay indistinguishable.

However, the values we calculated correspond to perfect experimental conditions. In order to get more realistic data, we should generate the Monte Carlo data with a general purpose event generator, which also takes into account different factors such as final state radiation and detector effects. This will be done in a following analysis with the event generator Pythia and the detector simulation ATLFAST.

Appendix A

Matrix Element Calculation

A.1 2UED Feynman Rules

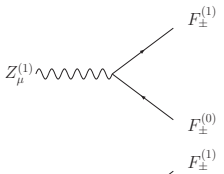

$= -ig_W \gamma^\mu P_{L/R}$

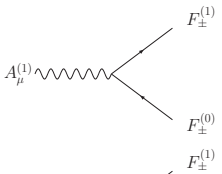

$= -ig_W \gamma^\mu P_{L/R}$

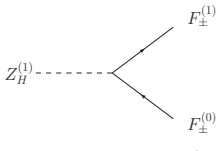

$= -ig_W P_{L/R}$

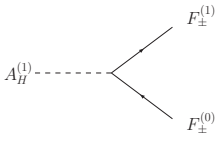

$= -ig_W P_{L/R}$

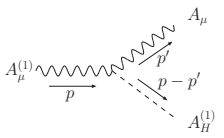

$\propto \epsilon^{\mu\nu\alpha\beta} \varepsilon_\mu^*(p - p') \varepsilon_\nu(p) p_\alpha p'_\beta$

A.2 Matrix Element Squared

$$
\begin{aligned}
|\mathcal{M}_{VFVS}|^2 = \frac{1}{m_D^2} 8 \big(& (p_a p_B) \big(m_C^2 m_D^2 (p_a p_c)(p_b p_B) - 2 \big(2(p_b p_D)(p_c p_D) m_C^2 m_B^2 \\
& + (p_b p_c) m_C^2 m_D^2 m_B^2 - 2 m_D^2 (p_b p_C)(p_c p_C) m_B^2 - 4 (p_b p_C)(p_c p_D)(p_C p_D) m_B^2 \\
& + 4 (p_b p_B)(p_B p_D)(p_c p_D) m_C^2 + 2 (p_b p_B)(p_B p_c) m_C^2 m_D^2 + (p_a p_C)(p_b p_B)(p_c p_C) m_D^2 \\
& - 4 m_D^2 (p_b p_B)(p_B p_C)(p_c p_C) - m_C^2 (p_a p_D)(p_b p_B)(p_c p_D) \\
& + 2 (p_a p_C)(p_b p_B)(p_c p_D)(p_C p_D) - 8 (p_b p_B)(p_B p_C)(p_c p_D)(p_C p_D) \big) \big) \\
& + (p_a p_b) \big(2 \big((p_a p_C) \big((p_c p_C) m_D^2 + 2 (p_c p_D)(p_C p_D) \big) - m_C^2 (p_a p_D)(p_c p_D) \big) m_B^2 \\
& + (p_a p_c) \big(-m_B^2 \big) m_C^2 m_D^2 + (p_a p_B) \big((p_B p_c) m_D^2 m_C^2 + 2 (p_B p_D)(p_c p_D) m_C^2 \\
& - 2 (p_B p_C) \big((p_c p_C) m_D^2 + 2 (p_c p_D)(p_C p_D) \big) \big) \big) - \big(m_A^2 - m_B^2 \big) \big((p_b p_c) m_B^2 m_C^2 m_D^2 \\
& + 2 \big(\big(m_C^2 (p_b p_D)(p_c p_D) - (p_b p_C) \big((p_c p_C) m_D^2 + 2 (p_c p_D)(p_C p_D) \big) \big) m_B^2 \\
& + (p_b p_B) \big((p_B p_c) m_D^2 m_C^2 + 2 (p_B p_D)(p_c p_D) m_C^2 \\
& - 2 (p_B p_C) \big((p_c p_C) m_D^2 + 2 (p_c p_D)(p_C p_D) \big) \big) \big) \big) \big)
\end{aligned}
\tag{A.1}
$$

$$
|\mathcal{M}_{VFSV}|^2 = -\frac{8 (p_a p_B)^2 \big(m_D^2 (p_b p_c) + 2 (p_b p_D)(p_c p_D) \big)}{m_D^2}
\tag{A.2}
$$

$$
\begin{aligned}
|\mathcal{M}_{SFVS}|^2 = -8 \big(& (p_a p_b) \big(-m_B^2 (p_a p_c) + (p_a p_B)(p_B p_c) \big) \\
& + (p_a p_B) \big((p_a p_c)(p_b p_B) - 2 m_B^2 (p_b p_c) - 4 (p_b p_B)(p_B p_c) \big) \\
& - \big(m_A^2 - m_B^2 \big) \big(m_B^2 (p_b p_c) + 2 (p_b p_B)(p_B p_c) \big) \big)
\end{aligned}
\tag{A.3}
$$

$$
|\mathcal{M}_{SFSV}|^2 = \frac{8 \big(m_B^2 - 2 (p_a p_B) \big) (p_a p_B)^2 \big(m_C^2 (p_b p_c) - 2 (p_b p_C)(p_c p_C) \big)}{m_A^2}
\tag{A.4}
$$

$$
\begin{aligned}
|\mathcal{M}_{FVS}|^2 = -16 \big(& (p_a p_B) \big(-2 m_B^2 (p_b p_C) + (p_b p_B)((p_a p_C) - 4 (p_B p_C)) \big) \\
& + (p_a p_b) \big(-m_B^2 (p_a p_C) + (p_a p_B)(p_B p_C) \big) \\
& - \big(m_A^2 - m_B^2 \big) \big(m_B^2 (p_b p_C) + 2 (p_b p_B)(p_B p_C) \big) \big)
\end{aligned}
\tag{A.5}
$$

Appendix B

Invariant Mass Distributions

B.1 Structures

Decay $D \to cC \to cbB \to cbaA$ with masses $m_A \leq m_B \leq m_C \leq m_D$.

$$
\begin{aligned}
(m_{ab}^{max})^2 &= \frac{(m_C^2 - m_B^2)(m_B^2 - m_A^2)}{m_B^2} \\
(m_{ac}^{max})^2 &= \frac{(m_D^2 - m_C^2)(m_B^2 - m_A^2)}{m_B^2} \\
(m_{c2}^{max})^2 &= \frac{(m_D^2 - m_C^2)(m_B^2 - m_A^2)}{2m_C^2 - m_D^2}
\end{aligned} \tag{B.1}
$$

B.1.1 The Far-Lepton–Photon Invariant Mass Distribution

$$
\frac{dP}{dm_{l_f\gamma}^2} = C1_f \tag{B.2}
$$

B.1.2 The Near-Lepton–Photon Invariant Mass Distribution

$$
\frac{dP}{dm_{l_n\gamma}^2} = \begin{cases} C1_n & 0 \leq m \leq m_{ac}^{max}\frac{m_B}{m_C} \\ C2_n & m_{ac}^{max}\frac{m_B}{m_C} < m \leq m_{ac}^{max} \end{cases} \tag{B.3}
$$

B.1.3 The High Lepton-Photon Invariant Mass Distribution

Hierarchy A11: $m_{ab}^{max} < m_{ac}^{max}\frac{m_B}{m_C} < m_{ac}^{max} < m_{c2}^{max}$

$$
\frac{dP}{dm_{l\gamma h}^2} = \begin{cases} C1_{hA11} & 0 \leq m \leq m_{ab}^{max} \\ C2_{hA11} & m_{ab}^{max} < m \leq m_{ac}^{max}\frac{m_B}{m_C} \\ C3_{hA11} & m_{ac}^{max}\frac{m_B}{m_C} < m \leq m_{c2}^{max} \end{cases} \tag{B.4}
$$

Hierarchy A12: $m_{ac}^{max}\frac{m_B}{m_C} < m_{ab}^{max} < m_{ac}^{max} < m_{c2}^{max}$

$$\frac{dP}{dm_{l\gamma h}^2} = \begin{cases} C1_{hA12} & 0 \leq m \leq m_{ac}^{max}\frac{m_B}{m_C} \\ C2_{hA12} & m_{ac}^{max}\frac{m_B}{m_C} < m \leq m_{ab}^{max} \\ C3_{hA12} & m_{ab}^{max} < m \leq m_{c2}^{max} \end{cases} \tag{B.5}$$

Hierarchy A2: $m_{ac}^{max}\frac{mB}{mC} > m_{a2}^{max} > m_{ac}^{max} > m_{ab}^{max}$

$$\frac{dP}{dm_{l\gamma h}^2} = \begin{cases} C1_{hA2} & 0 \leq m \leq m_{ac}^{max}\frac{m_B}{m_C} \\ C2_{hA2} & m_{ac}^{max}\frac{m_B}{m_C} < m \leq m_{c2}^{max} \\ C3_{hA2} & m_{c2}^{max} < m \leq m_{ab}^{max} \end{cases} \tag{B.6}$$

Hierarchy B1: $m_{ab}^{max} < m_{ac}^{max}\frac{m_B}{m_C} < m_{ac}^{max}$

$$\frac{dP}{dm_{l\gamma h}^2} = \begin{cases} C1_{hB1} & 0 \leq m \leq m_{ab}^{max} \\ C2_{hB1} & m_{ab}^{max} < m \leq m_{ac}^{max}\frac{m_B}{m_C} \\ C3_{hB1} & m_{ac}^{max}\frac{m_B}{m_C} < m \leq m_{ac}^{max} \end{cases} \tag{B.7}$$

Hierarchy B2: $m_{ac}^{max}\frac{m_B}{m_C} < m_{ab}^{max} < m_{ac}^{max}$

$$\frac{dP}{dm_{l\gamma h}^2} = \begin{cases} C1_{hB2} & 0 \leq m \leq m_{ac}^{max}\frac{m_B}{m_C} \\ C2_{hB2} & m_{ac}^{max}\frac{m_B}{m_C} < m \leq m_{ab}^{max} \\ C3_{hB2} & m_{ab}^{max} < m \leq m_{ac}^{max} \end{cases} \tag{B.8}$$

B.1.4 The Low Lepton-Photon Invariant Mass Distribution

Hierarchy A1: $m_{ab}^{max} < m_{ac}^{max} < m_{c2}^{max}$

$$\frac{dP}{dm_{l\gamma l}^2} = C1_{lA1} \tag{B.9}$$

Hierarchy A2: $m_{c2}^{max} < m_{ac}^{max} < m_{ab}^{max}$

$$\frac{dP}{dm_{l\gamma l}^2} = \begin{cases} C1_{lA2} & 0 \leq m \leq m_{c2}^{max} \\ C2_{lA2} & m_{c2}^{max} < m \leq m_{ac}^{max} \end{cases} \tag{B.10}$$

Hierarchy B: $m_{ab}^{max} < m_{ac}^{max}$

$$\frac{dP}{dm_{l\gamma l}^2} = C1_{lB} \tag{B.11}$$

B.1.5 Relations

$$
\begin{aligned}
&C1_f = C3_{A2}\\
&C1_n = C2_{hA11} = C2_{hB1}\\
&C2_n = C3_{hA11} = C3_{hA12} = C3_{hB1} = C3_{hB2} = C2_{lA2}\\
&C1_{hA11} = C1_{hA12} = C1_{hA2} = C1_{hB1} = C1_{hB2}\\
&C2_{hA12} = C2_{hA2} = C2_{hB2}\\
&C1_{lA1} = C1_{lA2} = C1_{lB}
\end{aligned}
\tag{B.12}
$$

B.2 Coefficients

B.2.1 FSFG

$$
C1_f = \frac{m_B^2}{\left(m_A^2 - m_B^2\right)\left(m_B^2 - m_C^2\right)} \tag{B.13}
$$

$$
C1_n = \frac{m_B^2 m_C^2 \log\left[\frac{m_B^2}{m_C^2}\right]}{\left(m_A^2 - m_B^2\right)\left(m_B^2 - m_C^2\right)\left(m_C^2 - m_D^2\right)} \tag{B.14}
$$

$$
C2_n = \frac{m_B^2 m_C^2 \log\left[\frac{m^2 m_B^2}{\left(m_A^2 - m_B^2\right)\left(m_C^2 - m_D^2\right)}\right]}{\left(m_A^2 - m_B^2\right)\left(m_B^2 - m_C^2\right)\left(m_C^2 - m_D^2\right)} \tag{B.15}
$$

$$
C1_{hA11} = -\frac{m_B^2 m_C^2 \left(m^2 + 2\left(m^2 - m_A^2 + m_B^2\right)\operatorname{arccoth}\left[\frac{m^2 - 2m_A^2 + 2m_B^2}{m^2}\right]\right)}{\left(m_A^2 - m_B^2\right)\left(m^2 - m_A^2 + m_B^2\right)\left(m_B^2 - m_C^2\right)\left(m_C^2 - m_D^2\right)} \tag{B.16}
$$

$$
C2_{hA12} = -\frac{m_B^2 m_C^2 \left(m^2 + \left(m^2 - m_A^2 + m_B^2\right)\log\left[-\frac{\left(m^2 - m_A^2 + m_B^2\right)\left(m_C^2 - m_D^2\right)}{m^2 m_C^2}\right]\right)}{\left(m_A^2 - m_B^2\right)\left(m^2 - m_A^2 + m_B^2\right)\left(m_B^2 - m_C^2\right)\left(m_C^2 - m_D^2\right)} \tag{B.17}
$$

$$
\begin{aligned}
C1_{lA1} = \Bigg(& m_B^2 m_C^2 \Bigg(2m^2 - m_A^2 + m_B^2 - \frac{(m^2 - m_A^2 + m_B^2) m_D^2}{m_C^2} \\
& + (m^2 - m_A^2 + m_B^2) \log\left[\frac{m_B^2 (m^2 - m_A^2 + m_B^2)}{(-m_A^2 + m_B^2) m_C^2}\right] \Bigg) \Bigg) \\
& / \Big((m_A^2 - m_B^2)(m^2 - m_A^2 + m_B^2)(m_B^2 - m_C^2)(m_C^2 - m_D^2) \Big)
\end{aligned}
\tag{B.18}
$$

B.2.2 VFVS

$$C1_f = \Big(3m_B^4(2m^4m_B^2 - 2m^2(m_A^2 - m_B^2)(m_B^2 - m_C^2) + (m_A^2 - m_B^2)^2 \times (m_B^2 - m_C^2))\Big)/\Big((m_A^2 - m_B^2)^3(m_B^2 - m_C^2)^2(2m_B^2 + m_C^2)\Big) \tag{B.19}$$

$$\begin{aligned} C1_n = \Big(&6m_B^2m_C^2((m_B^2 - m_C^2)(4m^2m_B^2m_C^2(m_C^2 - 2m_D^2) \\ &+ (m_A^2 - m_B^2)(m_C^2 - m_D^2)(m_B^2m_C^2 - 2(2m_B^2 + m_C^2)m_D^2)) \\ &- 2m_B^2(2m^2m_C^2(m_B^2 + m_C^2)(m_C^2 - 2m_D^2) \\ &+ (m_A^2 - m_B^2)(m_C^2 - m_D^2)(m_C^4 - 2(m_B^2 + 2m_C^2)m_D^2))\log\left[\frac{m_B}{m_C}\right])\Big) \\ &/\Big((m_A^2 - m_B^2)^2(m_B^2 - m_C^2)^2(2m_B^2 + m_C^2)(m_C^2 - m_D^2)^2(m_C^2 + 2m_D^2)\Big) \end{aligned} \tag{B.20}$$

$$\begin{aligned} C2_n = \Bigg(&6m_B^2m_C^2\Bigg(m_C^2(2m^4m_B^4m_C^2 - (m_A^2 - m_B^2)^2(m_C^2 - m_D^2) \\ &\times (3m_B^2m_C^2 - 2(5m_B^2 + m_C^2)m_D^2) + m^2m_B^2(m_A^2 - m_B^2) \\ &\times (-2m_C^4 + m_B^2(3m_C^2 - 10m_D^2))) + m_B^2(m_A^2 - m_B^2)(2m^2m_C^2(m_B^2 + m_C^2) \\ &\times (m_C^2 - 2m_D^2) + (m_A^2 - m_B^2)(m_C^2 - m_D^2)(m_C^4 - 2(m_B^2 + 2m_C^2)m_D^2)) \\ &\times \log\left[\frac{(m_A^2 - m_B^2)(m_C^2 - m_D^2)}{m^2m_B^2}\right]\Bigg)\Bigg) \\ &/\Big((m_A^2 - m_B^2)^3(m_B^2 - m_C^2)^2(2m_B^2 + m_C^2)(m_C^2 - m_D^2)^2(m_C^2 + 2m_D^2)\Big) \end{aligned} \tag{B.21}$$

$$\begin{aligned} C1_{hA11} = \Bigg(&3m_B^4m_C^2\Bigg(m^2(-2(m_A^2 - m_B^2)^4(m_C^2 - m_D^2) \\ &\times (m_C^4 + 2m_B^2m_D^2 - 8m_C^2m_D^2) + 6m^8m_B^2(m_C^4 - 4m_C^2m_D^2 + 2m_D^4) \\ &- 2m^6(m_A^2 - m_B^2)(m_C^6 + 6m_C^4m_D^2 - 8m_C^2m_D^4 \\ &+ 9m_B^2(m_C^4 - 4m_C^2m_D^2 + 2m_D^4)) + m^4(m_A^2 - m_B^2)^2 \\ &\times (5m_C^6 + 34m_C^4m_D^2 - 44m_C^2m_D^4 + m_B^2(19m_C^4 - 78m_C^2m_D^2 + 40m_D^4)) \\ &- m^2(m_A^2 - m_B^2)^3(m_B^2(7m_C^4 - 34m_C^2m_D^2 + 20m_D^4) \\ &- m_C^2(m_C^4 - 44m_C^2m_D^2 + 44m_D^4))) - 2(m_A^2 - m_B^2)(m^2 - m_A^2 + m_B^2)^3 \\ &\times (2m^2m_C^2(m_B^2 + m_C^2)(m_C^2 - 2m_D^2) + (m_A^2 - m_B^2)(m_C^2 - m_D^2) \\ &\times (m_C^4 - 2(m_B^2 + 2m_C^2)m_D^2))\log\left[1 - \frac{m^2}{m^2 - m_A^2 + m_B^2}\right]\Bigg)\Bigg) \\ &/\Big((m_A^2 - m_B^2)^3(m^2 - m_A^2 + m_B^2)^3(m_B^2 - m_C^2)^2 \\ &\times (2m_B^2 + m_C^2)(m_C^2 - m_D^2)^2(m_C^2 + 2m_D^2)\Big) \end{aligned} \tag{B.22}$$

$$
\begin{aligned}
C2_{hA12} = \Bigg(& 3m_B^4 m_C^2 \Bigg(\frac{1}{(m^2 - m_A^2 + m_B^2)^3} (2(m_A^2 - m_B^2)^5 (m_B^2 + 2m_C^2) \\
& \times (m_C^4 - 5m_C^2 m_D^2 + 4m_D^4) + 2m^{10} m_B^2 (5m_C^4 - 12m_C^2 m_D^2 + 6m_D^4) \\
& - m^4 (m_A^2 - m_B^2)^3 (-25m_C^6 + 152m_C^4 m_D^2 - 92m_C^2 m_D^4 \\
& + m_B^2 (11m_C^4 + 8m_C^2 m_D^2 - 4m_D^4)) - 2m^8 (m_A^2 - m_B^2) \\
& \times (-m_C^2 (m_C^4 - 14m_C^2 m_D^2 + 8m_D^4) + 2m_B^2 (8m_C^4 - 17m_C^2 m_D^2 + 9m_D^4)) \\
& - 2m^2 (m_A^2 - m_B^2)^4 (9m_C^6 - 47m_C^4 m_D^2 + 32m_C^2 m_D^4 \\
& + m_B^2 (2m_C^4 - 15m_C^2 m_D^2 + 10m_D^4)) + m^6 (m_A^2 - m_B^2)^2 \\
& \times (-11m_C^6 + 102m_C^4 m_D^2 - 60m_C^2 m_D^4 + m_B^2 (35m_C^4 - 56m_C^2 m_D^2 + 32m_D^4))) \\
& + 2(m_A^2 - m_B^2)(2m^2 m_C^2 (m_B^2 + m_C^2)(m_C^2 - 2m_D^2) + (m_A^2 - m_B^2) \\
& \times (m_C^2 - m_D^2)(m_C^4 - 2(m_B^2 + 2m_C^2) m_D^2)) \\
& \times \log \left[\frac{(m^2 - m_A^2 + m_B^2)(-m_C^2 + m_D^2)}{m^2 m_C^2} \right] \Bigg) \Bigg) \\
& / \Big((m_A^2 - m_B^2)^3 (m_B^2 - m_C^2)^2 (2m_B^2 + m_C^2)(m_C^2 - m_D^2)^2 (m_C^2 + 2m_D^2) \Big)
\end{aligned}
\tag{B.23}
$$

$$
\begin{aligned}
C1_{lA1} = \Bigg(& 3m_B^4 m_C^2 \Bigg(\frac{1}{m_B^2 m_C^2} (2m^{10} m_B^4 (-2m_C^6 + 12m_C^4 m_D^2 - 9m_C^2 m_D^4 + 2m_D^6) \\
& + (m_A^2 - m_B^2)^5 (m_B^2 - m_C^2)(m_C^2 - m_D^2)(4m_C^4 m_D^2 \\
& + m_B^2 (-3m_C^4 + 7m_C^2 m_D^2 + 2m_D^4)) + 2m^8 m_B^2 (m_A^2 - m_B^2) \\
& \times (-2m_C^8 + 14m_C^6 m_D^2 - 11m_C^4 m_D^4 + 2m_C^2 m_D^6 \\
& + m_B^2 (9m_C^6 - 44m_C^4 m_D^2 + 30m_C^2 m_D^4 - 8m_D^6)) + m^2 (m_A^2 - m_B^2)^4 \\
& \times (12m_C^6 m_D^2 (m_C^2 - m_D^2) - m_B^2 m_C^2 (m_C^6 + 16m_C^4 m_D^2 - 19m_C^2 m_D^4 + 10m_D^6) \\
& + m_B^4 (3m_C^6 - 10m_C^4 m_D^2 + 5m_C^2 m_D^4 + 10m_D^6)) - m^6 (m_A^2 - m_B^2)^2 \\
& (-4m_C^8 m_D^2 + 4m_C^6 m_D^4 + m_B^4 (28m_C^6 - 116m_C^4 m_D^2 + 71m_C^2 m_D^4 - 26m_D^6) \\
& + m_B^2 m_C^2 (-10m_C^6 + 76m_C^4 m_D^2 - 61m_C^2 m_D^4 + 14m_D^6)) + m^4 (m_A^2 - m_B^2)^3 \\
& \times (12m_C^6 m_D^2 (-m_C^2 + m_D^2) + m_B^4 (14m_C^6 - 52m_C^4 m_D^2 + 29m_C^2 m_D^4 - 22m_D^6) \\
& + m_B^2 m_C^2 (-10m_C^6 + 74m_C^4 m_D^2 - 59m_C^2 m_D^4 + 18m_D^6))) \\
& + 2(m_A^2 - m_B^2)(m^2 - m_A^2 + m_B^2)^3 (2m^2 m_C^2 (m_B^2 + m_C^2)(m_C^2 - 2m_D^2) \\
& + (m_A^2 - m_B^2)(m_C^2 - m_D^2)(m_C^4 - 2(m_B^2 + 2m_C^2) m_D^2)) \\
& \times \log \left[\frac{(m_B^2 - m_A^2) m_C^2}{m_B^2 (m^2 - m_A^2 + m_B^2)} \right] \Bigg) \Bigg) / \Big((m_A^2 - m_B^2)^3 (m^2 - m_A^2 + m_B^2)^3 \\
& (m_B^2 - m_C^2)^2 (2m_B^2 + m_C^2)(m_C^2 - m_D^2)^2 (m_C^2 + 2m_D^2) \Big)
\end{aligned}
\tag{B.24}
$$

B.2.3 VFSV

$$
C1_f = \frac{m_B^2}{(-m_A^2 + m_B^2)\,(-m_B^2 + m_C^2)} \tag{B.25}
$$

$$C1_n = \frac{2m_B^2 m_C^2 \left(-\left(m_B^2 - m_C^2\right)\left(m_C^2 - 2m_D^2\right) + 2m_C^2\left(m_B^2 - 2m_D^2\right)\log\left[\frac{m_B}{m_C}\right]\right)}{\left(m_A^2 - m_B^2\right)\left(m_B^2 - m_C^2\right)^2\left(m_C^4 + m_C^2 m_D^2 - 2m_D^4\right)} \tag{B.26}$$

$$\begin{aligned} C2_n = -\Bigg(& 2m_B^2 m_C^4 \Bigg((m_C^2 - 2m_D^2)(m^2 m_B^2 - (m_A^2 - m_B^2)(m_C^2 - m_D^2)) \\ & + (m_A^2 - m_B^2)(m_B^2 - 2m_D^2)(-m_C^2 + m_D^2) \\ & \times \log\left[\frac{m^2 m_B^2}{(m_A^2 - m_B^2)(m_C^2 - m_D^2)}\right]\Bigg)\Bigg) \\ & / \left(\left(m_A^2 - m_B^2\right)^2\left(m_B^2 - m_C^2\right)\left(m_C^2 - m_D^2\right)^2\left(m_C^2 + 2m_D^2\right)\right) \end{aligned} \tag{B.27}$$

$$\begin{aligned} C1_{hA11} = \Bigg(& m_B^2 m_C^4 \Bigg(m^2(2m^6 m_B^2(m_C^2 - 2m_D^2) - 2(m_A^2 - m_B^2)^3(m_C^2 - m_D^2) \\ & \times (m_B^2 - 2m_C^2 + 2m_D^2) - m^4(m_A^2 - m_B^2)(-3m_C^4 + 4m_C^2 m_D^2 \\ & + m_B^2(7m_C^2 - 12m_D^2)) + m^2(m_A^2 - m_B^2)^2(-9m_C^4 + 16m_C^2 m_D^2 - 4m_D^4 \\ & + m_B^2(7m_C^2 - 10m_D^2))) - 4(m_A^2 - m_B^2)(m^2 - m_A^2 + m_B^2)^3 \\ & \times (m_B^2 - 2m_D^2)(m_C^2 - m_D^2)\mathrm{arccoth}\left[\frac{m^2 - 2m_A^2 + 2m_B^2}{m^2}\right]\Bigg)\Bigg) \\ & / \Big((m_A^2 - m_B^2)^2(m^2 - m_A^2 + m_B^2)^3(m_B^2 - m_C^2)^2 \\ & \times (m_C^2 - m_D^2)^2(m_C^2 + 2m_D^2)\Big) \end{aligned} \tag{B.28}$$

$$\begin{aligned} C2_{hA12} = \Bigg(& 2m_B^2 m_C^4 \Bigg(\frac{1}{2(m^2 - m_A^2 + m_B^2)^3 m_C^2}(2m_B^2(-m_A^2 + m_B^2)^3 \\ & \times (m_C^4 - 3m_C^2 m_D^2 + 2m_D^4) + m^6(3m_C^6 - 4m_C^4 m_D^2 \\ & + m_B^2(m_C^4 - 6m_C^2 m_D^2 + 4m_D^4)) + 2m^2(m_A^2 - m_B^2)^2(2(m_C^3 - m_C m_D^2)^2 \\ & + m_B^2(3m_C^4 - 10m_C^2 m_D^2 + 6m_D^4)) - m^4(m_A^2 - m_B^2) \\ & \times (9m_C^6 - 16m_C^4 m_D^2 + 4m_C^2 m_D^4 + m_B^2(5m_C^4 - 20m_C^2 m_D^2 + 12m_D^4))) \\ & + (m_B^2 - 2m_D^2)(-m_C^2 + m_D^2)\log\left[-\frac{(m^2 - m_A^2 + m_B^2)(m_C^2 - m_D^2)}{m^2 m_C^2}\right]\Bigg)\Bigg) \\ & / \left(\left(m_A^2 - m_B^2\right)\left(m_B^2 - m_C^2\right)^2\left(m_C^2 - m_D^2\right)^2\left(m_C^2 + 2m_D^2\right)\right) \end{aligned} \tag{B.29}$$

$$
\begin{aligned}
C1_{lA1} = \Bigg(& m_B^2 \Big(-2m^8 m_B^2 m_C^4 (m_C^2 - 2m_D^2) + (m_A^2 - m_B^2)^4 (m_B^2 - m_C^2) \\
& \times (m_C^6 - 6m_C^4 m_D^2 + 7m_C^2 m_D^4 - 2m_D^6) - m^2 (m_A^2 - m_B^2)^3 (m_C^2 - m_D^2) \\
& \times (m_C^6 + 11 m_C^4 m_D^2 - 6 m_C^2 m_D^4 + m_B^2 (m_C^4 - 15 m_C^2 m_D^2 + 6 m_D^4)) \\
& + m^6 (m_A^2 - m_B^2)(-2m_C^8 - 2m_C^6 m_D^2 + 7 m_C^4 m_D^4 - 2 m_C^2 m_D^6 \\
& + m_B^2 (6m_C^6 - 6 m_C^4 m_D^2 - 7 m_C^2 m_D^4 + 2 m_D^6)) - m^4 (m_A^2 - m_B^2)^2 \\
& \times (-6m_C^8 - 2 m_C^6 m_D^2 + 17 m_C^4 m_D^4 - 6 m_C^2 m_D^6 \\
& + m_B^2 (4 m_C^6 + 8 m_C^4 m_D^2 - 21 m_C^2 m_D^4 + 6 m_D^6)) \\
& - 2(m_A^2 - m_B^2)(m^2 - m_A^2 + m_B^2)^3 m_C^4 (m_B^2 - 2m_D^2)(m_C^2 - m_D^2) \\
& \times \log \left[\frac{(-m_A^2 + m_B^2) m_C^2}{m_B^2 (m^2 - m_A^2 + m_B^2)} \right] \Big) \Bigg) \Big/ \Big((m_A^2 - m_B^2)^2 (m^2 - m_A^2 + m_B^2)^3 \\
& \times (m_B^2 - m_C^2)^2 (m_C^2 - m_D^2)^2 (m_C^2 + 2m_D^2) \Big)
\end{aligned} \tag{B.30}
$$

B.2.4 SFVS

$$
\begin{aligned}
C1_f = & \Big(3m_B^4 (2m^4 m_B^2 - 2m^2 (m_A^2 - m_B^2)(m_B^2 - m_C^2) + (m_A^2 - m_B^2)^2 \\
& \times (m_B^2 - m_C^2)) \Big) \Big/ \Big((m_A^2 - m_B^2)^3 (m_B^2 - m_C^2)^2 (2m_B^2 + m_C^2) \Big)
\end{aligned} \tag{B.31}
$$

$$
\begin{aligned}
C1_n = - \Bigg(& 6m_B^4 m_C^2 \Big((m_B^2 - m_C^2)(-4m^2 m_C^2 - (m_A^2 - m_B^2)(m_C^2 - m_D^2)) \\
& + 2m_C^2 (2m^2 (m_B^2 + m_C^2) + (m_A^2 - m_B^2)(m_C^2 - m_D^2)) \log \left[\frac{m_B}{m_C} \right] \Big) \Bigg) \\
& \Big/ \Big((m_A^2 - m_B^2)^2 (m_B^2 - m_C^2)^2 (2m_B^2 + m_C^2)(m_C^2 - m_D^2)^2 \Big)
\end{aligned} \tag{B.32}
$$

$$
\begin{aligned}
C2_n = & \Bigg(6m_B^4 m_C^4 \Big(2m^4 m_B^2 m_C^2 + m^2 (m_A^2 - m_B^2)(3m_B^2 - 2m_C^2)(m_C^2 - m_D^2) \\
& - 3(m_A^2 - m_B^2)^2 (m_C^2 - m_D^2)^2 - (m_A^2 - m_B^2)(m_C^2 - m_D^2) \\
& \times (2m^2 (m_B^2 + m_C^2) + (m_A^2 - m_B^2)(m_C^2 - m_D^2)) \\
& \times \log \left[\frac{m^2 m_B^2}{(m_A^2 - m_B^2)(m_C^2 - m_D^2)} \right] \Big) \Bigg) \\
& \Big/ \Big((m_A^2 - m_B^2)^3 (m_B^2 - m_C^2)^2 (2m_B^2 + m_C^2)(m_C^2 - m_D^2)^3 \Big)
\end{aligned} \tag{B.33}
$$

$$
\begin{aligned}
C1_{hA11} = \Bigg(& 3m_B^4 m_C^4 \Bigg(m^2(6m^8 m_B^2 - 2m^6(m_A^2 - m_B^2)(9m_B^2 + m_C^2) \\
& + m^4(m_A^2 - m_B^2)^2(19m_B^2 + 5m_C^2) - 2(m_A^2 - m_B^2)^4(m_C^2 - m_D^2) \\
& - m^2(m_A^2 - m_B^2)^3(7m_B^2 - m_C^2 + 2m_D^2)) - 2(m_A^2 - m_B^2) \\
& \times (m^2 - m_A^2 + m_B^2)^3(2m^2(m_B^2 + m_C^2) + (m_A^2 - m_B^2)(m_C^2 - m_D^2)) \\
& \times \log\left[1 - \frac{m^2}{m^2 - m_A^2 + m_B^2}\right] \Bigg) \Bigg) \Big/ \Big((m_A^2 - m_B^2)^3 (m^2 - m_A^2 + m_B^2)^3 \\
& \times (m_B^2 - m_C^2)^2 (2m_B^2 + m_C^2)(m_C^2 - m_D^2)^2 \Big)
\end{aligned} \tag{B.34}
$$

$$
\begin{aligned}
C2_{hA12} = \Bigg(& 3m_B^4 m_C^4 \Bigg(\frac{1}{(m^2 - m_A^2 + m_B^2)^3 m_C^2 (m_C^2 - m_D^2)} \\
& \times \Big(2m^{10} m_B^2 m_C^2 (5m_C^2 - 3m_D^2) + 2(m_A^2 - m_B^2)^5 (m_B^2 + 2m_C^2)(m_C^2 - m_D^2)^2 \\
& - 2m^8 (m_A^2 - m_B^2) m_C^2 (-m_C^4 + m_C^2 m_D^2 + 2m_B^2 (8m_C^2 - 5m_D^2)) \\
& - 2m^2 (m_A^2 - m_B^2)^4 (m_C^2 - m_D^2)(9m_C^4 - 7m_C^2 m_D^2 + m_B^2 (2m_C^2 - 3m_D^2)) \\
& - m^4 (m_A^2 - m_B^2)^3 (-25m_C^6 + 39m_C^4 m_D^2 - 14m_C^2 m_D^4 \\
& + m_B^2 (11m_C^4 - m_C^2 m_D^2 - 6m_D^4)) + m^6 (m_A^2 - m_B^2)^2 \\
& \times (-11m_C^6 + 15m_C^4 m_D^2 - 4m_C^2 m_D^4 + m_B^2 (35m_C^4 - 21m_C^2 m_D^2 - 2m_D^4)) \Big) \\
& + 2(m_A^2 - m_B^2)(2m^2(m_B^2 + m_C^2) + (m_A^2 - m_B^2)(m_C^2 - m_D^2)) \\
& \times \log\left[-\frac{(m^2 - m_A^2 + m_B^2)(m_C^2 - m_D^2)}{m^2 m_C^2} \right] \Bigg) \Bigg) \\
& \Big/ \Big((m_A^2 - m_B^2)^3 (m_B^2 - m_C^2)^2 (2m_B^2 + m_C^2)(m_C^2 - m_D^2)^2 \Big)
\end{aligned} \tag{B.35}
$$

$$
\begin{aligned}
C1_{lA1} = \Bigg(& 3m_B^4 \Bigg(-(m_A^2 - m_B^2)^5 (m_B^2 - m_C^2)(3m_C^4 - 4m_C^2 m_D^2 + m_D^4) \\
& + 2m^{10} m_B^2 (-2m_C^4 - 2m_C^2 m_D^2 + m_D^4) - m^6 (m_A^2 - m_B^2)^2 \\
& \times (-10m_C^6 - 16m_C^4 m_D^2 + 7m_C^2 m_D^4 + m_B^2 (28m_C^4 + 28m_C^2 m_D^2 - 13m_D^4)) \\
& + m^4 (m_A^2 - m_B^2)^3 (-10m_C^6 - 22m_C^4 m_D^2 + 9m_C^2 m_D^4 \\
& + m_B^2 (14m_C^4 + 28m_C^2 m_D^2 - 11m_D^4)) + 2m^8 (m_A^2 - m_B^2) \\
& \times (-2m_C^6 - 2m_C^4 m_D^2 + m_C^2 m_D^4 + m_B^2 (9m_C^4 + 8m_C^2 m_D^2 - 4m_D^4)) \\
& + m^2 (m_A^2 - m_B^2)^4 (m_B^2 (3m_C^4 - 16m_C^2 m_D^2 + 5m_D^4) \\
& - m_C^2 (m_C^4 - 14m_C^2 m_D^2 + 5m_D^4)) + 2(m_A^2 - m_B^2)(m^2 - m_A^2 + m_B^2)^3 \\
& \times m_C^4 (2m^2(m_B^2 + m_C^2) + (m_A^2 - m_B^2)(m_C^2 - m_D^2)) \\
& \times \log\left[\frac{(1 - \frac{m_A^2}{m_B^2}) m_C^2}{m^2 - m_A^2 + m_B^2} \right] \Bigg) \Bigg) \Big/ \Big((m_A^2 - m_B^2)^3 (m^2 - m_A^2 + m_B^2)^3 \\
& \times (m_B^2 - m_C^2)^2 (2m_B^2 + m_C^2)(m_C^2 - m_D^2)^2 \Big)
\end{aligned} \tag{B.36}
$$

B.2.5 SFSV

$$C1_f = \frac{m_B^2}{\left(-m_A^2+m_B^2\right)\left(-m_B^2+m_C^2\right)} \tag{B.37}$$

$$C1_n = \frac{2m_B^2 m_C^2\left(-m_B^2+m_C^2+2m_B^2\log\left[\frac{m_B}{m_C}\right]\right)}{\left(m_A^2-m_B^2\right)\left(m_B^2-m_C^2\right)^2\left(m_C^2-m_D^2\right)} \tag{B.38}$$

$$\begin{aligned} C2_n = -\Bigg(&2m_B^2 m_C^2\Bigg(m_C^2(m^2m_B^2-(m_A^2-m_B^2)(m_C^2-m_D^2)) \\ &+ m_B^2(-m_A^2+m_B^2)(m_C^2-m_D^2)\log\left[\frac{m^2m_B^2}{(m_A^2-m_B^2)(m_C^2-m_D^2)}\right]\Bigg)\Bigg) \\ &/\left((m_A^2-m_B^2)^2(m_B^2-m_C^2)^2(m_C^2-m_D^2)^2\right) \end{aligned} \tag{B.39}$$

$$\begin{aligned} C1_{hA11} = \Bigg(&m_B^2 m_C^2\Bigg(m^2(2m^6m_B^2m_C^2-2(m_A^2-m_B^2)^3(m_B^2-2m_C^2)(m_C^2-m_D^2) \\ &+ m^2(m_A^2-m_B^2)^2(-9m_C^4+6m_C^2m_D^2+m_B^2(7m_C^2-4m_D^2)) \\ &- m^4(m_A^2-m_B^2)(-3m_C^4+2m_C^2m_D^2+m_B^2(7m_C^2-2m_D^2))) \\ &+ 2m_B^2(m_A^2-m_B^2)(m^2-m_A^2+m_B^2)^3(m_C^2-m_D^2) \\ &\times\log\left[1-\frac{m^2}{m^2-m_A^2+m_B^2}\right]\Bigg)\Bigg)/\Big((m_A^2-m_B^2)^2(m^2-m_A^2+m_B^2)^3 \\ &\times(m_B^2-m_C^2)^2(m_C^2-m_D^2)^2\Big) \end{aligned} \tag{B.40}$$

$$\begin{aligned} C2_{hA12} = \Bigg(&2m_B^2 m_C^2\Bigg((m^6m_C^2(m_B^2+3m_C^2-2m_D^2) \\ &+ 2m_B^2(-m_A^2+m_B^2)^3(m_C^2-m_D^2)+2m^2(m_A^2-m_B^2)^2 \\ &\times(3m_B^2m_C^2+2m_C^4-2(m_B^2+m_C^2)m_D^2)-m^4(m_A^2-m_B^2) \\ &\times(9m_C^4-6m_C^2m_D^2+m_B^2(5m_C^2-2m_D^2)))/(2(m^2-m_A^2+m_B^2)^3) \\ &+ m_B^2(m_C^2-m_D^2)\log\left[\frac{m^2m_C^2}{(m^2-m_A^2+m_B^2)(-m_C^2+m_D^2)}\right]\Bigg)\Bigg) \\ &/\left((m_A^2-m_B^2)(m_B^2-m_C^2)^2(m_C^2-m_D^2)^2\right) \end{aligned} \tag{B.41}$$

$$
\begin{aligned}
C1_{lA1} = \Bigg(& 2m_B^2 m_C^2 \Big(\big(-2m^8 m_B^2 m_C^4 + (m_A^2 - m_B^2)^4 (m_B^2 - m_C^2)(m_C^4 - m_D^4) \\
& - m^2 (m_A^2 - m_B^2)^3 (m_C^2 - m_D^2)(m_C^4 - 3m_C^2 m_D^2 + m_B^2 (m_C^2 + 3m_D^2)) \\
& + m^6 (m_A^2 - m_B^2)(-m_C^2 (2m_C^4 - 2m_C^2 m_D^2 + m_D^4) \\
& + m_B^2 (6m_C^4 - 2m_C^2 m_D^2 + m_D^4)) - m^4 (m_A^2 - m_B^2)^2 \\
& \times (-3m_C^2 (2m_C^4 - 2m_C^2 m_D^2 + m_D^4) + m_B^2 (4m_C^4 - 4m_C^2 m_D^2 + 3m_D^4)) \Big) \\
& / \Big(2(m_A^2 - m_B^2)(m^2 - m_A^2 + m_B^2)^3 m_C^2 \Big) + m_B^2 (-m_C^2 + m_D^2) \\
& \log \left[\frac{(m_B^2 - m_A^2) m_C^2}{m_B^2 (m^2 - m_A^2 + m_B^2)} \right] \Big) \Bigg) / \Big((m_A^2 - m_B^2)(m_B^2 - m_C^2)^2 (m_C^2 - m_D^2)^2 \Big)
\end{aligned}
\tag{B.42}
$$

Appendix C

χ^2 Probabilities

C.1 2 Bins

C.1.1 GMSB Mass Spectrum

Lepton-Photon Invariant Mass

	FSFG	VFVS	VFSV	SFVS	SFSV
FSFG	—	0.533	0.376	0.482	0.241
VFVS		—	0.794	0.185	0.072
VFSV			—	0.112	0.040
SFVS				—	0.638
SFSV					—

Lepton-Lepton Invariant Mass

	FSFG	VFVS	VFSV	SFVS	SFSV
FSFG	—	0.930	0.000	0.824	0.000
VFVS		—	0.000	0.756	0.000
VFSV			—	0.000	0.000
SFVS				—	0.000
SFSV					—

High–Lepton-Photon Invariant Mass

	FSFG	VFVS	VFSV	SFVS	SFSV
FSFG	—	0.019	0.110	0.000	0.008
VFVS		—	0.000	0.000	0.747
VFSV			—	0.000	0.000
SFVS				—	0.000
SFSV					—

Low–Lepton-Photon Invariant Mass

	FSFG	VFVS	VFSV	SFVS	SFSV
FSFG	—	0.146	0.026	0.999	0.000
VFVS		—	0.000	0.146	0.031
VFSV			—	0.026	0.000
SFVS				—	0.000
SFSV					—

Lepton-Lepton-Photon Invariant Mass

	FSFG	VFVS	VFSV	SFVS	SFSV
FSFG	—	0.186	0.000	0.000	0.000
VFVS		—	0.000	0.000	0.000
VFSV			—	0.277	0.000
SFVS				—	0.000
SFSV					—

C.1.2 2UED Mass Spectrum

Lepton-Photon Invariant Mass

	FSFG	VFVS	VFSV	SFVS	SFSV
FSFG	—	0.961	0.874	0.936	0.983
VFVS		—	0.912	0.974	0.979
VFSV			—	0.938	0.891
SFVS				—	0.953
SFSV					—

Lepton-Lepton Invariant Mass

	FSFG	VFVS	VFSV	SFVS	SFSV
FSFG	—	0.574	0.074	0.200	0.000
VFVS		—	0.019	0.065	0.000
VFSV			—	0.612	0.000
SFVS				—	0.000
SFSV					—

High–Lepton-Photon Invariant Mass

	FSFG	VFVS	VFSV	SFVS	SFSV
FSFG	—	0.624	0.684	0.142	0.139
VFVS		—	0.370	0.051	0.321
VFSV			—	0.287	0.059
SFVS				—	0.003
SFSV					—

Low–Lepton-Photon Invariant Mass

	FSFG	VFVS	VFSV	SFVS	SFSV
FSFG	—	0.929	0.670	0.513	0.544
VFVS		—	0.607	0.485	0.605
VFSV			—	0.820	0.302
SFVS				—	0.208
SFSV					—

Lepton-Lepton-Photon Invariant Mass

	FSFG	VFVS	VFSV	SFVS	SFSV
FSFG	—	0.783	0.925	0.220	0.677
VFVS		—	0.712	0.134	0.888
VFSV			—	0.257	0.610
SFVS				—	0.101
SFSV					—

C.2 5 Bins

C.2.1 GMSB Mass Spectrum

Lepton-Photon Invariant Mass

	FSFG	VFVS	VFSV	SFVS	SFSV
FSFG	—	0.430	0.112	0.035	0.005
VFVS		—	0.009	0.005	0.006
VFSV			—	0.228	0.000
SFVS				—	0.000
SFSV					—

Lepton-Lepton Invariant Mass

	FSFG	VFVS	VFSV	SFVS	SFSV
FSFG	—	0.992	0.000	0.878	0.000
VFVS		—	0.000	0.968	0.000
VFSV			—	0.000	0.000
SFVS				—	0.000
SFSV					—

High–Lepton-Photon Invariant Mass

	FSFG	VFVS	VFSV	SFVS	SFSV
FSFG	—	0.043	0.000	0.000	0.008
VFVS		—	0.000	0.000	0.000
VFSV			—	0.001	0.000
SFVS				—	0.000
SFSV					—

Low–Lepton-Photon Invariant Mass

	FSFG	VFVS	VFSV	SFVS	SFSV
FSFG	—	0.589	0.008	0.000	0.000
VFVS		—	0.000	0.000	0.000
VFSV			—	0.007	0.000
SFVS				—	0.000
SFSV					—

Lepton-Lepton-Photon Invariant Mass

	FSFG	VFVS	VFSV	SFVS	SFSV
FSFG	—	0.221	0.000	0.000	0.000
VFVS		—	0.000	0.000	0.000
VFSV			—	0.002	0.000
SFVS				—	0.000
SFSV					—

C.2.2 2UED Mass Spectrum

Lepton-Photon Invariant Mass

	FSFG	VFVS	VFSV	SFVS	SFSV
FSFG	—	1.000	0.996	0.997	1.000
VFVS		—	0.999	0.999	1.000
VFSV			—	1.000	0.999
SFVS				—	0.998
SFSV					—

Lepton-Lepton Invariant Mass

	FSFG	VFVS	VFSV	SFVS	SFSV
FSFG	—	0.964	0.356	0.687	0.000
VFVS		—	0.094	0.289	0.000
VFSV			—	0.986	0.000
SFVS				—	0.000
SFSV					—

High–Lepton-Photon Invariant Mass

	FSFG	VFVS	VFSV	SFVS	SFSV
FSFG	—	0.988	0.991	0.542	0.606
VFVS		—	0.911	0.271	0.881
VFSV			—	0.759	0.402
SFVS				—	0.031
SFSV					—

Low–Lepton-Photon Invariant Mass

	FSFG	VFVS	VFSV	SFVS	SFSV
FSFG	—	0.999	0.922	0.504	0.801
VFVS		—	0.849	0.387	0.900
VFSV			—	0.937	0.310
SFVS				—	0.057
SFSV					—

Lepton-Lepton-Photon Invariant Mass

	FSFG	VFVS	VFSV	SFVS	SFSV
FSFG	—	0.973	0.967	0.572	0.525
VFVS		—	0.811	0.347	0.608
VFSV			—	0.772	0.159
SFVS				—	0.043
SFSV					—

Bibliography

[1] A. J. Barr, Phys. Lett. **B596**, 205 (2004), hep-ph/0405052.

[2] C. D. Hoyle *et al.*, Phys. Rev. **D70**, 042004 (2004), hep-ph/0405262.

[3] S. R. Coleman and J. Mandula, Phys. Rev. **159**, 1251 (1967).

[4] P. Binetruy, Oxford, UK: Oxford Univ. Pr. (2006) 520 p.

[5] P. Fayet and J. Iliopoulos, Phys. Lett. **B51**, 461 (1974).

[6] L. O'Raifeartaigh, Nucl. Phys. **B96**, 331 (1975).

[7] I. Hinchliffe and F. E. Paige, Phys. Rev. **D60**, 095002 (1999), hep-ph/9812233.

[8] T. Appelquist, H.-C. Cheng, and B. A. Dobrescu, Phys. Rev. **D64**, 035002 (2001), hep-ph/0012100.

[9] B. A. Dobrescu and E. Ponton, JHEP **03**, 071 (2004), hep-th/0401032.

[10] G. Burdman, B. A. Dobrescu, and E. Ponton, JHEP **02**, 033 (2006), hep-ph/0506334.

[11] E. Ponton and L. Wang, JHEP **11**, 018 (2006), hep-ph/0512304.

[12] B. A. Dobrescu, K. Kong, and R. Mahbubani, JHEP **07**, 006 (2007), hep-ph/0703231.

[13] G. Burdman, B. A. Dobrescu, and E. Ponton, Phys. Rev. **D74**, 075008 (2006), hep-ph/0601186.

[14] C. G. Lester and M. A. Parker, *Model independent sparticle mass measurements at ATLAS*, PhD thesis, Cambridge Univ., Geneva, 2001, Presented on 12 Dec 2001.

[15] D. J. Miller, P. Osland, and A. R. Raklev, JHEP **03**, 034 (2006), hep-ph/0510356.

[16] J. M. Smillie and B. R. Webber, JHEP **10**, 069 (2005), hep-ph/0507170.

[17] L.-T. Wang and I. Yavin, JHEP **04**, 032 (2007), hep-ph/0605296.

[18] M. Biglietti *et al.*, ATL-PHYS-PUB-2007-004.

[19] A. Alves and O. Eboli, Phys. Rev. **D75**, 115013 (2007), 0704.0254.

[20] M. R. Buckley, H. Murayama, W. Klemm, and V. Rentala, (2007), 0711.0364.

[21] M. Dine, A. E. Nelson, and Y. Shirman, Phys. Rev. **D51**, 1362 (1995), hep-ph/9408384.

[22] M. E. Peskin and D. V. Schroeder, *An Introduction to Quantum Field Theory* (Westview Press, 1995), chap. 5.2.

[23] E. Cremmer *et al.*, Phys. Lett. **B79**, 231 (1978).

[24] E. Cremmer *et al.*, Nucl. Phys. **B147**, 105 (1979).

[25] F. del Aguila, A. Culatti, R. Munoz-Tapia, and M. Perez-Victoria, Nucl. Phys. **B504**, 532 (1997), hep-ph/9702342.

[26] C. Athanasiou, C. G. Lester, J. M. Smillie, and B. R. Webber, JHEP **08**, 055 (2006), hep-ph/0605286.

[27] M. Jamin and M. E. Lautenbacher, Comput. Phys. Commun. **74**, 265 (1993).

[28] A. Pukhov *et al.*, (1999), hep-ph/9908288.

[29] N. D. Gagunashvili, Prepared for PHYSTATO5: Statistical Problems in Particle Physics, Astrophysics and Cosmology, Oxford, England, United Kingdom, 12-15 Sep 2005.

[30] T. Sjostrand, S. Mrenna, and P. Skands, JHEP **05**, 026 (2006), hep-ph/0603175.

[31] L. P. Elzbieta Richter-Was, Daniel Froidevaux, ATL-PHYS-98-131 (1998).